EFFECTS OF ESTRADIOL AND SELECTIVE ESTROGEN RECEPTOR AGONISTS ON BIOCHEMICAL ENDPOINTS IN THE BRAIN: A COMPARISON BETWEEN TRANSITIONAL AND SURGICAL MENOPAUSE RAT MODELS

by

Ziv Z. Kirshner

Bachelor of Science, ORT Braude College of Engineering, 2009

Submitted to the Graduate Faculty of the

School of Pharmacy in partial fulfillment

of the requirements for the degree of

Doctor of Philosophy

University of Pittsburgh

2019

UNIVERSITY OF PITTSBURGH

SCHOOL OF PHARMACY

This dissertation was presented

by

Ziv Z. Kirshner

It was defended on

October 29, 2019

and approved by

Wen Xie, MD, PhD, Professor, Pharmaceutical Science

Regis R. Vollmer, PhD, Professor Emeritus, Pharmaceutical Sciences

Donald B. DeFranco, PhD, Professor, Molecular Biophysics and Biochemistry

Dissertation Director: Robert B. Gibbs, PhD, Professor, Pharmaceutical Science

EFFECTS OF ESTRADIOL AND SELECTIVE ESTROGEN RECEPTOR AGONISTS ON BIOCHEMICAL ENDPOINTS IN THE BRAIN: A COMPARISON BETWEEN TRANSITIONAL AND SURGICAL MENOPAUSE RAT MODELS

Ziv Z. Kirshner, PhD

University of Pittsburgh, 2019

Women spend the last third of their lifetime postmenopause, with cessation of ovarian activity and diminished production of systemic estrogen. The loss of ovarian estrogen production is correlated with age-related cognitive decline, dementia and a shift in brain metabolism from glucose to ketone bodies. Estrogen treatment may prevent or reverse these changes. Our goal is to understand how the loss of ovarian function and estrogen replacement therapy affect metabolism and function of brain regions that are involved in cognitive functions. In this study, we evaluated the differences between surgical (ovariectomized, OVX) to transitional (ovatotoxin-treated, 4-vinylcyclohexene diepoxide, VCD) menopause rat models in comparison to normally cycling rats and with agonists treatments for the selective activation of estrogen receptor α (ERα), ERβ and G-protein coupled estrogen receptor 1 (GPER-1). Our endpoints were chosen to represent pivotal targets in major metabolic, energy, cytoskletal and neurological pathways which are modulated by estrogens with corresponding effects on neuronal or cognitive functions. Overall these studies established a highly reliable method to relatively quantify proteins in brain homogenates, a direct comparison of metabolic endpoints between OVX, VCD and cycling animals as well as the effects of ER agonists between OVX and VCD rats in two time points of continuous treatment (1- and 6-weeks) and three brain regions: hippocampus (HPC), frontal cortex (FCX) and striatum (STR). These studies illustrates that type and onset of menopause have versatile impact on brain metabolism, glucose utilization, cytoskeletal and cholinergic endpoints. We also demonstrated the differences in response to selective activation of different estrogen receptors and provided an

insight into changes that occur in across duration of treatment, menopause models and treatments with selective estrogen receptor agonists. These can serve as a pre-clinical map for the development of more selective estrogen replacement therapy for postmenopausal women.

Table of Contents

List of Tables

List of Figures

List of Abbreviations

Abbreviation / Acronym	Description / Definition
%CV	Percent coefficient of variation
ACh	Acetylcholine
AD	Androstenedione
AD	Alzheimer's disease
AR	Androgen Receptor
ATP-CL	ATP citrate lyase
BDNF	Brain-derived neurotrophic factor
BFCN	Basal forebrain cholinergic neurons
ChAT	Choline acetyltransferase
CNS	Central Nervous System
D	Diestrus
DMP	Delayed matching-to-position
DPN	Diarylpropionitrile (selective ERβ agonist)
E2	17β-estradiol
EDTA	Ethylenediaminetetraacetic
ELISA	Enzyme-linked immunosorbent assay
ER-X	Estrogen Receptor X
ERα	Estrogen Receptor Alpha
ERβ	Estrogen Receptor Beta
ESI	Electrospray ionization
FCX	Frontal cortex
G-1	Selective GPER-1 agonist (CAS# 881639-98-1)
GAPDH	Glyceraldehyde 3-phosphate dehydrogenase
GPER-1	G-protein coupled estrogen receptor 1
Gq-mER	Gq-Membranalic Estrogen Receptor
HKP	House-keeping protein
HPC	Hippocampus
HPCD	Hydroxypropyl-ß-cyclodextran
HPLC	High Performance Liquid Chromatography
ICC	Intraclass correlation coefficient
IGFR-1	Insulin-like growth factor receptor 1
LTP	Long-term potentiation
mtER	Mitochondrial estrogen receptor
MW	Molecular weight
OVX	Ovariectomized
P	Proestrus
PDH	Pyruvate dehydrogenase
PFK	Phosphofructokinase

PMSF	Phenylmethylsulfonyl Fluoride
PPT	Propyl pyrazole triol, selective ERα agonist
PVDF	Polyvinylidene difluoride
RIA	Radioimmunoassay
ROS	Reactive oxygen species
SDS	Sodium dodecyl sulfate
STR	Striatum
T	Testosterone
T_{AF}	Alswalmeh-Feldt F-test
TBS	Tris-buffered saline
TP	Total protein
TrkB	Tropomyosin receptor kinase B
VCD	4-vinylcyclohexene diepoxide (Ovatotoxin)
WB	Western Blot

Preface

Bs”d

First and foremost, I would like to thank my advisor, Prof. Robert B. Gibbs, for his mentorship, support, encouragement and guidance. His intriguing approach to science created in me a natural enthusiasm towards answering meaningful scientific questions. The values and investigative attitudes which I learned from Prof. Gibbs became an integral part of who I am and will be carried with me along my future scientific endeavors.

I would also like to express my deepest appreciation to the committee members, Prof. Wen Xie, Prof. Emeritus Regis R. Vollmer and Prof. Donald B. Defranco. For their devotion, commitment to advise and for providing valuable feedbacks through my graduate studies. Also, I sincerely thankful to our collaborators, Dr. Jeffrey K. Yao z”l, Prof. Heather Bimonte-Nelson and Prof. Gregory Brewer, who been very supportive in creating fruitful studies.

I am very grateful to all our lab members Douglas E. Nelson, Junyi Li, Tao Long and Di Rao who supported my development and studies. Beyond working together and the personal relationships, they demonstrated to me how collaboration between individual parts of a larger project can move together towards productive discoveries. I would also like to extend my deepest gratitude to the faculty and staff of the School of Pharmacy. I am extremely thankful to: Dr. Patricia D Kroboth, Dr. Randall B. Smith, Dr. Samuel M. Poloyac, Dr. Barry Gold, Dr. Paul Schiff, Dr. Maggie Folan, Lori M. Altenbaugh, Dolores M Hornick. The professional academic culture, the continuous support and the personal open-minded approach were of enormous value to my development.

I am deeply indebted to my immediate family for their continuous support and reassurance. To my mother, Sigalit Yaccov-Kazashecter z”l, who inherit to me her lifelong values of perusing higher education, passion to science and the path to create meaningful contributions. Although she passed away in 2008, she clearly foreseen my passion to science and my professional future beforehand. To my wife, Chen H. Kirshner, for her unambiguous support and for delivering to us our two amazing children during my studies: Nevo Y. Kirshner and Noya S. Kirshner. To my sister, Adi Kirshner, who took up on herself enormous responsibility to take care of my younger brothers Orel Kirshner and Daniel Kirshner in Israel. I am grateful to all of their encouragement, patience, constructive advice and prefunded belief in me.

I am extremely grateful to my larger circle of supporters. The Internations Sepharadic Education Foundation (ISEF) who supports my education in the past +12 years. To the close circle of friends: Eli Ganah z”l, Yehuda Sasi and Dr. Stephan Greene for their personal advice and support alongside my academic studies.

My dissertation document encapsulates several years of scientific exploration which were the fruits of many hypotheses, paradigms and scientific thoughts. These studies disclosed many findings of beauty in the mysterious universe of life. While I am very proud of these discoveries, they are not only my personal celebration and were made with the combined efforts of all those who supported me. My own reward is the prolonged experience of seeking and ultimately finding.

From my heart I thank you all,

Sincerely,

Ziv

1.0 Introduction

1.1 Effects of Estrogen on Cognitive Functions and Behavior

Today, the increase in lifespan and medical care results in women spending the last third of their lifetime postmenopause (Takahashi & Johnson, 2015). Women, usually above 45-years old, undergo a perimenopausal transition period where levels of reproductive hormones, produced by the ovaries, are fluctuating. This results in irregular menstrual periods and in later stages to a cessation of menstruation. Perimenopause ends when a women enters a menopausale stage defined by 12 consecutive month of amenorrhea (absence of menstruation) and consistent low circulating estradiol and progesterone as well as elevated gonadotropins (Dalal & Agarwal, 2015; McCarrey & Resnick, 2015). Physiological symptoms (e.g. hot flushes, chills sleep disruptions, mood changes and worsening cognitive performance), that emerge from the systemic loss of reproductive hormones, may start early at perimenopause and continue through menopause. In some women, these symptoms may continue post-menopause with an increased risk of neurological decline (Brinton, Yao, Yin, Mack, & Cadenas, 2015; Hoga, Rodolpho, Goncalves, & Quirino, 2015; McCarrey & Resnick, 2015; Takahashi & Johnson, 2015). The overall nature of these side effects is indicative of disruption in multiple estrogen-regulated pathways which impact cognitive functions.

Estrogen therapy in women has beneficial effects on the brain that include lower prevalence of age-related cognitive decline and dementia, as well as benefits on specific cognitive tasks (Gibbs, 2010). Yet, most of these estrogen-mediated effects have been seen in younger women that undergo surgical menopause or in perimenopausal stages, while fewer beneficial effects have

been observed by estrogen therapy in older postmenopausal women (Gibbs, 2010; McCarrey & Resnick, 2015). Certain differences in response to estrogen therapy can be explained by the 'Critical Period Hypothesis' which suggests that the ability of estrogens to confer protection from cognitive decline exists for a short time after menopause and that responsiveness to estrogen decreases with age and time after menopause. In the brain, estrogens regulate signaling and transcriptional pathways, glucose metabolism, mitochondrial ATP-production and neuronal functions as well as coordinate certain metabolic functions between the brain and periphery (Rettberg, Yao, & Brinton, 2014). These effects are mediated by estrogen receptors which act by both genomic and secondary signaling pathways to affect metabolic, energetic and neurochemical functions. These receptor-mediated pathways may become uncoupled from their original function before perimenopause or become responsive to different estrogen receptors. This change in response to estrogen is associated with changes in age, type of menopause, time from when menopause started as well as when treatment initiated and duration of treatment (Gibbs, 2010). The broader goal of the current studies is to evaluate neurochemical factors involved in the cognitive decline of post-menopausal women and to evaluate potential therapeutic strategies. The majority of this work has focused on characterizing the differences between normally cycling rats to rat models of surgical (ovariectomized) and transitional (neuro-toxin induced) menopause. We also characterized the response of each menopause rat model to short- and long- term treatments with selective estrogen-receptor agonists. Results of these studies improve the understanding of metabolic changes associated with surgical and transitional menopause in rat models and illustrates new strategies for the development of more selective hormone replacement therapy in women.

1.1.1 Estrogen Effects on Cognitive Functions

Many beneficial effects of estrogens were observed in rodents and are mediated by estrogen receptors in a region-dependent manner to modulate different neurotransmitter systems (Barth, Villringer, & Sacher, 2015; Gibbs, 2010; B. S. McEwen, Akama, Spencer-Segal, Milner, & Waters, 2012). Some of those effects include improvement in cognitive performance (Daniel, 2006) and prevention of age-related cognitive decline (Frick, 2009; Gibbs & Gabor, 2003). Estrogen-mediated mechanisms on neurons, such as hippocampal spine maturation, synaptogenesis, and effects on memory processes were also demonstrated (B. S. McEwen et al., 2012). Yet, most of the mechanisms by which estrogen affect behaviors and cognitive functions are unknown and involve several brain regions, multiple neurotransmitters and significant changes to energy and metabolism in the brain (Gibbs, 2010; B. S. McEwen et al., 2012; Rettberg et al., 2014). In postmenopausal women, impairment of spatial learning ability is associated with the loss of ovarian hormones. One effect of estrogen treatment is to maintain or restore spatial learning. In rats, this effect is mediated by estrogenic actions on basal forebrain cholinergic neurons (BFCN).

BFCNs provide primary afferents into the hippocampus and cerebral cortex (Mesulam, 1996) which in turn affect learning, memory, attention and regeneration processes. In aged or in ovariectomized rats, several functions of cholinergic neurons become impaired as measured by lower activity levels of choline acetyltransferase (ChAT), high affinity choline uptake (HACU), and acetylcholine (ACh) release (Abraham, Koszegi, Tolod-Kemp, & Szego, 2009; Gibbs, 2010). These impairments in cholinergic functions can be prevented or recovered by estrogen treatments (Abraham et al., 2009; Gibbs, 1999, 2010; Gibbs, Nelson, Anthony, & Clarkson, 2002). Disruption to BFCN pathways has an impact on spatial learning and memory. For example, *Gibbs et al.* have shown that estradiol enhance the acquisition of the delayed matching-to-position (DMP) T-maze

task by increasing key cholinergic functions such as HACU and ACh release (Gibbs, 2000; Gibbs & Johnson, 2007). Estrogen effects on cognitive performance on the DMP maze were completely abolished by selective loss of BFCNs positioning them as essential for mediating estradiol effect on the DMP maze task (Gibbs & Johnson, 2007; Johnson, Zambon, & Gibbs, 2002). Collectively, these studies demonstrate the role of BFCNs in cognitive functions and that estrogen treatment can maintain the integrity of cholinergic function as a mechanism to prevent age-related decline in spatial learning.

Another mechanism by which estrogen can influence BFCNs is by maintenance of the metabolic capacity in the brain to prevent selective loss of cholinergic cells caused by limited availability of glycolytic fuels. During aging and with the loss of ovarian function, energy production in the brain is shifting to higher use of ketone bodies and lower use of glucose (Brinton et al., 2015; Frank, Brown, & Clegg, 2014; Rettberg et al., 2014). Cholinergic neurons are particularly susceptible to the lower availability in glucose, in byproducts of glycolytic metabolism and the subsequent reduction in the availability of acetyl-CoA. The decrease in ATP production and lower levels of acetyl-CoA results in inhibition of ChAT, lower ACh levels, lower rate of ACh release, reduction in synaptic function and correlates with death rate of cholinergic neurons (Szutowicz, Bielarczyk, Jankowska-Kulawy, Pawelczyk, & Ronowska, 2013; Szutowicz et al., 2014). Estrogen treatment in OVX or aged rats, as well as in women, maintaining the levels of glucose metabolism by regulation of glucose transport, mitochondrial functions and production of ATP and acetyl-CoA (Brinton et al., 2015; Rettberg et al., 2014). This in turn can prevent the loss of cholinergic neurons due to energetic imbalance (Rettberg et al., 2014; Szutowicz et al., 2013; Szutowicz et al., 2014). Together, these examples illustrates how estrogen treatment can be of

therapeutic value and better understanding of those mechanisms can support the development of better treatments for women.

1.2 Estrogen Receptors

Effects of estrogen are mediated by signaling through two nuclear receptors (ERα and ERβ) and by the membrane-associated G-protein coupled estrogen receptor 1 (GPER1) (Cui, Shen, & Li, 2013). ERα and ERβ are highly conserved with structural homology and six functional domains and when activated can induce gene transcription (Sanchez, Nguyen, Rocha, White, & Mader, 2002). In their membrane-associate form, mERα and mERβ, are localized in specific membrane compartments Boulware, 2007 #26), capable of activating several second messenger signaling pathways in neurons- and region- specific manners (Micevych, Mermelstein, & Sinchak, 2017).

GPER1 was identified more recently (Moriarty et al., 2006; (Brailoiu et al., 2007) and shown to mediate rapid estrogen signaling in neurons and other cell lines such as: ovarian cancer (Albanito et al., 2007), breast cancer (Thomas, Pang, Filardo, & Dong, 2005), endothelial cancer (Vivacqua et al., 2006) and others (Filardo, 2002; Funakoshi, Yanai, Shinoda, Kawano, & Mizukami, 2006; Luine, 1985; Revankar, Cimino, Sklar, Arterburn, & Prossnitz, 2005). Limited evidence supports the presence of additional estrogen receptors (e.g. ER-X, Gq-mER and cytoplasmic ERα-36 variant), that can either be activated by estrogens or with structural homology to traditional ERs. Yet, the existence of these receptors is still debatable. Selective agonists for the activation of ERα, ERβ and GPER-1 available commercially and illustrated by structure in Figure 1.

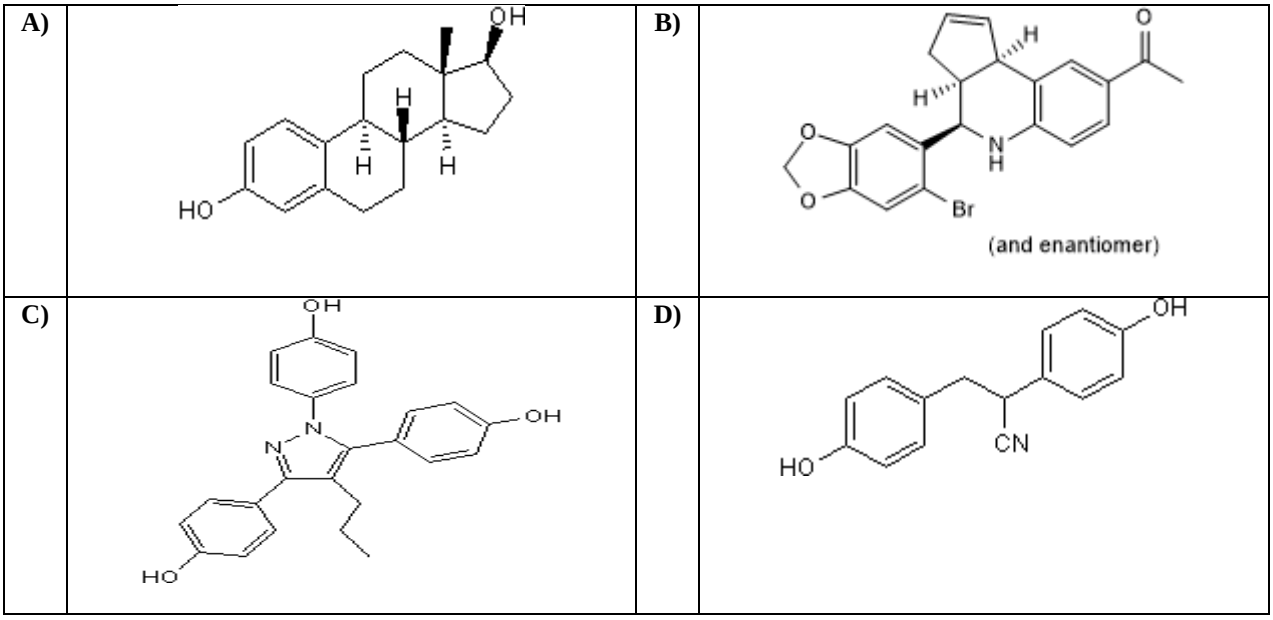

Figure 1: Structures of (A) E2, (B) G-1 (selective GPER-1 agonist), (C) PPT (selective ERα agonist) and (D) DPN (selective ERβ agonist). Compound structure image adapted from TOCRIS.com by catalog numbers 2824, 3577, 1426 and 1494 respectively.

Expression of estrogen receptors across the brain is highly dynamic and change as function of age and in response to levels of circulating hormones as illustrated in Figure 2 (Mott & Pak, 2013). For example, ERα degradation induced by estradiol may be regulated through proteasome-mediated pathways whereas agonist treatment may induce ERα degradation by lysosome-mediated pathway (Wijayaratne & McDonnell, 2001) as well as by activated ERβ (Bartella et al., 2012). In aged rats, estrogen binding in the hypothalamus and anterior pituitary is lower compare to young rats (Funabashi et al., 2000; Rubin, Fox, & Bridges, 1986). This change in estrogen binding may be attributed to age-associated reduction in the expression of ERs, a shift in ratios of ERs or a change in the intracellular receptor localization. While age alone does not eliminate ERα expression, changes in circulating estrogens as well as other factors can determine the levels of ERα expression in the brain (Funabashi et al., 2000; Wilson et al., 2002). Loss of ovarian E2, followed by 10-weeks of estrogen deprivation, can also lead to a decrease in the expression of ERα

in the hippocampus, with minimal effect on the expression of ERβ (Q. G. Zhang et al., 2011). Overall these suggests that expression of ERs can be changes with age and both the onset and duration of estrogen treatments following the loss of ovarian hormones.

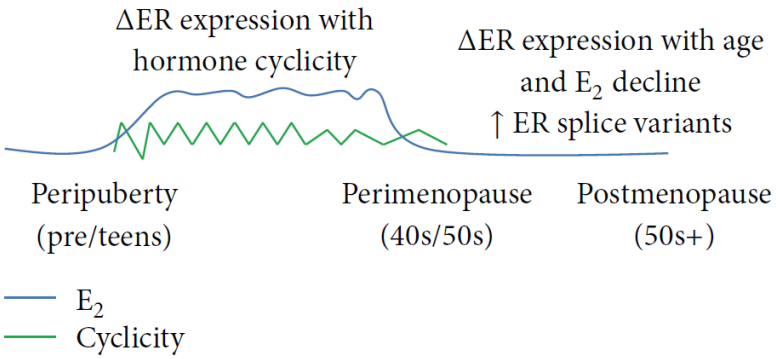

Figure 2: Illustration of a simplified model for changes in the expression and distribution of estrogen receptors in the brain as function of age and circulating levels of estrogen throughout the female life span. Blue line demonstrate levels of E2 as they change with age from peripuberty (left side) to perimenopause and postmenopause (right side). From puberty to beginning of the perimenopause a cyclicity line (green) illustrates the hormonal fluctuations and how they plateau towards age of menopause. During this puberty period, changes (Δ) in the expression of estrogen receptors are mostly associated with hormone cyclicity. At postmenopausal stage expression of ER declines due to the loss of circulating estrogens, but alternative splicing of ER gene expression can increase and diversify the ER gene expression profile. Illustration adapted from (Mott & Pak, 2013).

Signaling of membrane-associated ERs were shown to be highly specific with regards to brain region, the type of neuron and complexity of signal activation (e.g. dependent or independent from other membrane or intracellular proteins) (Boulware et al., 2005 ; Grove-Strawser, Boulware, & Mermelstein, 2010; Manavathi & Kumar, 2006; B. McEwen, 2002; Meitzen & Mermelstein, 2011; Micevych et al., 2017). For example, *Mermelstein et al.* demonstrated in hippocampal neurons from female rats how estrogen activation of mERα is associated with expression of caveolin 1 and activates either metabotropic glutamate receptor 1 (mGluR1) or mGluR5 signaling

(Micevych et al., 2017). In other hippocampal neurons, estrogen is acting through mERβ in association with caveolin 3 and activation of either mGluR2 or mGluR3 (Grove-Strawser et al., 2010). In the striatum, mERs activation was paired with a different sets of mGluRs (Meitzen & Mermelstein, 2011). Estrogens were also shown to activate several other receptors (directly and indirectly via ERs) on membranes of neurons, such as of insulin-like growth factor receptor 1 (IGFR-1), Brain-derived neurotrophic factor (BDNF) and Tropomyosin receptor kinase B (TrkB) receptors (Cersosimo & Benarroch, 2015). Overall ERs are co-localized in defined membranalic compartments with other membrane-associated proteins to interact with diverse set of membrane-receptors and activate or inhibit both rapid and genomic actions (Cersosimo & Benarroch, 2015; Frick, 2009; Micevych et al., 2017).These suggests that mechanism of ERs are highly selective, with great complexity, neuron-specific and multiple estrogen-mediated pathways can act within the same cell (Figure 3). Changes in the expression of ERs over the estrus cycle, in age and with how and when loss of ovarian function occurs are adding to this complexity. This work was aimed to address and resolve specific variables of this complexity.

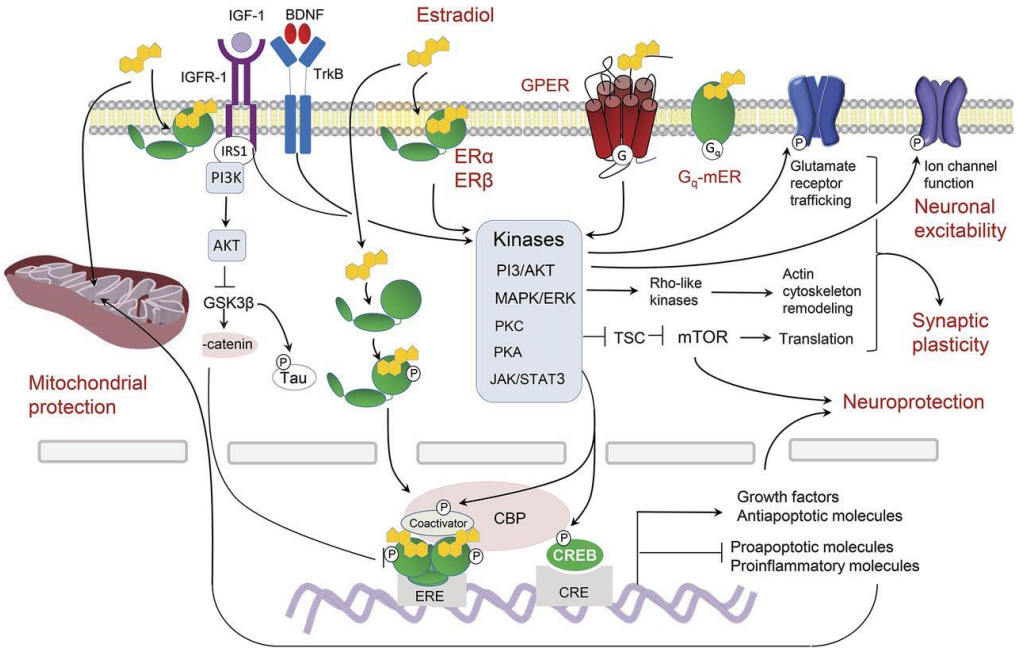

Figure 3: Illustration of estrogen signaling in the brain. Adapted from *Cersosimo et al.* (Cersosimo & Benarroch, 2015).

1.3 Estrogen Activity is Region Specific

While estrogen can regulate proteins activation by direct binding (e.g. allosteric modulation) many of the effects are mediated via ERs (Levin, 2009; Moura & Petersen, 2010; T. W. Wu, Chen, & Brinton, 2011).When ER is activated in a ligand-dependent manner (e.g. E2-Receptor complex formation), ERα and ERβ can induce direct or tethered genomic activity as well as cytosol-initiated non-genomic actions (Lynch, Winiecki, Vanderhoof, Riccio, & Jasnow, 2016). ERα and ERβ can also be activated by signaling of specific growth factors in ligand-independent fashion (e.g. kinase activation) (Lynch et al., 2016) and evidence suggests that ligand-independent activation of GPER-1 by kinase pathways (such as MAPK) is also possible (Gao et al., 2018; Gros et al., 2011; Lau, Chan, Guo, & Wong, 2008; Shanle & Xu, 2011). All three estrogen receptors (ERα, ERβ and GPER) can also initiate rapid cytoplasmic signaling in region and cell type dependent manner (Heldring et al., 2007; Meitzen & Mermelstein, 2011; Micevych et al., 2017; Sarvari et al., 2010; Vargas et al., 2016). Limited evidence also exists for other estrogen-related receptors with either structure similarity to ERs or response to E2 treatment (Saito & Cui, 2018; C. D. Toran-Allerand, 2004; C. Dominique Toran-Allerand et al., 2002).

In the HPC, androgen receptors (ARs) are abundant mostly in CA1 and some in CA3 regions (Simerly, Chang, Muramatsu, & Swanson, 1990) whereas for estrogen, ERα levels are higher than ERβ in CA1-CA3 region; and ERβ, but not ERα, is abundant in the Dentate gyrus, subiculum and Tenia tecta hippocampal areas (Milner et al., 2005; Milner et al., 2001; Paul J.

Shughrue, Lane, & Merchenthaler, 1997). GPER-1 expressed in all three regions (HPC, FCX and STR) with highest expression in the HPC compare to lower levels in the FCX and STR (Brailoiu et al., 2007; Hammond, Nelson, & Gibbs, 2011). Interestingly, majority of the cholinergic neurons in the HPC express GPER-1, and both E2 and G1 (GPER-1 agonist) increase hippocampal ACh release in response to elevated potassium (Hammond et al., 2011). There are many effects of estrogen on the HPC include modulation of synaptic plasticity, connectivity and increase in dendritic spines with functional outcomes on memory (Hammond, Mauk, Ninaci, Nelson, & Gibbs, 2009; C. Li et al., 2004; Noah J. Sandstrom & Williams, 2001; N. J. Sandstrom & Williams, 2004; Spencer et al., 2008; Woolley, 2007). At least some of the effects on hippocampal plasticity and spinogenesis are mediated by ERβ membrane-initiated signaling (Flanagan-Cato, 2011; Micevych et al., 2017; Woolley & McEwen, 1994). In the FCX, both ERα and ERβ are expressed (P. J. Shughrue & Merchenthaler, 2000) and can regulate calcium signaling pathway, dopaminergic, serotonergic, and glutamatergic neurotransmission (Sarvari et al., 2010) as well as response to estrogen treatment by enhancing plasticity, long-term potentiation (LTP) and increase dendritic spines density (Brailoiu et al., 2007; B. McEwen, 2002; Mitra et al., 2003; Srivastava et al., 2008; Wallace, Frankfurt, Arellanos, Inagaki, & Luine, 2007; Woolley & McEwen, 1994). In the STR, ERβ expression is more dominant and ERα expression is limited to the Caudate putamen region (Mitra et al., 2003; Paul J. Shughrue & Merchenthaler, 2001). About 99% of cholinergic neurons in the STR express GPER-1 (Brailoiu et al., 2007; Hammond et al., 2011).

1.4 Effects of Estrogen on Energy and Metabolism are linked to Cognitive Functions

Estrogens have a large repertoire of effects on cellular metabolism and energy production, which in turn affect multiple memory and learning systems across brain regions. In the brain, estrogens can modulate central control of food intake and energy expenditure by acting on specific neuronal circuits in the hypothalamus, cortex and brainstem (e.g. with systemic consequences on glucose availability and energetic-balance in the CNS) (Mauvais-Jarvis, Clegg, & Hevener, 2013; Vasconsuelo, Milanesi, & Boland, 2013). On the cellular level, effects of estrogen range from changes in glucose uptake, regulation of transmembrane channels activity, shifting mitochondrial bioenergetics balance and the levels of reactive oxygen species (ROS) and cytosolic metabolism, all with crucial impacts on cell survival, proliferation and function (Chen, Cammarata, Baines, & Yager, 2009; Korol & Wang, 2018; Lejri, Grimm, & Eckert, 2018; Mauvais-Jarvis et al., 2013; Rettberg et al., 2014; Russell, Jones, & Newhouse, 2019). These effects are associated with the effects of estrogen on cytoskeletal proteins, which serve as a necessary component for the cross talk between estrogenic effects on mitochondria, nucleus and plasma membrane (Brill et al., 2016; Vasconsuelo et al., 2013). Some of the targets for estrogenic actions are illustrated below in Figure 9. Chapter 3 (section 3.3.3.1) describes in more depth the effects and mechanisms of estrogen actions on cytoplasmic, mitochondrial and cytoskeletal proteins related to neurochemical and metabolism endpoints.

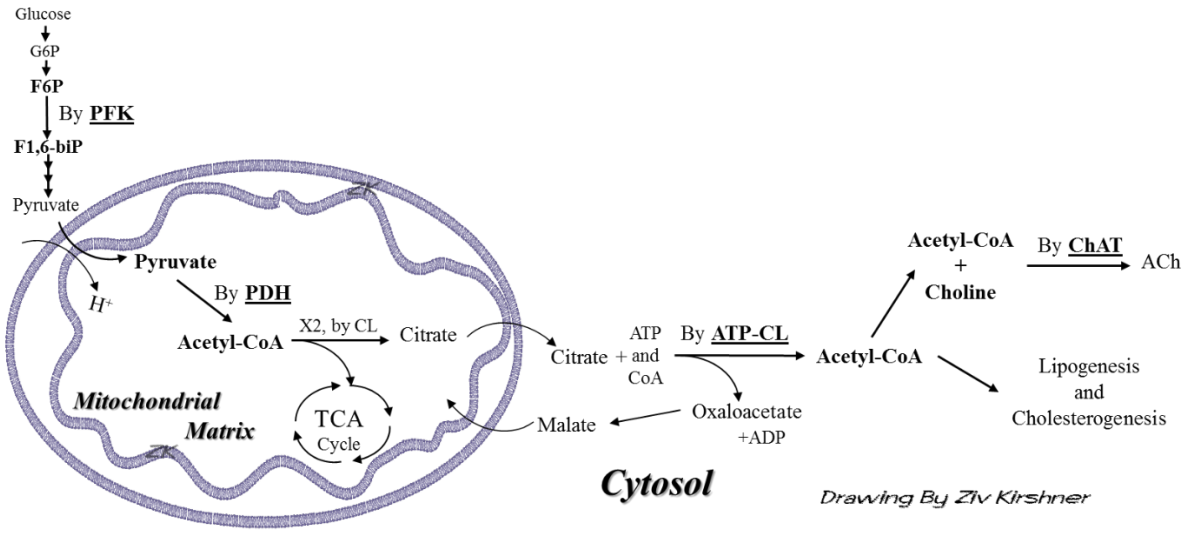

Figure 4: Illustration of metabolic pathways involve in glucose utilization, glycolysism cytosolic acetyl-coA production and acetylcholine production.

Effects of estrogen on energy and metabolism are mediated by multiple mechanism. The mitochondria expresses both ERα and ERβ, as well as the GPER-1 receptor, which collectively named mitochondrial estrogen receptors (mtERs) (Gazit et al., 2016). To modulate mitochondrial function, estrogens can act directly on glycolytic proteins inside the mitochondria (e.g. allosteric modulation of PDH), change mitochondrial gene expression, activate mtERs or induce indirect effects on mitochondrial functions by cytoplasmic or nuclear actions (Chen, Cammarata, et al., 2009; Rettberg et al., 2014; Velarde, 2014; Yang et al., 2004).

Estrogens also can profoundly affect the brain by influencing critical cellular and metabolic pathways (Brinton, 2008; Chen, Brown, & Russo, 2009; Lopez & Tena-Sempere, 2015; Mauvais-Jarvis et al., 2013). For example, estrogen regulates glucose uptake and utilization, mitochondrial ATP production and oxidative stress in the brain (Rettberg et al., 2014). In astrocytes, estrogens affect glucose sensing and anti-inflammatory activity (Fuente-Martin et al., 2013; Garcia-Caceres et al., 2016) and have sexually dimorphic effects on fatty acid oxidation and the production of

ketone bodies (Argente-Arizon, Guerra-Cantera, Garcia-Segura, Argente, & Chowen, 2017). In neurons, estrogens influence cellular bioenergetics and metabolic pathways with corresponding effects on ATP production which, in turn, can affect synaptic plasticity and neurotransmitter production (Brinton et al., 2015; Chen, Brown, et al., 2009). Androgens also affect cellular and metabolic pathways in the brain. For example, testosterone (T) increases pyruvate dehydrogenase (PDH) activity, increases Acetyl-CoA production, and enhances the TCA-cycle (Toro-Urrego, Garcia-Segura, Echeverria, & Barreto, 2016; Traish, Abdallah, & Yu, 2011; Vasconsuelo et al., 2013; Yan et al., 2017). Some of these effects are mediated, at least in part, by conversion of T to estradiol (Toro-Urrego et al., 2016). Following the loss of ovarian hormones, these mechanisms may mediate some of the metabolic changes seen in the brain of postmenopausal women. Thus, it is important to understand whether and how the loss of ovarian hormones (i.e., menopause) affects basic cellular and metabolic pathways in the brain.

In rats, mitochondrial dysfunction in the brain has been associated with age, age-related neuro-degenerative diseases and the shift in brain metabolism from glucose to ketone bodies. With age, there is increase in the levels of ROS and reductions in ATP production, glucose metabolism and in the activity of the mitochondrial electron transport chain. These changes are accompanied by an increase in the levels and utilization of ketone bodies in the brain, and increase in the gene expression for proteins involve in fatty acid oxidation and ketogenic pathways (Lejri et al., 2018). These bioenergetic changes were strongly correlated to increase hallmarks of Alzheimer's disease (AD) such as aggregation of beta-sheet and neurofibrillary tangles (Swerdlow & Khan, 2004) and were observed in women with AD (Brinton et al., 2015; Grimm, Mensah-Nyagan, & Eckert, 2016; Yao et al., 2012; Yao, Rettberg, Klosinski, Cadenas, & Brinton, 2011). Furthermore, the severity

of those changes has been correlated with cognitive impairments as well as progression of AD (Yao et al., 2009).

Age-associated changes to mitochondria and bioenergetics balance are exacerbated by the loss of ovarian estrogens and can be reversed by estrogen therapy. In rats, genes and activity of enzymes involved in glycolytic functions, as well as glucose uptake, were lower; whereas genes involved in fatty acid uptake and utilization were increased in both ovariectomized and irregularly cycling rats (Mosconi et al., 2017; Yao et al., 2012; Yin et al., 2015). These metabolic changes were correlated with lower levels of estrogen and reduced synaptic plasticity, which is a neuro-anatomical hallmark of cognitive performance (Mosconi et al., 2017). Effects of estrogen treatments on the protection of mitochondrial functions were also observed in clinical studies. For example, women receiving E2 or conjugated equine estrogens with progesterone had higher levels of glucose uptake than untreated women (Mosconi et al., 2009). Overall, estrogen treatments can moderate morphological changes, mitochondrial dysfunction and the increase in utilization of ketone-bodies associated with aging and the loss of ovarian function. These effects on energy and metabolism slowing or preventing the impact on specific neuronal circuits (e.g. cholinergic neurons) leading to the maintenance of cognitive functions (Russell et al., 2019). Yet, the mechanistic complexity, cell specificity and regional differences require a more selective approach to identify a selective regimen that can prevent cognitive decline based on age, how ovarian function was lost (e.g. surgical or transitional) and the duration of treatment.

1.5 Overview of Thesis

Our goal is to better understand how loss of circulating estrogens and estrogen replacement affect brain regions involved in cognitive processes. We selected pivotal proteins which are known to be modulated by estrogens and involve in metabolism, energy production, cytoskeleton andmarkers of cholinergic neurons. We first developed a multiplex methodology with normalization to total protein stain as a tool for measuring relative amounts of proteins (Chapter 2). We then to characterized the effects of surgical (ovariectomized, OVX) and transitional (ovatotoxin-treated, 4-vinylcyclohexene diepoxide, VCD) models of menopause as well as normally cycling animals in proestrus and diestrus stages (Chapter 3). In these studies, three regions of the brain were examined. The hippocampus because of its critical role in learning and memory consolidation. The frontal cortex because of its role in learning, attention, and cognitive performance. And the striatum because it is a major component of the extrapyramidal motor system and plays an important role in associative and motor learning. We then characterized the effects of treatment with estrogen or selective ER agonists (Chapter 4). These studies evaluated changes in three brain regions (HPC, FCX and STR) with both short- and long- term treatments (1- and 6- weeks). In Chapter 5, we co-localized GPER1 within orexin neurons in the lateral hypothalamus of rats. Orexinergic neurons project to basal forebrain cholinergic neurons and estrogen may act on orexinergic-GPER1 cells to mediate indirect effects on the cholinergic system. These themes are described in greater detail in the following chapters.

2.0 Development of a Normalization Method for Multiplex Fluorescence Western Blotting using Total Protein as a Loading Control

2.1 Use of the REVERT® total protein stain as a loading control demonstrates significant benefits over the use of housekeeping proteins when analyzing brain homogenates by Western blot: An analysis of samples representing different gonadal hormone states

Western blot is routinely used to quantify differences in the levels of target proteins in tissues. Standard methods typically use measurements of housekeeping proteins to control for variations in loading and protein transfer. This is problematic, however, when housekeeping proteins also are affected by experimental conditions such as injury, disease, and/or gonadal hormone manipulations. Our goal was to evaluate an alternative and perhaps superior method for conducting Western blot analysis of brain tissue homogenates from rats with distinct physiologically relevant gonadal hormone states. Tissues were collected from the hippocampus, frontal cortex, and striatum of young adult female rats that either were ovariectomized to model surgical menopause, or were treated with the ovatotoxin 4-vinylcyclohexene diepoxide (VCD) to model transitional menopause. Tissues also were collected from rats with a normal estrous cycle killed at proestrus when estradiol levels are high, and at diestrus when estradiol levels are low. Western blot detection of α-tubulin, β-actin, and GAPDH was performed and were compared for

sensitivity and reliability with a fluorescent total protein stain (REVERT®). Results show that the total protein stain was much less variable across samples and had a greater linear range than α-tubulin, β-actin, or GAPDH. The stain was stable and easy to use, and did not interfere with the immunodetection or multiplexed detection of the housekeeping proteins. In addition, we show that normalization of our data to total protein, but not to GAPDH, revealed significant differences in α-tubulin expression in the hippocampus as a function of treatment, and that gel-to-gel consistency in measuring differences between paired samples run on multiple gels was significantly better when data were normalized to total protein than when normalized to GAPDH. These results demonstrate that the REVERT® total protein stain can be used in Western blot analysis of brain tissue homogenates to control for variations in loading and protein transfer, and provides significant advantages over the use of housekeeping proteins for quantifying changes in the levels of multiple target proteins.

2.2 Introduction

Gonadal hormones affect the brain through a multitude of mechanisms involving all regions of the cell. Estradiol in particular has been shown to produce well-documented effects on cellular metabolism, synaptic plasticity, brain growth and development, neuronal maintenance and repair, sex and social behaviors, and learning and memory (Alexander, Irving, & Harvey, 2017; Brinton et al., 2015; Coyoy, Guerra-Araiza, & Camacho-Arroyo, 2016; Gibbs, 2010; Hansberg-Pastor, Gonzalez-Arenas, Pina-Medina, & Camacho-Arroyo, 2015; Heberden, 2017; Nguyen, Ducharme, & Karama, 2016; Vasconsuelo et al., 2013). These effects are mediated by estrogen

receptors (ERs) and correspond with changes in both gene and protein expression in specific regions of the brain.

Several methods are available to study changes in protein expression in brain. These include spectrometry methods such as HPLC and LC/MS; and also antibody-dependent methods such as enzyme-linked immunosorbent assay (ELISA), radioimmunoassay (RIA) and Western blot. Western blot evolved from northern blotting with the addition of electrophoretic transfer and the use of secondary antibodies to allow protein quantification by optical densitometry (Alwine, Kemp, & Stark, 1977; Renart, Reiser, & Stark, 1979). Further advances such as the acquisition of images using high dynamic range detectors (such as CCDs) and the use of fluorescently-labeled secondary antibodies have led to increased detection sensitivity, a broader linear range of signal quantification, and have enabled multiplex detection of multiple proteins simultaneously (Morseman, Moss, Zoha, & Allnutt, 1999; Poor, Santa, & Sittampalam, 1988; Sternberg, 1983). Quantitative Western blot became a common and well-established methodology as a result of being easy to perform, cost-efficient, and its ability to be used with a variety of visualization methods for quantifying relative amounts of protein.

A common practice in quantitative Western blot analysis is to normalize the intensity of bands representing target proteins to a house-keeping protein (HKP) that is present in high abundance and assumed to be unaffected by treatment. This controls for variations in loading and transfer that can affect band intensity and quantification. In studies involving estrogen regulation of proteins in the central nervous system, it is common practice to normalize target proteins to one of three HKPs, ß-actin, GAPDH, or α-tubulin.

To verify how common this is, we conducted a search of publications using the Pubmed advanced search engine to identify publications in which (a) circulating estrogens were

manipulated in rats or mice by either ovariectomy and/or estradiol treatment, and (b) Western blot methods were used to quantify changes in one or more target proteins in the brain. Our analysis was limited to 50 papers published in the last 4 years (2013-2017). The specific HKPs that were used to normalize Western blot data were noted and frequency of use was quantified. The results of this survey are summarized in Table 1. Of the 50 publications surveyed, 32 (64%) normalized target proteins to actin, 9 (18%) normalized to GAPDH, and 9 (18%) normalized to tubulin.

Studies have reported, however, that, in many tissues, these same HKPs are themselves targets of estrogen regulation (Hansberg-Pastor et al., 2015). This raises concerns about the use of HKPS in the estrogen field as normalization controls for Western blot analyses, and about the interpretation of data based on these methods.

An alternative approach is to use total protein (TP) staining in place of HKPs as an internal control. TP stain enables one to combine signal densitometry from all proteins in a defined MW range in order to represent the TP content. Some TP stains can be applied on a gel to represent amount of loaded protein; while some can be applied directly on polyvinylidene difluoride (PVDF) or nitrocellulose membrane. In each case, signal generated by the TP stain represents the whole-sample proteome. Therefore, any set of changes caused by hormonal manipulations will be proportional to the TP content and less variable between samples. Indeed, a number of studies have reported on the use of TP as a reliable loading control for Western blot quantification (Collins, An, Peller, & Bowser, 2015; Eaton et al., 2013; Gilda & Gomes, 2013; Moritz, 2017; Moritz, Marz, Reiss, Schulenborg, & Friauf, 2014; Rivero-Gutierrez, Anzola, Martinez-Augustin, & de Medina, 2014; Romero-Calvo et al., 2010; Taylor, Berkelman, Yadav, & Hammond, 2013; Welinder & Ekblad, 2011; Zeng et al., 2013). Despite these advantages and the lack of a reliable HKP, normalization by TP stain has not yet been evaluated as a suitable loading control for protein

quantification in brain samples obtained at different stages of the estrus cycle or following other gonadal or hormonal manipulations.

Here we evaluated the REVERT® (LI-COR, Inc) TP stain as an internal control in Western blot analyses. This was compared with commonly used HKPs to quantify changes in the levels of target proteins in the brains of rats being used to model surgical vs. transitional menopause, as well as in tissues collected at proestrus and diestrus.

Our results demonstrate significant benefits of using TP to normalize loading when quantifying protein levels by Western blot. In addition, we detected significant effects of menopausal model on HKPs, but not TP, and show that these differences are of sufficient magnitude to alter conclusions about effects of ovarian manipulations on protein expression. We conclude that the described TP stain is a more reliable and precise method than the alternative of using a single common HKP as an internal control when evaluating effects of hormone manipulations on target proteins in the central nervous system.

Table 1: Housekeeping proteins used in publicly available Western blot data in which circulating estrogens were manipulated in rats or mice by either ovariectomy and/or estradiol treatment, and changes in one or more target proteins in the brain were quantified.

Year	DOI	HKP Used	Reference
2017	10.1016/j.brainres.2017.02.004	GAPDH	(Z. L. Zhang et al., 2017)
2017	10.1080/01616412.2016.1252875	actin	(Bernal-Mondragon et al., 2017)
2017	10.1242/bio.021022	actin	(Guo, Deng, Bo, & Yang, 2017)
2017	10.1111/jne.12429	actin	(Black, Witty, & Daniel, 2016)
2017	10.18632/oncotarget.19768	actin	(Fan, Li, Wang, Zhong, & Cui, 2017)
2017	10.1159/000475433	actin	(L. Li et al., 2017)
2017	10.1016/j.jsbmb.2017.05.001	actin	(Jover-Mengual et al., 2017)

Year	DOI	HKP Used	Reference
2017	10.1016/j.jns.2017.02.034	actin	(Y. Zhang, Huang, Wang, Wang, & Wang, 2017)
2017	10.1002/jcp.26083	GAPDH	(Lu, Ma, Jin, Zhu, & Cao, 2018)
2017	10.1016/j.brainres.2017.02.006	GAPDH	(Tulsulkar, Ward, & Shah, 2017)
2017	10.1016/j.neuroscience.2016.12.025	GAPDH	(S. Kumar, Singh, Singh, Goswami, & Singru, 2017)
2017	10.1016/j.ygcen.2016.12.004	actin	(de Jesus et al., 2017)
2017	10.1080/01616412.2016.1250459	actin	(Vahidinia et al., 2017)
2016	10.1007/s12035-016-0155-1	tubulin	(Candeias et al., 2016)
2016	10.1007/s12031-016-0785-9	actin	(Yazgan, Yazgan, Ovey, & Naziroglu, 2016)
2016	10.1210/en.2016-1197	actin	(Grissom & Daniel, 2016)
2016	10.1515/hmbci-2016-0008	GAPDH	(Govindaraj & Rao, 2016)
2016	10.1016/j.bbr.2016.01.009	actin	(De Jesus-Burgos, Gonzalez-Garcia, Cruz-Santa, & Perez-Acevedo, 2016)
2016	10.1016/j.mce.2015.11.015	tubulin	(Sa, Fonseca, Teixeira, & Madeira, 2016)
2016	10.1016/j.bbi.2015.11.013	actin	(Hwang et al., 2016)
2016	10.1111/ejn.13121	GAPDH	(Graham, Gardner Gregory, Hussain, Brake, & Pfaus, 2015)
2015	10.18632/oncotarget.5433	actin	(Rao, Shults, Pinceti, & Pak, 2015)
2015	10.1016/j.lfs.2015.09.013	GAPDH	(Radhika, Govindaraj, Sarangi, & Rao, 2015)
2015	10.1159/000437268	actin	(Benmansour, Adeniji, Privratsky, & Frazer, 2016)
2015	10.1016/j.neuroscience.2015.04.049	tubulin	(Shrestha & Briski, 2015)
2015	10.1016/j.npep.2015.02.001	tubulin	(Alenazi, Ibrahim, & Briski, 2015)

Year	DOI	HKP Used	Reference
2015	10.1016/j.bbr.2015.03.003	actin	(Wibowo, Calich, Currie, & Wassersug, 2015)
2015	10.1016/j.brainres.2015.02.001	tubulin	(Del Bianco-Borges & Franci, 2015)
2015	10.1111/febs.13207	tubulin	(Sa, Fonseca, Teixeira, & Madeira, 2015)
2014	10.1186/s12974-014-0171-x	actin	(Cunningham et al., 2014)
2014	10.1111/jnc.12998	actin	(Xu, Gu, & Shen, 2015)
2014	10.1016/j.brainres.2014.09.013	actin	(J. Li et al., 2014)
2014	10.1016/j.neulet.2014.08.045	actin	(Koh, 2014a)
2014	10.1016/j.brainres.2014.07.003	tubulin	(Lima, Ota, Cabral, Del Bianco Borges, & Franci, 2014)
2014	10.1016/j.exger.2014.07.018	actin	(Moran, Garrido, Cabello, Alonso, & Gonzalez, 2014)
2014	10.1371/journal.pone.0102194	actin	(Zeynalov, Rezvani, Miyazaki, Liu, & Littleton-Kearney, 2014)
2014	10.1016/j.psyneuen.2014.03.016	actin	(Y. C. Wu, Du, van den Buuse, & Hill, 2014)
2014	10.1016/j.neulet.2014.05.006	actin	(Koh, 2014b)
2014	10.1371/journal.pone.0096232	tubulin	(Mori, Matsuda, Yamawaki, & Kawata, 2014)
2014	10.1161/STROKEAHA.113.001499	actin	(Broughton et al., 2014)
2014	10.1016/j.neulet.2013.11.007	actin	(Cai et al., 2014)
2014	10.1007/s00213-013-3310-7	actin	(Nelson, Springer, & Daniel, 2014)
2013	10.1523/JNEUROSCI.2001-13.2013	GAPDH	(W. W. Wu, Bryant, Dorsa, Adelman, & Maylie, 2013)
2013	10.1186/1471-2202-14-104	GAPDH	(Bernal-Mondragon, Rivas-Arancibia, Kendrick, & Guevara-Guzman, 2013)
2013	10.1016/j.jsbmb.2013.07.007	tubulin	(Dietrich, Humphreys, & Nardulli, 2013)

Year	DOI	HKP Used	Reference
2013	10.1210/en.2013-1235	actin	(Mahavongtrakul, Kanjiya, Maciel, Kanjiya, & Sinchak, 2013)
2013	10.1101/lm.026732.112	actin	(Fortress, Fan, Orr, Zhao, & Frick, 2013)
2013	10.1016/j.exger.2013.02.010	actin	(Moran, Garrido, Alonso, Cabello, & Gonzalez, 2013)
2013	10.1016/j.bbrc.2013.02.117	actin	(Wada-Kiyama et al., 2013)
2013	10.1210/en.2012-1698	actin	(Witty, Gardella, Perez, & Daniel, 2013)

2.3 Materials and Methods

2.3.1 Ethics statement

All procedures were carried out in accordance with PHHS policies on the use of animals in research, and with the approval of the University of Pittsburgh's Institutional Animal Care and Use Committee.

2.3.2 Animals

Young adult (3mo old) female Sprague-Dawley rats were purchased from Harlan Sprague-Dawley Laboratories, Inc. Rats were housed individually with free access to food and water, and maintained on a 12-hr light/dark cycle.

2.3.3 **Experimental design and treatments**

Rats were randomly assigned to one of four groups, proestrus (P), diestrus (D), 4-vinylcyclohexene diepoxide (VCD)-treatments and ovariectomy (OVX). Regularly cycling animals underwent daily vaginal smears to assess cycle stage (Goldman, Murr, & Cooper, 2007). Rats were euthanized on proestrus (n=8) or diestrus (n=7) and brain tissues were collected. Additional rats were used to model surgical and transitional menopause. Transitional menopause was modeled by administering daily injections of the ovatotoxin VCD at 80 mg/kg diluted in sesame oil at a volume of 2.5 µl/g body weight for 30 days (n=16). This regimen has been shown to destroy >95% of primary ovarian follicles with little toxicity to stromal cells or to other organs, and no other lasting toxic effects (Hoyer, Devine, Hu, Thompson, & Sipes, 2001; Muhammad et al., 2009; Van Kempen et al., 2014; Van Kempen, Milner, & Waters, 2011). An additional group of intact rats underwent daily vehicle injections of sesame oil. After 30 days of injection, the vehicle-treated rats underwent bilateral ovariectomy (OVX). Ovariextomy was conducted in-house using a lateral approach. Rats were anesthetized with ketamine (70 mg/Kg) and xylazine (14 mg/Kg). An incision was made and the apical tip of the uturus and ovaries were exposed. The apical tip of the uterus was tied off with 6-0 suture silk and the ovaries removed. The peritoneum was then sutured shut with 6-0 suture silk and the skin closed with two 9 mm suture clips. Rats that had received 30-days VCD treatment underwent a sham surgery which included anesthesia and the abdominal incisions, but no removal of the ovaries. Animals were placed onto a warm heating pad during recovery. Ketofen (3mg/Kg, i.p.) was administrated twice per day for three days to reduce discomfort. Topical antibiotic ointment was applied for 3-days to prevent infection. At 1 or 6 weeks following surgery, rats were euthanized with an overdose of ketamine (280 mg/kg)

and xylazine (56 mg/kg) and tissues were collected for analysis. This resulted in a total of 6 treatment groups: P, D, Ovx-1W, Ovx-6W, VCD-1W, and VCD-6W.

2.3.4 **Collection of Tissues**

Rats were anesthetized and decapitated. Brains were rapidly removed and dissected on an ice-cold petri dish. Tissues from the hippocampus (HPC), striatum (STR), and frontal cortex (FCX) were collected and snap frozen on dry ice. Serum was also collected and stored at –200C for quantification of hormone levels.

2.3.5 **Analysis of Hormone Levels by UPLC-MS-MS**

Serum levels of 17β-estradiol (E2), testosterone (T) and androstenedione (AD) were quantified by UPLC-MS/MS as described (J. Li, Oberly, Poloyac, & Gibbs, 2016). Briefly, for E2 analysis, samples were spiked with internal standard 25 µl 2,4,16,16,17-d5-17 beta-estradiol (1 ng/ml in methanol). After extraction samples were derivatized with dansyl chloride. E2 was eluted using a Waters Acquity UPLC BEH C18, 1.7 µm, 2.1 X 150 mm reversed-phase column, with an acetonitrile: water (0.1% formic acid) gradient. MS detection and quantification were achieved in the positive mode with a Thermo Fisher TSQ Quantum Ultra mass spectrometer interfaced via an electrospray ionization (ESI) probe with the Waters UPLC Acquity solvent delivery system. Transitions used for analysis were 506 → 171 for E2, and 511 →171 for the deuterated internal standard. Area under the peak was quantified and used to determine absolute levels of E2/mL of sample by comparison with a series of standards.

Testosterone (T) and Androstenedione (AD) levels were quantified by a modification of the method described by Cawood (Cawood et al., 2005) and using methods similar to the quantification of E2 described above. Briefly, samples were spiked with 0.25 ng/ml D3-testosterone or D7-androstenedione as the internal standard. T and AD was eluted from the same column as E2, with a methanol:water (0.1% formic acid and 2 mM ammonium acetate) gradient from 50 to 85% methanol. Transitions used for T analysis were 289 → 97 for T and 292 → 97 for the deuterated T; transitions used for AD analysis were 287→ 100 for AD and 294 → 100 for the deuterated AD. The lower limits of detection were 2.5 pg/mL for E2 and 10.0 pg/mL for T and AD.

2.3.6 **Processing and Analysis of Brain Tissues Samples**

Brain tissues were thawed in freshly-prepared cold lysis buffer (10 µl buffer per 1 µg tissue) containing: 1% protease inhibitor cocktail, 0.5% Sodium deoxycholate, 0.001M ethylenediaminetetraacetic acid (EDTA), 0.15M NaCl, 0.01M Sodium fluoride, 0.1% Sodium dodecyl sulfate (SDS), Tris-HCl (50mM, pH=7.4), 0.001M Sodium orthovanadate (Na3VO4) and 0.001M phenylmethylsulfonyl fluoride (PMSF). All reagents were purchased from Sigma-Aldrich. Samples were then sonicated at 4˚C 6 times at 30-seconds ea. for total of 3-minutes. An aliquot of each sample was used to determine protein concentration by Bradford assay (Bradford, 1976).

2.3.7 **SDS-PAGE**

Samples were diluted to 2.4 µg/µl in sonication buffer mixed with an equal volume of 2X Laemmli Sample Buffer (BIO-RAD Cat#1610737) containing 5% (v/v) 2-mercaptoethanol.

Samples were then heated to 98˚C for 7-minutes. Samples were loaded onto commercially-prepared 12% Mini-PROTEAN® TGX™ gels. Samples were loaded at a volume of 10 µl per lane to achieve a total of 12 µg protein per lane. This loading concentration was confirmed to ensure that signals from each of our targets fell within their linear detection range. In addition, for each brain region, a dilution series was generated using a mixture of homogenates containing twenty samples to equally represent each of our animal models. The combined mixture was used to test and compare the range for linear detection and quantification of TP and individual targets. The Chameleon 700 pre-stained protein ladder (LI-COR) was included on all gels. Samples were run for 2-hours at 100 V using a running buffer containing: 25 mM Tris-HCL, 192 mM glycine and 0.1% SDS. Upon completion of the run, samples were transferred (2-hr, 100 V, 4˚C) to Immobilon FL PVDF membrane (Millipore) using a transfer buffer (25 mM Tris-HCl, 192 mM glycine, 10% v/v methanol, pH 8.3).

2.3.8 **Total Protein Membrane Stain**

After transfer, PVDF membranes were directly stained for TP detection using LI-COR REVERT™ Kit according to the manufacturer's instructions. Briefly, membranes were submerged in REVERT for 5 minutes, washed 2X for 30 seconds each with wash solution (LI-COR, 6.7% (v/v) glacial acetic acid, 30% (v/v) methanol, in water) and imaged immediately. Membranes were scanned using the 700 nm channel of the Odyssey® imaging system (LI-COR) at a scanning resolution of 169 µm and a 'normal' image quality setting. TP stain was then removed by 5 minutes incubation in reversal solution (LI-COR, 0.1 M sodium hydroxide, 30% (v/v) methanol, in water) with gentle shaking and then imaged again to verify that no residual signal remained.

Membranes were than blocked for 1 hour at room temperature in Odyssey® TBS blocking buffer (LI-COR, 927-50000) and incubated overnight at 4˚C with mixture of primary antibodies: against α-tubulin (Abcam, ab52866, rabbit monoclonal anti-α-tubulin, 1:5000), β-Actin (Abcam, ab6276, mouse polyclonal anti-β-actin, 1:5000), and GAPDH (Abcam, ab181602, rabbit polyclonal anti-GAPDH, 1:5000).

The next morning, membranes were washed 3X for 10 min each with TBS-T (50 mM Tris-HCL at pH=7.4, 150 mM NaCl and 0.1% Tween-20) and incubated for 1 hr at room temperature in TBS-T containing secondary antibodies of goat anti-mouse IgG (LI-COR IRDye 800CW, cat#32210) and goat anti-rabbit IgG (LI-COR IRDye800CW, cat#32211) each at 1:5,000 dilution.

2.3.9 **Image Acquisition and Data Analysis**

All PVDF-membranes were analyzed using the Odyssey application software (Ver 3.0.30) by acquiring integrated intensity values of defined bands. Densitometry of single-band targets (e.g. GAPDH) were measured in a rectangular area automatically defined by the software. Manual adjustments were made to contain all detectable signal for a band and background was subtracted using the software's averaging protocol. Signal from the TP stain was measured in accordance with manufactures protocol by manually applying a rectangular area at a select range of molecular weights (e.g.50-90KDa; see below). For comparison of samples on the same gel, relative quantification was achieved by normalizing each target to the value of either TP or to an individual HKP. In some cases these ratios were then normalized to an average of the same target from proestrus animals on the same gel, to facilitate between-gel comparisons.

All linear ranges of quantification were obtained by graphing integrated intensities of serial dilutions and choosing a range of dilutions with the highest linearity represented by least-squares analysis.

2.3.10 Analysis of the consistency of TP densitometry across different molecular ranges

The TP stain produced bands of varied intensities depending on loading and molecular weight. Signals for specific molecular weight ranges were analyzed for consistency. The following ranges were evaluated: 30-160KDa, 15-160KDa, 30-90KDa, 30-50KDa, 50-160KDa and 50-90KDa. Signal consistency for each range was determined by calculating the percent coefficient of variation (%CV). Samples representing each of the treatment groups were loaded onto the same gel (total n=12; OVX (n=4), VCD-treated (n=4), diestrus (n=2), proestrus (n=2); each at 12 µg/lane). The %CV was calculated for the mean of all 12 samples per gel for each of 2 gels.

2.3.11 Analysis of the consistency of the signals for each of the HKPs vs TP

Analysis of the consistency of the HKP signals across treatment groups was evaluated similarly to above. Samples representing each of the treatment groups were loaded onto the same gel (12/gel). %CV for each of the HKPs and for TP was calculated from the same membrane by multiplexing images. This experiment was repeated twice per brain region.

2.3.12 Statistical comparison of normalizing to GAPDH vs TP when evaluating effects on α-tubulin

Evidence for effects of ovarian status on α-tubulin was detected. We therefore set out to test whether the effects were significantly different when data were normalized to TP vs. the commonly used HKP GAPDH. Densitometry data for α-tubulin was normalized to GAPDH and separately to TP using values obtained simultaneously from the same PVDF membrane. This was repeated twice. Differences between proestrus and diestus were evaluated by two-tailed T-test. In addition, differences among all 6 groups were evaluated by one-way ANOVA. Statistical comparisons were conducted using JMP Pro software (SAS, version 13.0.0) and statistical significance was defined as $p < 0.05$.

2.4 Results

2.4.1 Hormone levels

Serum levels of E2, T and AD are summarized in Table 1. As expected, levels of all three hormones were significantly higher at proestrus than at diestrus (E2: $t(13)=7.14$, $p<0.0001$; T: $t(13)=2.91$, $p<0.02$; AD: $t(13)=3.38$, $p<0.005$). Following ovariectomy, the levels of all three hormones were below the levels of detection. In rats treated with VCD, levels of E2, T, and AD were significantly lower than levels detected in proestrus rats ($p<0.05$ in all cases), and did not differ significantly from levels detected in diestrus rats. However, levels of both androgens were much higher than detected in Ovx rats. This was the case at both 1-w and at 6-w following the

completion of VCD treatments. This is consistent with the selective depletion of ovarian follicles and the preservation of surrounding interstitial cells following VCD treatment (Acosta et al., 2009; Koebele et al., 2017; Mayer, Devine, Dyer, & Hoyer, 2004; Mayer, Dyer, Eastgard, Hoyer, & Banka, 2005; Van Kempen et al., 2011).

Table 2: Summary of Serum hormone levels in cycling, ovariectomized and VCD-treated rats

Hormone	Proestrus [pg/ml]	Diestrus [pg/ml]	OVX-1 [pg/ml]	OVX-6 [pg/ml]	VCD-1 [pg/ml]	VCD-6 [pg/ml]
	n=8	n=7	n=7	n=7	n=8	n=8
17β-Estradiol	52.6±4.5	16.3±1.7*	-	-	16.4±7.6**	8.0±4.9**
Testosterone	210.5±41.8	78.8±6.4*	-	-	88.2±46.5**	66.0±19.7**
Androstenedione	220.9±40.8	71.5±6.6*	-	-	87.3±31.8**	55.7±16.3**

Values indicate mean ± SEM. Hyphen mark values below detection limit and asterisks shows significant difference from proestrus. * $p<0.02$, two-tailed t-test. ** $p<0.001$, one-way ANOVA.

2.4.2 Consistency of the REVERT® TP stain across samples and for different ranges of molecular weight

Analysis of the consistency of the TP signal across treatment groups for different ranges of molecular weight are summarized in Figure 5. TP staining produced a consistent densitometry pattern with higher optical density in areas where more proteins are present (Fig 5A). The lowest fluorescence intensity was in the range between 50 to 90 KDa while the widest range (15 to 160 KDa) produce approximately 3.5X more signal (Fig 5B). Regardless of these differences the %CV for each MW range fell between 5.22% and 6.17% (Fig 5C). Highest variability was observed in the 30 to 160 KDa range while lowest variability was observed in the 50 to 90 KDa range (e.g.

signal from proteins below 50 KDa and above 90 KDa had high variability with impact on the selected Mw range). These values remained consistent regardless of treatment (not shown). Thus, all subsequent analyses used the MW range of 50-90 KDa for normalizing targets to TP.

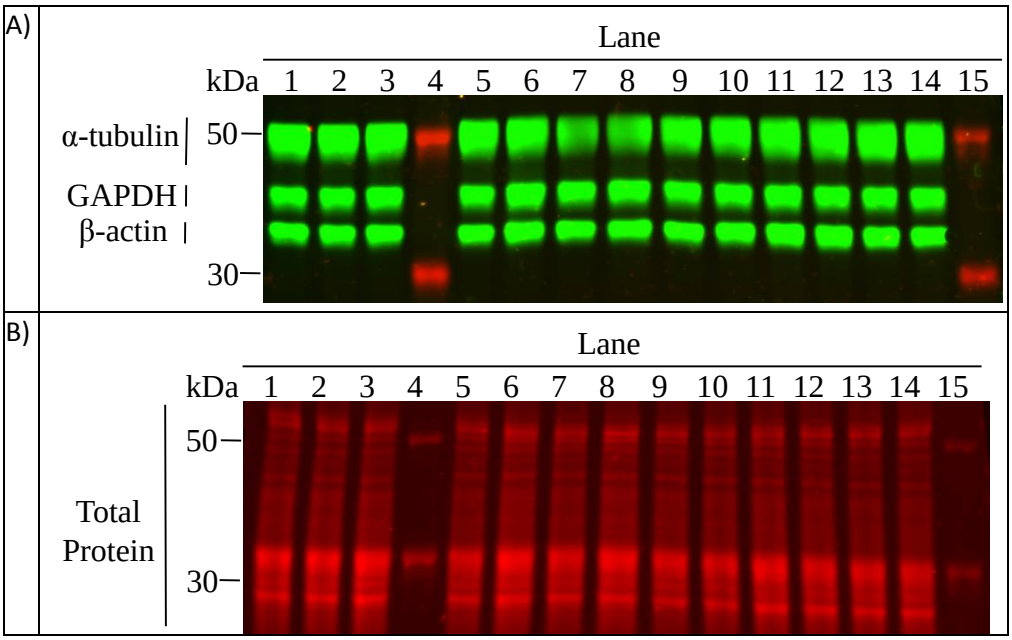

Figure 5: Fluorescence signal densitometry of TP stain is less variable than individual HKPs. (A) representative image of PVDF membrane with different bands of individual HKPs (green): GAPDH (36KDa), β-actin (42KDa) and α-tubulin (50KDa); and (B) a TP stain produced on the same membrane (red). Note the apparent consistency in TP signal across lanes loaded with different samples (12µg-protein/lane).

A)

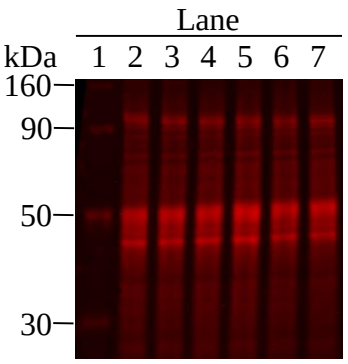

B)

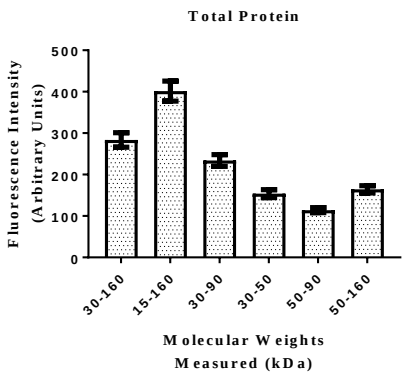

C)

MW Range (KDa)	30-160	15-160	30-90	30-50	50-90	50-160
%CV	6.17%	6.04%	6.03%	6.10%	5.22%	5.34%

Figure 6: Comparative analysis of the variability in TP signal across different ranges of MW for samples of regional brain homogenates. (A) Image of PVDF membrane showing TP stain of six different hippocampal homogenates for MWs ranging from 30-160 KDa. (B) Analysis of fluorescence intensity for different ranges of molecular weight from 12 samples run on a single gel (not shown). Bars represent the mean fluorescence intensity ± SEM for each MW range. (C) %CV calculated from the same 12 samples summarized in B. Note the consistent and low variability in TP measurements across multiple MW ranges.

2.4.3 **Comparison of the linear dynamic range for measuring TP vs. HKPs**

Figure 6 shows an image of TP and HKPs detected in lanes loaded with different amounts of protein. Linear dynamic range was evaluated by plotting fluorescence intensity vs. protein loading. To avoid possible bias associated with treatment, twenty samples were selected across all treatment groups and were combined. This was done for each brain region. These combined samples were then loaded at concentrations ranging from 0.5 to 80 µg protein per lane. Results obtained from all three brain regions were similar. Representative graphs are shown in Figure 6. For TP, signal remained linear across a wide range from 0.5 to 40 µg/lane (Fig 6D, $R2>0.98$). In comparison, the effective linear range for the three HPKs was much more limited. GAPDH: 5 to 15 µg/lane (Fig 6E, $R2=0.93$); β-actin: 5 to 25 µg/lane (Fig 6F, $R2=0.91$); α-tubulin: 2 to 25

µg/lane (Fig 6G, R2>0.97). Based on these data, lanes were loaded with 15 µg protein for all subsequent analyses.

2.4.4 **Analysis of the consistency of TP vs. HKP staining**

The consistency of TP staining vs. staining for each of the HKPs was evaluated and compared for each of the three brain regions (Table 3, Fig 4). Note that the values represent %CV for data collected across all treatment groups. Data show that %CV for TP staining was substantially less than the %CV for each of the HKPs, regardless of brain region. In most cases, %CV for the HKP was 2-5X the %CV for TP staining. This is consistent with the supposition that levels of HKPs are affected by changes in ovarian status, thus resulting in greater variability when data are combined across treatment groups. The fact that variability for TP staining was very consistent across treatment groups supports the suitability of using TP rather than HKPs for normalization.

Table 3: Summary of calculated %CV for quantification of TP and individual HKPs

Brain Region	Gel 1				Gel 2			
	TP	GAPDH	β-actin	α-tubulin	TP	GAPDH	β-actin	α-tubulin
FCX	5.43%	16.71%	20.21%	9.54%	5.22%	27.51%	14.12%	18.87%
STR	7.37%	34.82%	31.08%	28.22%	11.10%	40.20%	36.09%	49.48%
HPC	7.84%	32.03%	20.74%	17.01%	13.03%	39.60%	30.20%	17.69%

Data obtained from multiplexing densitometry of TP, GAPDH, β-actin and α-tubulin signals from 2 gels. For each target, the %CV was calculated from 12 samples/gel representing OVX (n=4), VCD (n=4), diestrus (n=2) and proestrus (n=2). Note that %CV is consistently lower for measurements of TP vs. each of the HKPs.

2.4.5 **Effects of treatment on relative levels of α-tubulin**

Based on the supposition that HKPs can be affected by changes in ovarian status, we evaluated differences in relative levels of α-tubulin as a function of treatment. In addition, we compared results obtained by normalizing the α-tubulin data to TP vs. GAPDH. The results are summarized in Figure 7. After normalizing to TP, a significant increase in α-tubulin was detected in the HPC of VCD-treated rats relative to levels at proestrus (Fig 7A; $F(5,20)=4.62$, $p<0.006$). This effect was observed at both 1-week and 6-weeks following VCD treatment. In contrast, analysis of these same data normalized to GAPDH produced no significant effect (Fig 7B; $F(5,20)=2.63$, $p=0.055$). No significant effects of VCD treatment on α-tubulin were detected in the STR or FCX regardless of normalization (not shown). Hence the effect of VCD treatment on α-tubulin was region specific, and was detected only when data were normalized to TP and not to GAPDH.

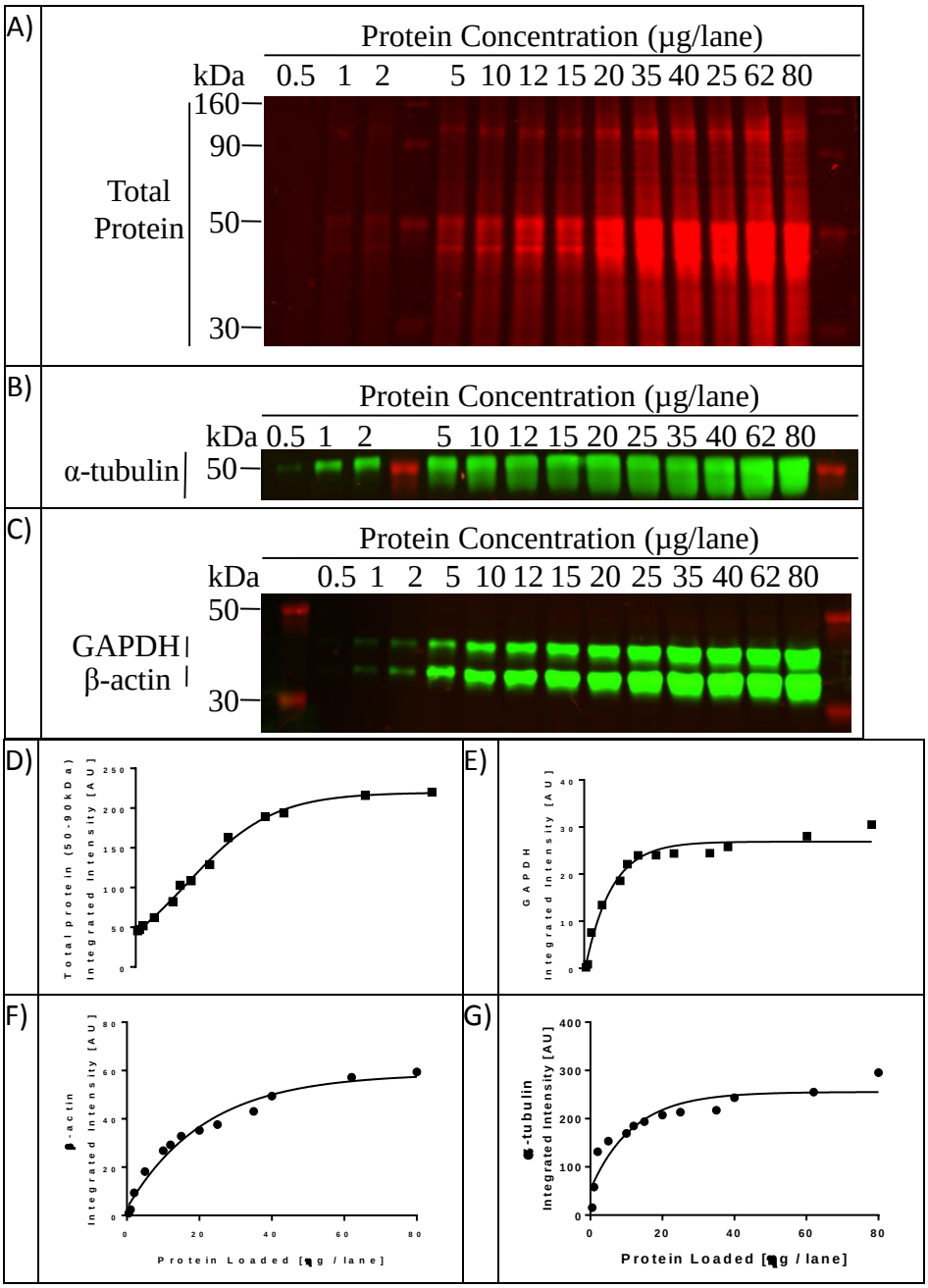

Figure 7: Analysis of linear range of detectability for TP and each HKP. Representative images of PVDF membranes stained with total-protein (A) and three HKPs (B,C) in a serial dilution of regional rat brain homogenates ranging from 0.5 µg to 80 µg per lane. (D-G) Graphs showing densitometric analysis. Lines show least-squares best fit across all points. For each curve, a dynamic range for quantification was defined by choosing the linear portion of the curve that yields the highest correlation. For example, note the rapid saturation of α-tubulin signal at 25µg/lane and the limited linear range of GAPDH (5 to 15 µg/lane) and β-actin (5 to 25 µg/lane). In contrast, REVERT® TP signal had a much wider linear range (0.5 to 40 µg/lane).

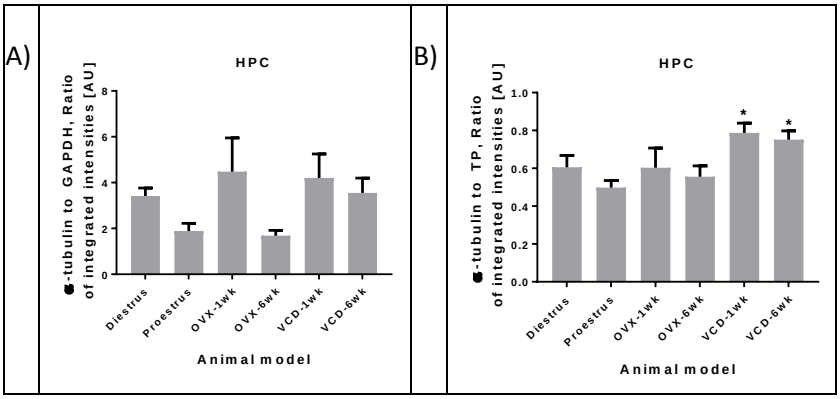

Figure 8: Effect of VCD treatment on α-tubulin expression in the HPC. Bars represent the mean ratio of integrated intensities ± SEM from n=5 per group. (A) Data normalized to GAPDH. (B) Same data normalized to TP. Note significant increase in b-Tubulin detected in VCD-treated rats relative to proestrus in (B). In contrast, no significant effect was detected in (A). *p<0.05 relative to proestrus by one-way ANOVA.

2.4.6 **Reproducibility of results across gels**

A concern in Western blot analysis is the reproducibility of results and the ability to combine results obtained from different gels. While signal intensity can vary greatly from gel-to-gel, it should be the case that the measurement of relative levels of a target protein in two different samples should be relatively consistent from one gel to another. We predicted that the gel-to-gel variability in such measurements would be lower when targets are normalized to TP than when normalized to an HKP. To test this, we used our existing data set and identified pairs of samples that were run on the same gel on at least two separate occasions. We identified a total of 32 samples, serving as 16 pairs from different treatments. For each pair, within the same gel, the percent difference between samples was calculated twice: once normalized to TP (100*[(Sample 1/TP) – (Sample 2/TP)]/(Sample 1/TP)), and once normalized to GAPDH (100*[(Sample

1/GAPDH) – (Sample 2/GAPDH)]/(Sample 1/GAPDH)). Identical calculations were made for the same pair of samples on a second gel (Table 2).

To compare the reliability of the two normalization procedures we calculated the intraclass correlation coefficients (ICCs) for the same 16 pairs when normalized by TP or by GAPDH. These ICC values reflect the variation of our data by each normalization method. The intraclass correlation coefficients were calculated using the reliability analysis platform on IBM SPSS Statistics Software Version 25. ICCs models were defined as two-way mixed effects, absolute agreement with multiple raters and 95% confidence interval. The calculated ICC value for samples normalized to TP was 0.892 (i.e., excellent reliability) while the calculated ICC value for samples normalized to GAPDH was 0.215 (i.e., poor reliability).

To determine whether the two calculated ICC values differ significantly, we used the Konishi–Gupta modified Z-test (TZ) where the null hypothesis H0 is that two ICCs are equal (Donner & Zou, 2002; Konishi, 1985; Konishi & Gupta, 1987). Our TZ test was calculated using raters values of k1=k2=2, intraclass estimates of r1A and r2A were substitutes with $\rho 1=1.26$, $\rho 2=0.29$ correspondingly and an inter class $\rho 12=0.44$. The final approximation to the Fisher's Z-transformation was TZ=TZM=2.83 with proportions of TZ >1.65 showing significance at $p<0.05$ level where H0 is rejected. We also compared our ICC Cronbach alpha values by a second method of Diedenhofen and Musch (Diedenhofen & Musch, 2016). The correlation between our underlying scores of the Cronbach alphas (0.95 and 0.50) was 0.2 and applied to the on-line web interface based on R-code resulting in $\chi 2= 4.6$, df=1 and $p<0.05$ level where H0 is rejected.

Thus, the ICC value obtained when data were normalized to TP was in the excellent reliability range (0.892) and differed significantly from the ICC valuate obtained when data were normalized to GAPDH (0.215).

Table 4: Reproducibility of α-tubulin expression data between pairs of samples when normalized by either TP or GAPDH.

Pair	TP Gel 1	TP Gel 2	GAPDH Gel 1	GAPDH Gel 2
1	1.22	1.08	0.78	1.01
2	1.35	1.32	1.40	1.35
3	1.13	1.03	1.42	1.09
4	1.22	1.06	1.67	1.35
5	1.42	1.11	1.61	1.16
6	1.11	1.03	1.10	1.15
7	1.43	1.12	1.56	1.25
8	0.78	0.61	1.17	0.75
9	1.31	1.25	1.54	1.20
10	0.37	0.50	1.36	1.11
11	1.33	1.27	1.30	1.35
12	0.98	0.90	1.26	0.80
13	0.98	1.01	1.46	1.18
14	1.17	1.03	1.61	1.10
15	1.41	1.35	1.37	1.44
16	1.14	1.12	1.21	1.16

Each number represents a ratio of sample 2 to sample 1 for each pair of samples analyzed on each of two gels. Data normalized to TP and (columns 2 & 3) and to GAPDH (columns 4 & 5). Data were analyzed for intra-class correlation coefficient as described in section 3.6.

2.5 Discussion

Our goal was to evaluate an alternative method for conducting Western blot analysis of brain homogenates from rats with distinct physiologically relevant gonadal hormone states. To accomplish this, experimental groups included models of surgical (OVX) and transitional (VCD-treated) menopause, and tissues from normal cycling rats collected at proestrus and at diestrus. Hormone measurements confirmed significantly higher serum levels of E2, T, and AD on proestrus than on diestrus and undetectable levels of all three hormones in OVX rats. In VCD-treated rats, E2 levels were undetectable which is consistent with the loss of ovarian follicles. In contrast, levels of T and AD were elevated compared with diestrus, consistent with the continued presence of ovarian interstitial cells which produce androgens (Mayer et al., 2004). These data are consistent with prior validations of this model (Koebele et al., 2017; Mayer et al., 2004; Mayer et al., 2005; Wright et al., 2008) and confirm that we successfully produced an array of physiologically relevant gonadal hormone conditions with which to evaluate the methodology.

Results show that direct application of the REVERT™ TP stain to PVDF membranes containing samples from the HPC, STR and FCX produced a stable fluorescence signal, with low variability and a wide linear range (0.5-40 µg/lane). In comparison, the linear range for quantification of GAPDH, ß-actin, or α-tubulin was much more limited. In addition, the TP signal across several ranges of molecular weights produced lower coefficients of variation (%CV) than individual HKPs. The higher variability in the HKP signals across treatments is consistent with literature showing that these HKPs can be affected by gonadal hormone status (discussed below). The impact of these findings is made evident by the observation that normalization of our data to TP, but not to GAPDH, detected significant differences in α-tubulin expression in the HPC as a function of treatment. Finally, we showed that gel-to-gel consistency in measuring differences

between paired samples run on multiple gels was significantly better when data were normalized to TP than when normalized to GAPDH. These findings are consistent with other recent reports describing the benefits of TP stains for normalizing Western blot analysis of rodent samples of other tissues including cerebrospinal fluid (Collins et al., 2015), sciatic nerve (Eaton et al., 2013), and liver (Rivero-Gutierrez et al., 2014). Our data extend these findings by demonstrating the utility of the REVERT® TP stain in Western blot analysis of brain tissues from rats of varying gonadal hormone status.

2.5.1 **Evidence that HKPs are affected by gonadal hormone status**

The fact that relatively high variability in HKP measurement was observed across treatment groups is not surprising given the many studies that have demonstrated significant regulation of housekeeping genes by gonadal hormones in a variety of tissues. For example, differences in the expression of GAPDH, actin and tubulin mRNAs were reported in samples from brain and other tissues of males vs. females, in obesity models, and in ovariectomized rats with and without estrogen treatment (B. Li et al., 2014; Liu & Xu, 2006; Martinez-Beamonte et al., 2011; Schroder, Pelch, & Nagel, 2009; Taki, Abdel-Rahman, & Zhang, 2014). Estradiol has been shown to regulate actin polymerization in a variety of tissues (Briz & Baudry, 2014; A. Kumar et al., 2015; Zhao et al., 2017), to alter microtubule stability in cancer cells and in hippocampal neurons (Briz & Baudry, 2014; Ikeda et al., 2010), and to alter the expression of GAPDH in endometrium and liver (Flamini et al., 2009; Rivero-Gutierrez et al., 2014). Estradiol also has been shown to bind to and induce rapid phosphorylation of GAPDH in hippocampal neurons and to increase GAPDH activity (Ramirez, Kipp, & Joe, 2001). Proteomic studies in brain samples revealed estradiol regulation of proteins involved in glucose utilization (including GAPDH), the

branching of actin filaments, and post-translational modification of tubulin (Hansberg-Pastor et al., 2015; Szego, Kekesi, Szabo, Janaky, & Juhasz, 2010). These changes in expression were brain region-specific, varied with treatment, and were affected by pregnancy, estrus- and menstrual-cycles.

Recent proteomic studies have attempted to identify suitable HKPs for Western blot quantification (Higdon & Kolker, 2015; H. G. Lee et al., 2016). Analysis of the human proteomic database ProteomicsDB identified 20 protein candidates with %CV<20% that have constitutive and ubiquitous expression. Notably, in this analysis GAPDH, β-actin and α -tubulin had %CV>20% qualifying them as unreliable for protein normalization (H. G. Lee et al., 2016). Another analysis of two different proteomic studies screened a total of 1297 proteins from 12 tissues and found that 107 of them had %CV < 30% variation within the same tissue (Higdon & Kolker, 2015). After comparing expression levels between the two studies, only 34 proteins consistently had %CV < 30% across the 12 tissues. Of these 34 proteins, an analysis of gene expression showed that only 14 had gene expression levels with %CV < 20% across 6 microarray studies. Note that this is still much greater than the variations observed in TP signal.

Collectively, these data demonstrate significant effects of gonadal status on GAPDH, actin and tubulin, as well as the difficulty in identifying HKPs suitable for normalizing Western blot data. Nevertheless, our small survey of recent reports suggests that the vast majority of Western blot analyses of hormonal effects on protein expression continue to use actin, tubulin, and GAPDH as normalization controls, often without first demonstrating that the HPKs are not also affected by treatment. Hence the need for a more consistent and reliable method.

2.5.2 **Considerations in Selecting a TP stain to normalize Western blot data**

When selecting a TP stain for use in Western blot analysis a number of factors need to be considered. Chief among these are an appropriate linear range consistent with the targets of interest and low sample-to-sample variability. Many of the currently available stains meet these criteria. Other factors include (1) reversibility, which can be an important consideration for samples of limited volume or if the stain interacts with subsequent immunodetection or spectrometric analysis of targets, (2) the ability to be used on membranes vs. gels, as membrane staining can account for inconsistencies in loading as well as transfer, and (3) compatibility with multiplexing for simultaneous detection of multiple targets. Many stains are available and each has its limitations. For example, Ponceau S is easily reversed, but reportedly loses sensitivity below 200 ng (Janes, 2015). In addition, Janes et al. (Janes, 2015) reported that the zero intercept of the Ponceau S densitometry could not be accurately estimated from a blank region of the PVDF membrane. This could compromise the ability to use Ponceau S for relative protein quantification. Coomasie Blue and Amido Black are sensitive down to 50 ng (Harper & Speicher, 2001), but have higher %CV than other TP stains and may block epitopes required for subsequent immunodetection (Moritz, 2017; Moritz et al., 2014; Tovey, Ford, & Baldo, 1987; Welinder & Ekblad, 2011). SYPRO Ruby is highly sensitive and is compatible with immunodetection techniques, but is irreversible (Berggren et al., 1999). These are just a few of the TP stains that have been commonly used in Western blot analysis.

The REVERT® TP stain displayed many desired characteristics of a non-specific TP stain including a broad linear range and excellent sample-to-sample consistency. In addition, the stain was stable for hours, yet easily reversed, could be applied directly to PVDF membranes thus controlling for inconsistencies in both protein loading and transfer, and was highly suited for use

in the quantification of multiple targets on a single gel. Importantly, we detected no bleed-through from the 700 nm channel to the 800 nm channel (Fig 5), and no apparent interference with the immunodetection of our targets. Normalization to the REVERT® TP stain also resulted in excellent gel-to-gel consistency in the detection of relative differences in the expression of a target protein between pairs of samples. These findings suggest that this methodology overcomes the limitations of HKPs and is an easy and reliable method of normalization for Western blot analysis of brain tissue homogenates.

2.5.3 **Limitations**

This study demonstrates some advantages of the REVERT® TP stain over HKPs for use in quantitative Western blot analysis of brain tissue homogenates; however, there are some limitations. (1) We make no claims as to the superiority of REVERT® TP stain over any other TP stains that are commonly available for use in Western blot analysis. Direct comparison with other TP stains was not conducted and was not a goal of this study. It should be noted that several other TP reagents have also been shown to produce high accuracy, low %CV and excellent detection sensitivity (Collins et al., 2015; Eaton et al., 2013; Moritz, 2017; Rivero-Gutierrez et al., 2014; Taylor et al., 2013; Thacker, Yeung, Staines, & Mielke, 2016). (2) Our studies were conducted using PVDF membrane and not on other media types such as nitrocellulose or nylon. It is possible that performance will vary on other media types. (3) While we did not detect any binding of the TP stain to our targets or interference with immunodetection of the targets, it is impossible to rule out such interactions with other targets. Such interactions need to be tested empirically and, if observed, may require modification of the protocol to the specific application.

2.5.4 **Summary**

Our goal was to evaluate an alternative method for conducting Western blot analysis of brain homogenates from rats with distinct physiologically relevant gonadal hormone states. Our results demonstrate that the REVERT™ TP stain can be applied directly to PVDF membranes for multiplex fluorescence detection with target proteins. The method is easy to apply and shows excellent sensitivity, linearity, and reproducibility. Detection of TP showed much less variability across samples than the detection of HKPs. In addition, we provide direct evidence that normalizing to TP can enable detection of an effect that is otherwise masked by the added variability associated with normalizing to an HKP. Finally, we show that gel-to-gel consistency in measuring differences between paired samples run on multiple gels was significantly better when data were normalized to TP than when normalized to GAPDH. Given the evidence that gonadal hormones can influence the expression and activity of HKPs in many tissues including brain, we strongly recommend the use of this methodology for quantifying protein expression by Western blot in studies involving gonadal hormone manipulations or different gonadal hormone states.

3.0 Impact of Surgical and Transitional Models of Menopause and Stages of the Estrous Cycle on the Expression of Enzymes Involve in Brain Metabolism, Acetyl-CoA Production and Integrity of Cholinergic Function

This chapter describes the first of two large 'omics' experiments, focused on relative quantification of proteins involve in glycolytic pathways, acetyl-CoA production, cytoskeletal proteins as well as a marker for integrity of the cholinergic system.

3.1 Studies Overview

Our goal is to understand how loss of circulating estrogens and estrogen replacement affect brain regions involved in cognitive processes. We recently conducted a large metabolomics study to characterize the effects of different models of menopause and treatment with estrogen receptor agonists on neurochemical endpoints in different regions of the brain. Here we characterize effects on the expression of several key enzymes involved in glucose utilization and energy production, specifically phosphofructokinase (PFK), glyceraldehyde 3-phosphate dehydrogenase (GAPDH), and pyruvate dehydrogenase (PDH). In addition, we evaluated effects on levels of ß-actin and α-tubulin, on choline acetyltransferase (ChAT) activity, and on levels of ATP citrate lyase (ATP-CL), an enzyme involved in the cytosolic production of Acetyl-CoA. Effects were measured in the hippocampus, frontal cortex and striatum (Section 3.3.3.1 describes in more depth the criteria for selection of targets and how estrogen modulate these proteins).

Overall two experiments were conducted. Experiment 1 compared the effects of ovariectomy, a model of surgical menopause, and VCD-treatments, a model of transitional menopause, with tissues from gonadally intact rats collected at proestrus and at diestrus stages of the estrous cycle. Experiment 2 (Chapter 4) evaluated the same endpoints in OVX and VCD-treated rats treated with estradiol or with selective ERα, ERß, or GPR30 agonists for 1 week or 6 weeks. Our findings demonstrate distinct differences in the expression of metabolic enzymes between cycling animals and models of surgical and transitional menopause. These differences were model-, region- and time- dependent, and were modulated by selective estrogen receptor agonists. The hippocampus was particularly sensitive to loss of ovarian function at the 1-week time-point whereas the frontal cortex was sensitive regardless of how or when ovarian function was lost. In addition, OVX rats appeared much more sensitive to agonist treatments than VCD-treated rats. This may contribute to differences in the effects of estrogen treatments on cognition and age-related cognitive decline in women that have experienced surgical vs. transitional menopause.

3.2 Introduction

The goal of this project was to characterize the effects of transitional and surgical menopause, as well as treatment with different estrogen receptor agonists, on metabolic pathways related to glucose utilization and energy production, acetyl-CoA production and cholinergic function.

Estrogens exert a profound influence on the brain including effects on brain architecture, synaptic function and plasticity (Alexander et al., 2017; B. S. McEwen, 2014), neurotransmitter

production and release (Babayan & Kramar, 2013; Y. Hara, Waters, McEwen, & Morrison, 2015), neuro-immunomodulation (ThyagaRajan, Hima, Pratap, Priyanka, & Vasantharekha, 2019; Yin, Yao, Brinton, & Cadenas, 2017) and neuronal survival (Baez-Jurado et al., 2019). In many cases these effects have been associated with significant enhancements of learning, memory, and attention (Colciago, Casati, Negri-Cesi, & Celotti, 2015; Frick, Kim, Tuscher, & Fortress, 2015; Gibbs, 2010; Hadjimarkou & Vasudevan, 2018; Tuscher, Fortress, & Frick, 2019). This has been demonstrated both in animals and in humans (Korol & Pisani, 2015; Luine, 2014; McCarrey & Resnick, 2015; Newhouse & Dumas, 2015). Loss of estrogens (e.g., following menopause) likewise is thought to contribute to cognitive decline both in normal aging and in association with specific neurodegenerative diseases like Alzheimer's disease and Parkinson's disease (Frick, 2009; Rettberg et al., 2014). Estrogen treatments have been shown to reverse some of these effects; however, not all studies agree and mechanisms are still poorly understood.

We hypothesize that several important variables contribute to the specific effects of menopause and estrogen treatments on brain function. Menopause refers to a loss of ovarian function with a corresponding reduction in ovarian estrogens. Ovariectomy or surgical menopause consists of the rapid and complete removal of the ovaries resulting in a complete loss of all ovarian hormones. In contrast, natural or transitional menopause is characterized by an accelerated loss of ovarian follicles, resulting in irregular fluctuations in ovarian hormones during the transition period, culminating in a substantial decline in ovarian production of estrogens and progesterone (Camp et al., 2012). With transitional menopause, ovarian stromal cells remain and continue to produce androgens, resulting in a substantial increase in the ratio of androgens:estrogens in the systemic circulation. Most women experience a transitional menopause occurring at approximately 50-55 years of age. Far fewer women (~13%) experience surgical menopause, and

many of these surgeries are conducted in much younger women (women in their 20s and 30s) to prevent ovarian and breast cancer associated with BRCA1 and BRCA2 mutations (Metcalfe et al., 2015).

Rodents do not experience follicular atresia resulting in a natural menopause. Consequently, most preclinical studies have used ovariectomy to study how loss of ovarian function affects the brain. Recently, a rodent model of progressive ovarian failure has been characterized (Hoyer et al., 2001; Lohff, Christian, Marion, Arrandale, & Hoyer, 2005; Lohff, Christian, Marion, & Hoyer, 2006; Van Kempen et al., 2011). This model involves daily injection of 4-vinylcyclohexene diepoxide (VCD), which selectively and over time destroys the majority of primordial and primary ovarian follicles (Springer et al., 1996). Rodents treated with appropriate daily doses of VCD experience a progressive loss of ovarian follicles. Stromal cells remain intact and continue to produce androgens, thus mirroring conditions that occur in natural menopause. Using this model, studies are beginning to show that effects of menopause as well as estrogen treatment on brain physiology and function can differ depending on when and how loss of ovarian function occurs (see (Koebele et al., 2017) for recent review).

Another important variable are the specific estrogen receptors that are responsible for the effects of estrogens in different regions of the brain. Three estrogen receptors have been identified. ERα and ERβ are nuclear receptors that function to activate or suppress the expression of specific genes (Arnal et al., 2017; Warner, Huang, & Gustafsson, 2016). These receptors also can be localized to membrane compartments where they participate in the rapid activation of signal transduction pathways (Dominguez & Micevych, 2010; Micevych et al., 2017; Wong et al., 2019). A membrane-associated G-protein coupled receptor 1, GPER1, also has been identified and participates in the rapid activation of signal transduction pathways (Alexander et al., 2017) as well

as in cross-talk with ERα- and ERβ- mediated pathways (Hadjimarkou & Vasudevan, 2018). There also is evidence for the existence of a variety of estrogen-related receptors which are structurally related to the identified ERs and can participate in mediating estrogen effects (as mentioned in Chapter 1.2) (Saito & Cui, 2018; C. D. Toran-Allerand, 2004; C. Dominique Toran-Allerand et al., 2002). These receptors are expressed by neurons and glial cells in different regions of the brain and determine the effects of estrogens on brain physiology and function.

The present study is part of a larger metabolomics study designed to characterize the effects of surgical (i.e., ovariectomy) and transitional (i.e., VCD-treatments) models of menopause, as well as treatment with different estrogen receptor agonists, on neurochemical endpoints in the brain. Here we used a modified Western blot methods, which was described in Chapter 2, to measure effects on the levels of three enzymes that play critical roles in glycolysis, i.e., phosphofructokinase (PFK), glyceraldehyde 3-phosphate dehydrogenase (GAPDH), and pyruvate dehydrogenase (PDH), in addition to levels of ß-actin and α-tubulin, ATP citrate lyase (ATP-CL), an enzyme involved in the cytosolic production of Acetyl-CoA. We also measured effects on choline acetyltransferase (ChAT) activity, the enzyme responsible for the production of acetylcholine from Acetyl-CoA and choline. Effects were measured in the hippocampus, frontal cortex and striatum, each of which has well documented roles in specific learning, memory and attentional processes. Results demonstrate significant differences between surgical and transitional menopause that are both time and brain-region dependent, and that may contribute to differences in the effects of estrogen treatments on brain physiology and function in women that have experienced surgical vs. transitional menopause.

3.3 Methods

3.3.1 Ethics statement

All procedures were carried out in accordance with PHHS policies on the use of animals in research, and with the approval of the University of Pittsburgh's Institutional Animal Care and Use Committee.

3.3.2 Animals

Young adult (3mo old) female Sprague-Dawley rats were used for all studies. Rats purchased from Harlan Sprague-Dawley Laboratories, Inc. Rats were housed individually with free access to food and water, maintained on a 12-hr light/dark cycle and were acclimated to the housing conditions for two weeks prior to the beginning of treatments or experiments.

We chose to use young adult for both the OVX and VCD models to avoid confounds associated with aging and reproductive senescence in rats. Unlike primates, mid-age rodents enter a stage of reproductive senescence characterized by dysfunction of the HPA axis where LH and GnRH surge allowing follicles to persist in estrogen production, leading to elevated estradiol levels and persistent estrus stage (Brinton et al., 2015; Cruz, Fernandois, & Paredes, 2017; LeFevre & McClintock, 1988; Shirai, Houle, & Mirsky, 2015). Thus, rodents are not considered to be a translational model for primate natural menopause and were mostly used as a postmenopausal model by ovariectomy. While most women experience natural menopause that occurs in mid-life,

a significant number of women undergo bilateral oophorectomy (referred to as ovariectomy in animals) enter a surgical (iatrogenic) menopause characterized by the complete loss of all ovarian hormones earlier in life (Davis et al., 2015; Rocca, Grossardt, & Shuster, 2014; Rocca, Grossardt, Shuster, & Stewart, 2012; Weber, Maki, & McDermott, 2014). Choosing to use young adults animals for the VCD model minimizing the impact of confounding variables and allows a direct comparison between OVX and VCD.

3.3.3 Experimental design and treatments

Two experiments were performed. **Experiment 1** (Chapter 3) evaluated the effects of surgical (OVX) vs. transitional (VCD-treated) menopause on protein expression and ChAT activity at 2 time points (1 week and 6 weeks), relative to gonadally intact controls sacrificed at proestrus and at diestrus. **Experiment 2** (Described in Chapter 4) evaluated the effects of estradiol and of selective estrogen receptor (ER) agonists on these same endpoints in OVX and VCD-treated rats, after 1 week and 6 weeks of treatment.

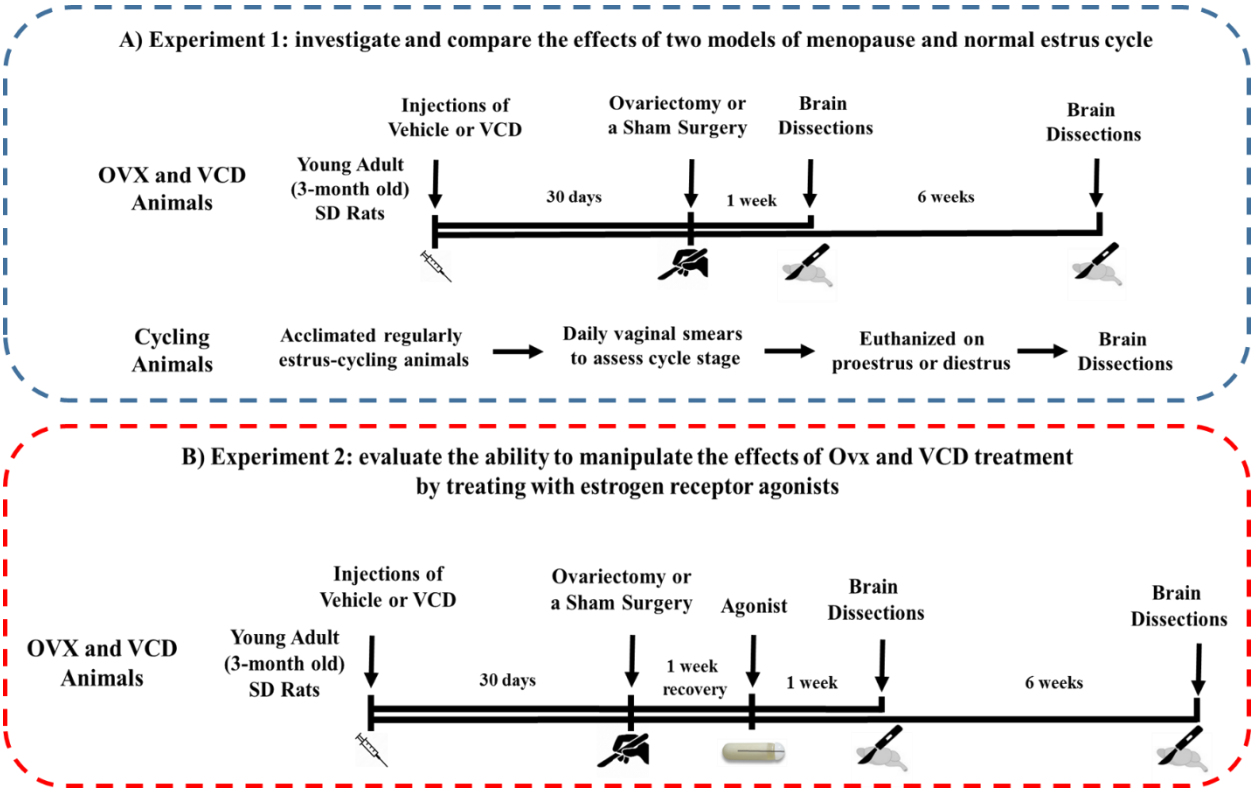

Figure 9: : Illustration of experimental designs involving OVX, VCD and cycling rat model. Two separate experiments were conducted. (A) (Experiment 1, Chapter 3)Transitional menopause modeled in young SD rats by daily injections of 4-vinylcyclohexene diepoxide (VCD) at 80 mg/kg for 30-days. This regimen destroys >95% of primary ovarian follicles with little toxicity to stromal cells or to other organs, and no other lasting toxic effects. For surgical menopause model, cycling animals were given daily vehicle injections of sesame oil and after 30-days of treatment underwent bilateral ovariectomy. Rats that completed 3-day VCD treatment underwent sham surgery. Cycle stage of regularly cycling rats were determined by daily vaginal smears. Rats were anesthetized at 1-week and 6-weeks from model establishment and tissues from the hippocampus (HPC), striatum (STR), and frontal cortex (FCX) were collected. This resulted in a total of 6 treatment groups: P, D, OVX-1W, OVX-6W, VCD-1W, and VCD-6W with at least n= 4 or higher per group. (B) (Experiment 2, Chapter 4) Following surgery, VCD and OVX rats were given 1-week recovery before beginning of treatments with estrogen receptor agonists. A mini osmotic pump was planted subcutaneously in the dorsal neck region for continuous administration of 5 µg/day of: 17ß-estradiol (E2), PPT (a selective ERα agonist), DPN (a selective ERß agonist), G-1 (a selective GPR30 agonist), or vehicle. Tissue from the HPC, STR and FCX were collected at 1-week and 6-weeks after beginning of agonist treatments.

3.3.3.1 Selection of Targets

Targets were selected using several criteria: (1) an identified pivotal role in at least one major metabolic pathway, (2) evidence that 17ß-estradiol (E2), testosterone (T) or androstenedione (AD) has direct and/or indirect effects on both the expression and function of the target, and (3) changes in the expression or activity of each target must be associated with functional effects on glucose metabolism or on a particular neuronal function related to acetylcholine production. The following proteins were selected for analysis:

Phosphofructokinase (PFK): PFK catalyzes the first irreversible commitment reaction in glycolysis where fructose-6-phosphate (F6P) and ATP converted into fructose-1,6-bisphosphate (F1,6BP) and ADP(Akram, 2013). In the brain, PFK determines glycolytic flux and is allosterically regulated by cofactors, metabolites and hormones (Kasten, Mhaskar, & Dunaway, 1993; McKenna, Dienel, Sonnewald, Waagepetersen, & Schousboe, 2012). Number of studies in various rat models demonstrated the effects of estrogen on glucose metabolism with particular changes to PFK expression and activity in several neurons and various brain regions (Chen, Brown, et al., 2009; Gupta, Srivastava, & Setty, 2012; Amalia Kostanyan & Karen Nazaryan, 1992; Tamrakar, Ibrahim, Gujar, & Briski, 2015) as well as in non-neuronal cell lines (Trenti et al., 2017).

Glyceraldehyde 3-phosphate dehydrogenase (GAPDH): GAPDH catalyzes the phosphorylation and conversion of glyceraldehyde-3-phosphate (G3P) to the energy-rich intermediate 1,3-bisphosphoglycerate (1,3BPG). In glycolysis, GAPDH regulate glycolytic flux in response to ATP demands, oxidative stress and levels of other metabolic pathways (M. N. Lee et

al., 2009; Seki & Gaultier, 2017; Suzuki et al., 2015). Studies demonstrate that GAPDH also has highly diverse functions beyond glycolysis (Chuang & Ishitani, 1996; M. R. Hara, Cascio, & Sawa, 2006; Nicholls, Li, & Liu, 2012; Sirover, 2012; Tristan, Shahani, Sedlak, & Sawa, 2011). For example, GAPDH can bind with tubulin to mediate intracellular transport of proteins (Hinckelmann et al., 2016; Volker & Knull, 1997; Volker & Knull, 1993) and can induce neuronal inhibition by catalyzing the phosphorylation of GABAA receptors (Laschet et al., 2004). Binding studies, using rat brain microsomal preparations in affinity columns and competitive binding assays found that BSA-conjugated E2 has about 10 times higher binding affinity than BSA-conjugated progesterone while BSA-conjugated T has very little binding with GAPDH (Joe & Ramirez, 2001). Consecutively, both E2 and progesterone modulate GAPDH activity in a dose dependent manner (Joe & Ramirez, 2001; Ramirez et al., 2001). E2 and T also have been reported to induce GAPDH translocation between the cytoplasm and plasma membrane, induce GAPDH phosphorylation, and higher mitochondrial expression of GAPDH, (Chen, Brown, et al., 2009; Joe, Kipp, & Ramirez, 2005; A. Kostanyan & K. Nazaryan, 1992; Robertson, Bhattacharyya, & Ing, 1998).

Pyruvate dehydrogenase (PDH): PDH catalyzes the decarboxylation of pyruvate and Coenzyme-A into acetyl-Coenzyme A (acetyl-CoA) and CO2. In rats and mice, both the activity and expression of PDH in the brain are modulated by sex hormones, and were particularly higher following E2 treatments in OVX rats (Gaignard et al., 2015; Irwin et al., 2011; Irwin et al., 2012; Nilsen, Irwin, Gallaher, & Brinton, 2007). In neurological disorders, PDH deficiency has been associated with impaired function of the astrocyte-neuron lactate shuttle resulting in the limitation of alternative pyruvate source in neurons and lower glycolytic metabolism (Jha, Jeon, & Suk, 2012;

Mergenthaler, Lindauer, Dienel, & Meisel, 2013). Low levels of PDH in different brain regions also lead to mitochondrial dysfunction in various endpoints (Hoshi et al., 1996; Park et al., 2018; Prasad, Rupar, & Prasad, 2011; Stacpoole, 2012).

ATP citrate lyase (ATP-CL): ATP-CL, also abbreviated as ACLY, catalyzes the cytosolic conversion of citrate to acetyl-CoA which, in turn, is critical for lipogenesis, cholesterogenesis, and for protein and histone acetylation. Cytoplasmic citrate comes primarily from efflux by the mitochondrial citrate transporter (CIC), although influx of extracellular citrate can also occur. (Catalina-Rodriguez et al., 2012; Gnoni, Priore, Geelen, & Siculella, 2009; Sun et al., 2010). Cytoplasmic citrate can regulate glycolysis by inhibiting PFK and PDH (Iacobazzi & Infantino, 2014). In addition to its other roles, acetyl-CoA is essential for the production of the neurotransmitter acetylcholine (Szutowicz, Jankowska, Blusztajn, & Tomaszewicz, 1999; Szutowicz, Tomaszewicz, Jankowska, & Kisielevski, 1994) and is co-localized with ATP-CL in cholinergic terminals (Szutowicz, Stepien, Bielarczyk, Kabata, & Lysiak, 1982).

Cytoskeletal Proteins: α-tubulin and β-actin: In neurons, cytoskeletal proteins play critical roles in axonal transport, dendritic spine morphology, and synaptic plasticity. Studies have demonstrated significant effects of estrogens and androgens on cellular levels of both actin and tubulin (Butler, Leigh, & Gallo, 2001; Joe et al., 2005; Jurasek et al., 2018), with corresponding effects on synaptic function (Frick et al., 2015; Hansberg-Pastor et al., 2015; Welling, Shackelford, Ervin, & Choleris, 2019) as well as on glycolytic enzymes (Hansberg-Pastor et al., 2015; Welling et al., 2019). E2 and T also have been shown to influence tubulin polymerization (Butler et al., 2001; Joe et al., 2005; Jurasek et al., 2018), and to modulate interactions between tubulin and

GAPDH (Hinckelmann et al., 2016; Vigelso et al., 2015; Volker & Knull, 1997; Volker & Knull, 1993). Changes in the levels of actin and tubulin have regional impact on neuronal plasticity, brain organization, cellular transport and involve in direct and indirect mechanisms of energy and metabolism (e.g. from metabolite transport to regulation of glycolytic enzymes as mentioned above) (Frick et al., 2015; Hansberg-Pastor et al., 2015; Welling et al., 2019). Sex hormones also have direct influence on α-tubulin and β-actin. Nanomolar concentrations of estradiol and testosterone have opposite effects on microtubule polymerization (Joe et al., 2005). While E2 disrupts the polymerization process, treatments with T stabilizes the formation of microtubules (Butler et al., 2001; Jurasek et al., 2018). Additionally, hormones modulate the relationship between GADH and tubulin as mentioned earlier (GAPDH section).

Choline acetyltransferase (ChAT): ChAT is the enzyme responsible for the formation of acetylcholine from choline and acetyl-CoA. ChAT activity often is used as an indicator of the integrity of cholinergic projections in humans as well as in animal models (Contestabile, Ciani, & Contestabile, 2008; Gibbs, 1998, 2010). Cholinergic dysfunction or changes in ChAT activity have been associated with several neurodegenerative diseases, while estrogen treatments been associated with higher ChAT activity in OVX rats and mice (Gibbs, 2010). Abnormalities in ChAT are associated with neurological conditions and is a therapeutic target for several diseases (Cha et al., 2016; D'Souza & Waldvogel, 2016; Gibbons & Dean, 2016; Oda, 1999; Richter et al., 2014).

Acosta et al. demonstrated notable difference in the activity of acetylcholinesterase (AChE) between OVX and VCD models (Acosta et al., 2009). Ovariectomy alone or following VCD treatment led to increased AChE activity in the HPC relative to VCD treatment alone. No change

in the activity of AChE was seen in the FCX region. Changes to AChE may impact the availability of free choline and limit synaptic choline recycling. Synaptic choline reuptake can be a rate limiting step of ACh production (Hassel, Solyga, & Lossius, 2008; Ray, Bailey, Simon, & Lahiri, 2012) and changes to AChE activity may be more beneficial for regeneration of cellular ACh than changes to ChAT activity.

3.3.3.2 Experiment 1 – Comparison of menopausal models

Rats were randomly assigned to one of four groups, proestrus (P), diestrus (D), 4-vinylcyclohexene diepoxide (VCD)-treatments and ovariectomy (OVX). Regularly cycling animals underwent daily vaginal smears to assess cycle stage (Goldman et al., 2007). Rats were euthanized on proestrus or diestrus and brain tissues were collected. Transitional menopause was modeled by administering daily injections of the ovatoxin VCD at 80 mg/kg diluted in sesame oil at a volume of 2.5 µl/g body weight for 30 days (n=16). This regimen has been shown to destroy >95% of primary ovarian follicles with little toxicity to stromal cells or to other organs, and no other lasting toxic effects (Hoyer et al., 2001; Muhammad et al., 2009; Van Kempen et al., 2014; Van Kempen et al., 2011). Remaining rats underwent daily vehicle injections of sesame oil. After 30 days of injection, the vehicle-treated rats received bilateral ovariectomy. Ovariectomy was conducted in-house using a lateral approach (Kirshner & Gibbs, 2018). Rats that completed 30-days VCD treatment underwent sham surgery which included anesthesia, the abdominal incisions and wound closure, but no removal of the ovaries. Rats were placed onto a warm heating pad during recovery. Ketofen (3mg/Kg, i.p.) was administrated twice per day for three days to reduce discomfort. Topical antibiotic ointment was applied for 3-days to prevent infection. At 1 or 6 weeks following surgery, rats were euthanized with an overdose of ketamine (280 mg/kg) and

xylazine (56 mg/kg) and tissues were collected for analysis. This resulted in a total of 6 treatment groups: P, D, OVX-1W, OVX-6W, VCD-1W, and VCD-6W with at least n= 4 or higher per group.

3.3.4 **Collection of Tissues**

Rats were anesthetized with ketamine and xylaxzine and then decapitated. Brains were rapidly removed and dissected using an ice-cold brain matrix (Kopf Instruments, Inc.) and a petri dish. Tissues from the hippocampus (HPC), striatum (STR), and frontal cortex (FCX) were collected, snap frozen on dry ice and kept at -800C. Cycle stage of regularly cycling rats were determined by daily vaginal smears and rats were euthanized on proestrus or diestrus. Trunk blood was collected from all rats and serum was processed and stored at –200C for quantification of hormone levels.

3.3.5 **Analysis of Hormone Levels by UPLC-MS-MS**

Serum levels of E2, T and AD were quantified by UPLC-MS/MS as recently described (J. Li et al., 2016; Long et al., 2018, 2019). T and AD levels were quantified by a modification of the method described by Cawood (Cawood et al., 2005) and using methods similar to the quantification of E2 (J. Li, Rao, & Gibbs, 2018; Long et al., 2018, 2019). The lower limits of detection were 2.5 pg/mL for E2 and 10.0 pg/mL for T and AD.

3.3.6 **Processing and Analysis of Brain Tissue Samples**

Brain tissues were thawed in cold sonication medium containing EDTA (10mM) and Triton X-100 (0.5%) in a ratio of 10 µl buffer to every 1 mg of wet weight tissue. Tissues were sonicated at 4˚C 6 times at 30-seconds ea. for a total of 3-minutes. Half of each sample was immediately aliquoted into a freshly-prepared cold Western-blot lysis buffer containing: 1% protease inhibitor cocktail (Sigma, P8340), 0.5% Sodium deoxycholate, 0.001M EDTA, 0.15M NaCl, 0.01M Sodium fluoride, 0.1% Sodium dodecyl sulfate (SDS), Tris-HCl (50mM, pH=7.4), 0.001M Sodium orthovanadate (Na3VO4) and 0.001M phenylmethylsulfonyl fluoride (PMSF). All reagents were purchased from Sigma-Aldrich, Inc. Remaining sample was used for measuring ChAT activity. An aliquot of each sample was used to determine protein concentration by Bradford assay (Bradford, 1976). Samples were stored in -80 ˚C prior to processing.

3.3.7 **SDS-PAGEs**

Brain homogenates were processed for SDS-PAGE and Western blot analysis using procedures recently developed and validated in our laboratory (Kirshner & Gibbs, 2018). Briefly, samples were diluted to 2.4 µg/µl in sonication buffer (containing: 1% protease inhibitor cocktail, 0.5% Sodium deoxycholate, 0.001M ethylenediaminetetraacetic acid (EDTA), 0.15M NaCl, 0.01M Sodium fluoride, 0.1% Sodium dodecyl sulfate (SDS), TriseHCl (50 mM, pH = 7.4), 0.001M Sodium orthovanadate (Na3VO4) and 0.001M phenylmethylsulfonyl fluoride (PMSF). All reagents were purchased from Sigma-Aldrich), mixed with an equal volume of Laemmli buffer (BIO-RAD, Cat# 1610737)), heated to 98˚C for 7-minutes and loaded onto commercially-prepared

12% Mini-PROTEAN® TGX™ gels. Samples were loaded at a volume of 10 µl per lane to achieve a total of 12 µg protein per lane. This loading concentration was confirmed to ensure that signals from each of our targets fell within their linear detection range (Kirshner & Gibbs, 2018). In addition, for each brain region, a dilution series was generated using a mixture of homogenates containing twenty samples to equally represent each of our animal models. The combined mixture was used to test and compare the range for linear detection and quantification of total protein (TP) and individual targets. The Chameleon 700 pre-stained protein ladder (LI-COR, Inc., Lincoln, NE, USA) was included on all gels. Samples were run for 2-hours at 100 V and were transferred for 2 hr, 100 V, 4˚C to Immobilon FL PVDF membrane (Millipore, Inc., Burlington, MA. USA).

3.3.8 Total Protein Membrane Stain for Normalization

After transfer, PVDF membranes were directly stained for total protein using the LI-COR REVERT™ Kit (LI-COR, Inc.) according to methods validated earlier (as described in Chapter 2 (Kirshner & Gibbs, 2018)). Briefly, membranes were submerged in REVERT for 5 minutes, washed two times for 30 seconds each with wash solution (LI-COR, Inc., 6.7% (v/v) glacial acetic acid, 30% (v/v) methanol, in water) and imaged immediately. Membranes were scanned using the 700 nm channel of the Odyssey® imaging system (LI-COR, Inc.) at a scanning resolution of 169 µm and a 'normal' image quality setting. TP stain was then removed by 5 minutes incubation in reversal solution (LI-COR, Inc., 0.1 M sodium hydroxide, 30% (v/v) methanol, in water) with gentle shaking and then imaged again to verify that no residual signal remained.

Membranes were then blocked for 1 hour at room temperature in Odyssey® TBS blocking buffer (LI-COR, Inc, cat#927-50000) and incubated overnight at 4˚C with a mixture of primary

antibodies (all from Abcam, Inc., Cambridge, UK): ATP-CL (rabbit polyclonal anti-ATP-CL, 1:1500, ab40793), PFK (rabbit polyclonal anti-PFK, 1:1500, ab154804), α-tubulin (rabbit polyclonal anti-α-tubulin, 1:5000, ab52866), PDH (mouse monoclonal anti-PDH-E1α subunit, 1:2000, ab110330), β-Actin (mouse polyclonal anti-β-actin, 1:5000, ab6276; Experiment 1 only), and GAPDH (rat polyclonal anti-GAPDH, 1:5000, ab181602).

The next morning, membranes were washed 3X for 10 min each with TBS-T (50 mM Tris-HCL at pH=7.4, 150 mM NaCl and 0.1% Tween-20) and incubated for 1 hr at room temperature in TBS-T containing secondary antibodies of goat anti-mouse IgG (LI-COR IR Dye 800CW, cat#32210) and goat anti-rabbit IgG (LI-COR IRDye800CW, cat#32211) each at 1:5,000 dilution.

3.3.9 **Image Acquisition and Data Analysis**

All PVDF-membranes were analyzed using the Odyssey application software (Ver 3.0.30) by acquiring integrated intensity values of defined bands. Densitometry of single-band targets were measured in a rectangular area automatically defined by the software. Manual adjustments were made to contain all detectable signal for a band and background was subtracted using the software's averaging protocol. Signal generated by the total protein stain was measured in accordance with the manufacturer's protocol by manually applying a rectangular area at a select range of molecular weights (e.g.50-90KDa; see below). For comparison of samples on the same gel, relative quantification was achieved by normalizing each target to the signal of total protein in the range of 50 to 90 KDa on the same lane. Previous studies determined that this molecular weight range has a wide linear range of detection as a function of protein loading and low signal variability across samples (Kirshner & Gibbs, 2018). These ratios were then normalized to an

average of the same target calculated from a set of control group samples (on the same gel) to facilitate between-gel comparisons. At least 3 samples from either the proestrus (experiment 1) or a vehicle-treated (experiment 2) control group were present on each gel and averaged within group to represent an intra-gel normalization factor. Prior studies from our laboratory revealed that this type of normalization enables us to perform between-gel comparisons with excellent between-gel consistency and an intraclass correlation coefficient of 0.89 (i.e., excellent reliability) (Kirshner & Gibbs, 2018). Figure 12 is a representative images for the detection of total protein stain (Fig. 12A) and multiple protein targets (Fig. 12B).

The linear range of quantification for each target was determined by graphing integrated intensities of serial dilutions and choosing a range of dilutions with the highest linearity represented by least-squares analysis.

3.3.10 **Choline acetyltransferase activity (ChAT) assay**

ChAT activity was measured using a modification of the radioenzymatic method of Fonnum (1969) (Sterri & Fonnum, 1980) as described by Pongrac and Rylett (1996) (Julie L. Pongrac & Rylett, 2002). Sonicated samples were thawed and diluted to a concentration of 0.8 mg/mL using cold sonication buffer. Accuracy of the working dilution was verified by a second, post-dilution protein assay. Reaction triplicates (5ul) from each sample dilution were then incubated in 37 ˚C water bath for 30min in the presence of 10X acetyl-CoA (Sigma, cat#A2056) and [3H]-acetyl-CoA (PerkinElmer, Waltham, MA, USA, Cat# NET290050UC) for 30,000 d.p.m/tube in a volume of 10ul with a final concentration of 0.25mM acetyl-coA, physostigmine sulfate (0.2mM, Sigma) and incubation buffer (containing: 20mM choline chloride, 20mM EDTA,

600mM NaCl and 50mM sodium sulfate buffer at pH 7.4). Reaction was timed and terminated by 4mL of reaction rinse at 40c containing 10mM sodium phosphate buffer (Sigma). Then, 1.6mL of acetonitrile (Sigma, Cat# 360457) containing 5mg/mL tetrephenylboron (TCI America, Portland, OR, USA, Cat# 143-66-8-A5130) was added and 6.4mL of followed by Insta-Fluor Plus (PerkinElmer, Cat# 6013167). Reaction samples were stored in 40c for 24 hours allowing phase separation. Amount of [3H]-acetylcholine produced was determined by counting total cpm emitted from the organic phase in 8mL EconoFluor scintillation cocktail (PerkinElmer, 6NE9699). Background was determined using identical tubes to which no sample was added (LKB beta-counter). Difference between total cpm and background cpm was used to estimate the total amount of ACh produced per sample. Aliquot of each diluted sample was used for determination of total protein in reaction tube and used for calculating ChAT activity. Average from three reaction tubes per sample were calculated and ChAT activity was represented as pmol of ACh synthesized / hr / mg protein.

3.3.11 **Statistical Analysis**

Statistical comparisons were conducted using JMP Pro software (SAS, version 13.0.0). Statistical significance was defined as $p < 0.05$ and results are presented as mean ± SEM.

Experiment 1:

Hormone levels, WB data and ChAT activity were first analyzed for differences between tissues collected at proestrus vs. diestrus by two-tailed t-test. Next, comparisons among all 6 groups were analyzed for each target by one-way ANOVA. For WB, each gel was designed to include representatives from all 6 groups and WB data were normalized to the proestrus group

(Kirshner & Gibbs, 2018). ChAT activity and WB data also were analyzed by 2-way ANOVA by using Model and Time as factors and omitting the data from normal cycling rats. Post-hoc comparisons were made using either a Tukey test to compare all groups or a Dunnet test to compare groups with the proestrus controls. These analyses were conducted for each end point in each region of the brain. For WB, an additional set of gels were run and included samples of OVX and VCD animals at 1 and 6 weeks (data not reported). These data were normalized to OVX-1W and demonstrate remarkable agreement with data generated by gels containing all 6-groups, demonstrating excellent reproducibility of these methods.

3.4 Results

3.4.1 Experiment 1: Comparison of Surgical and Transitional Models of Menopause Relative to Proestrus and Diestrus

3.4.2 Serum Hormone Levels

Serum levels of E2, T and AD are summarized in Figure 10 and Table 3. Analysis revealed that the levels of all three hormones were significantly higher at proestrus than at diestrus (for E2: $t(13) = 6.75$, $p < 0.001$; for T: $t(12) = 3.1$, $p < 0.01$; for AD: $t(13) = 2.78$, $p = 0.016$). Mean serum levels of circulating hormones in proestrus rats were E2: 50.6 ± 4.5, T: 186.9 ± 43.2 and AD: 196.5 ± 42.9, and levels in diestrus rats were 13.9 ± 2.8 pg/mL for E2, 92.2 ± 14.5 pg/mL for T, and 67.0 ± 7.2 pg/mL for AD. Two-way ANOVA revealed significant differences in hormone levels as a function of model and time (for E2: $F(3,26) = 3.05$, $p = 0.0464$; for T: $F(3,26) = 6.265$, $p = 0.0029$; and for AD: $F(3,26) = 3.97$, $p = 0.0188$). Post-hoc analyses revealed that in VCD-treated rats,

levels of E2, T and AD were significantly lower than levels in proestrus and did not differ significantly from levels detected in diestrus rats ($p < 0.05$ for all cases). None of these hormones were detectable in OVX rats, whereas VCD-treated rats had significantly higher levels of E2 and both androgens (T and AD) than OVX rats ($p < 0.05$ in each case). This was the case at both 1-w and at 6-w following the completion of VCD treatments. This is consistent with the selective depletion of ovarian follicles and the preservation of surrounding interstitial cells following VCD treatment (Acosta et al., 2009; Koebele et al., 2017; Mayer et al., 2004; Mayer et al., 2005; Van Kempen et al., 2011).

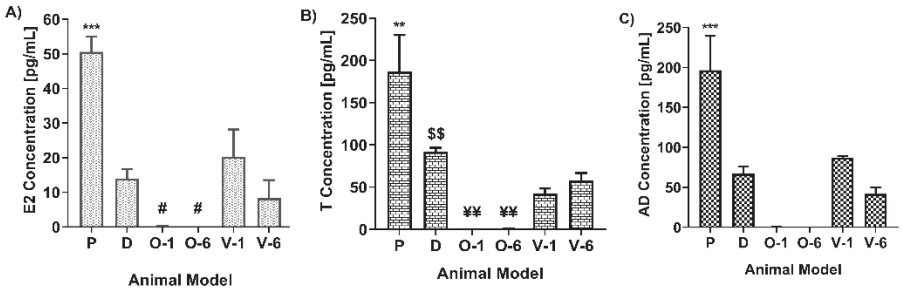

Figure 10: Serum hormone levels of (A) E2 (17β-estradiol), (B) T (testosterone) and (C) AD (androstenedione) by time (1- or 6- weeks) and rat model of: proestrus, diestrus, surgical (OVX; O) or transitional (VCD; V) menopause. All three hormones were below detection limits in OVX rats. One-way ANOVA: ** $p < 0.01$ and *** $p < 0.001$ are significant compare to all other groups; # $p < 0.05$ compare to VCD-1w; $$ $p < 0.01$ compare to P and ¥¥ $p < 0.01$ compare to P and D. Data shown as Mean ± SEM.

3.4.3 Comparison of target protein levels and ChAT activity in tissues collected at proestrus vs. diestrus

Figure 13 and Table 3 summarizes the levels of target proteins detected in tissues collected at proestrus vs. diestrus. Differences varied by brain region. For example, levels of ß-actin were

significantly lower at diestrus than at proestrus in the HPC ($t(6) = 3.25$, $p < 0.02$) and FCX ($t(6) = 4.16$, $p < 0.01$), with a strong trend in the STR ($t(6) = 2.27$, $p < 0.06$). In the FCX levels of the enzymes ATP-CL, PDH and GAPDH also were significantly lower at diestrus than at proestrus ($p < 0.05$ in each case), as well as a trend towards lower levels of α-tubulin ($t(6) = 2.16$, $p = 0.074$). In the STR levels of PDH were significantly higher in tissues collected at diestrus than at proestrus ($t(13) = 2.66$, $p = 0.02$). In contrast, no significant differences in ChAT activity were detected in tissues collected at diestrus vs. proestrus in any of the three brain regions examined.

3.4.4 Effects of OVX and VCD Treatments on target protein levels and ChAT activity in comparison with tissues collected at proestrus and diestrus

Both region-specific and time-dependent effects of OVX and VCD-treatments on target proteins were detected. These data are illustrated in Figures 11 and 13, summarized in Table 5, and are organized by brain region below.

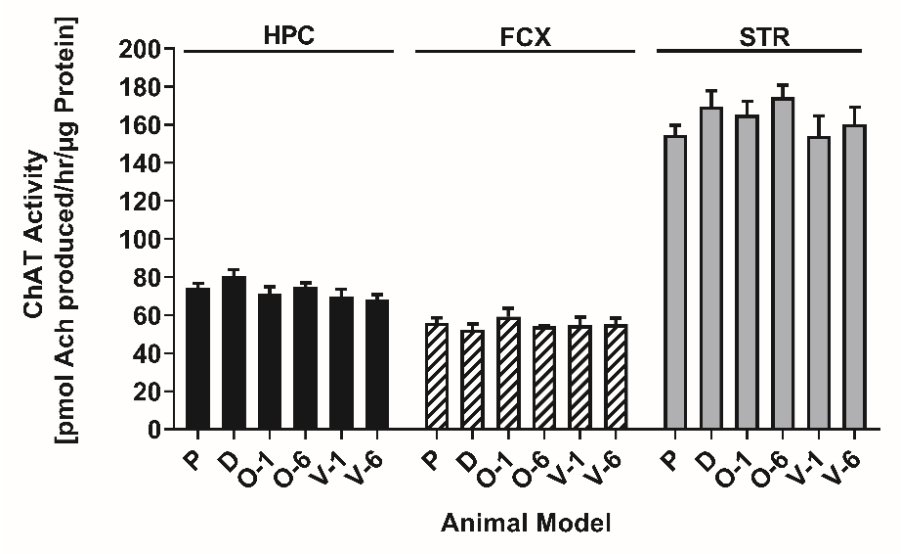

Figure 11: Activity of choline acetyltransferase (ChAT) in HPC, FCX and STR of proestrus (P), diestrus (D), surgical (OVX; O) or transitional (VCD; V) menopause rat models. Data shown as Mean ± SEM. No significant differences in ChAT activity were detected in tissues collected from gonadally intact rats at diestrus vs. proestrus and not in comparison to all other groups by either one-way or two-way ANOVA in any of the three brain regions examined.

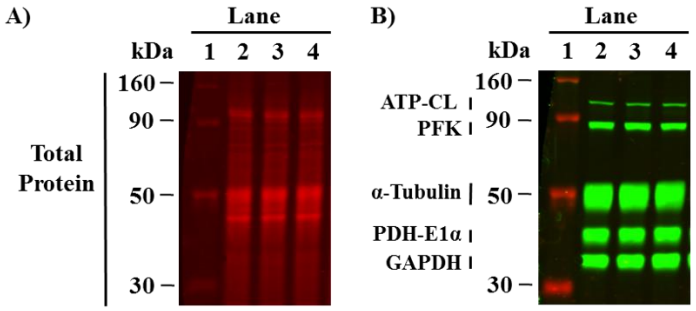

Figure 12: Representative images from a single PVDF membrane with multiplexed fluorescence signals densitometry of total protein stain and five individual proteins. (A) TP stain produced consist signal (red) across lanes loaded with different samples at 12 mg-protein/lane; and (B) densitometry of single-band targets were measured on the same membrane for: ATP-CL (122 KDa), PFK (85 KDa), α-tubulin (50 KDa), PDH-E1α (43 KDa) and GAPDH (36 KDa). Normalization to total protein allowed for between-gel comparisons along with wide linear range of detection and low signal variability as described earlier (Kirshner and Gibbs, 2018).

HPC

One-way ANOVAs revealed significant effects on levels of PFK ($F[5,39] = 4.4$, $p = 0.003$), α-tubulin ($F[5,18] = 10.08$, $p < 0.0001$) and PDH ($F[5,39] = 2.92$, $p = 0.025$), with trends for effects on levels of ATP-CL ($F[5,39] = 2.41$, $p = 0.06$) and GAPDH ($F[5,39] = 2.1$, $p = 0.08$). Post-hoc analyses revealed higher levels of PFK in VCD-1W than in OVX-1W ($p = 0.003$), and higher levels of PFK in OVX-6W than OVX-1W ($p = 0.026$). Levels of α-tubulin were higher in both VCD-6W and VCD-1W compared to P, D and OVX-1W and were higher in VCD-6W compared to OVX-6W ($p < 0.05$ for all comparisons). Levels of PDH were higher in OVX-1W than VCD-6W ($p = 0.01$).

Two-way ANOVAs of Model and Time (omitting the P and D data) revealed significant overall effects on levels of PFK ($F[1,26] = 3.19$, $p = 0.09$), α-tubulin ($F[1,12] = 18.04$, $p = 0.001$)and PDH ($F[1,26] = 7.56$, $p = 0.0107$). A main effect of Model was detected for α-tubulin ($F[3,12] = 6.1$, $p = 0.01$, VCD > OVX) and PDH ($F[1,26] = 7.56$, $p = 0.01$, OVX > VCD). A main effect of Time was detected for PDH ($F[1,26] = 9.83$, $p = 0.004$, 1w > 6w) and GAPDH ($F[1,26] = 6.5$, $p = 0.017$, 1w < 6w). There also was a significant Model * Time interaction on levels of PFK ($F[1,26] = 12.72$, $p = 0.0014$). Specifically, VCD-1W had higher levels of PFK than OVX-1W and VCD-6W had lower levels of PFK than OVX-6W. ANOVA also revealed a non-significant trend for an effect on ChAT activity in the HPC ($F[5,40] = 2.3$, $p = 0.063$) with lower activity in VCD-6W compared with diestrus ($p = 0.05$). No other effects on ChAT activity were detected in the HPC by one-way or by two-way analyses.

FCX

One-way ANOVAs revealed significant effects on levels of ATP-CL ($F[5,26] = 9.07$, $p = 0.0001$), PFK ($F[5,26] = 2.99$, $p = 0.029$) and PDH ($F[5,39] = 6.09$, $p = 0.0003$). Post-hoc analyses revealed that tissues collected at proestrus had higher levels of ATP-CL than tissues collected at diestrus ($p = 0.007$), OVX-1W ($p = 0.006$) and OVX-6W ($p = 0.004$). In addition, levels of ATP-CL in VCD-1W rats were significantly higher than in OVX-6W rats ($p = 0.04$) and higher in VCD-6W rats than in diestrus ($p = 0.004$), OVX-1W ($p = 0.003$) and OVX-6W ($p = 0.002$) rats. Levels of PFK were significantly higher in tissues collected at proestrus than in OVX-1W rats ($p = 0.035$). Levels of PDH likewise were significantly higher at proestrus than at diestrus or in OVX-1W, OVX-6W and VCD-6W rats (all $p < 0.03$). Two-way ANOVAs revealed an overall effect on ATP-CL ($F(3,18) = 8.55$, $p = 0.001$). A main effect of Model, but not time, was detected ($F[1,18] = 23.85$, $p = 0.0001$, VCD > OVX). No other significant main effects or interaction effects were detected. No significant effects on ChAT activity were detected in the FCX as a function of OVX or VCD treatments either by one-way or by two-way analyses.

STR

One-way ANOVA revealed significant effects on ATP-CL ($F[5,39] = 2.65$, $p = 0.037$), PFK ($F[5,39] = 8.2$, $p = 0.0001$) and β-actin ($F[5,18] = 4.91$, $p = 0.005$). Higher levels of ATP-CL expression were detected in VCD-1W compare to diestrus ($p = 0.045$) and PFK expression was higher in VCD-1W compare to proestrus ($p = 0.0005$), diestrus ($p = 0.011$), VCD-6W ($p = 0.0008$) and OVX-1W ($p = 0.014$). OVX-6W rats had significantly higher levels of PFK than proestrus ($p = 0.0076$), diestrus ($p = 0.017$), and VCD-6W rats ($p = 0.0116$). Expression of β-actin was higher

in OVX-1W rats than at diestrus ($p = 0.034$) and in OVX-6W rats than at diestrus ($p = 0.007$) or proestrus ($p = 0.04$).

Two-way ANOVA revealed a significant overall effect on levels of PFK ($F[3,26] = 11.71$, $p = 0.0001$). A significant Model * Time interaction ($F[1,26] = 33.88$, $p = 0.0001$) on the levels of PFK was detected. Post-hoc analysis revealed higher levels of PFK in VCD-1W as compare to OVX-1W, and lower PFK levels in VCD-6W than in OVX-6W. In addition, two-way ANOVA for ATP-CL showed a non-significant trend ($F(3,26)=2.36$, $p=0.095$). Tukey analysis revealed a main effect of Time on levels of ATP-CL ($F[1,26] = 6.07$, $p = 0.021$) where ATP-CL levels were higher at 1-week than at 6-weeks. No significant effects on ChAT activity were detected in the STR by either one-way or two-way analyses.

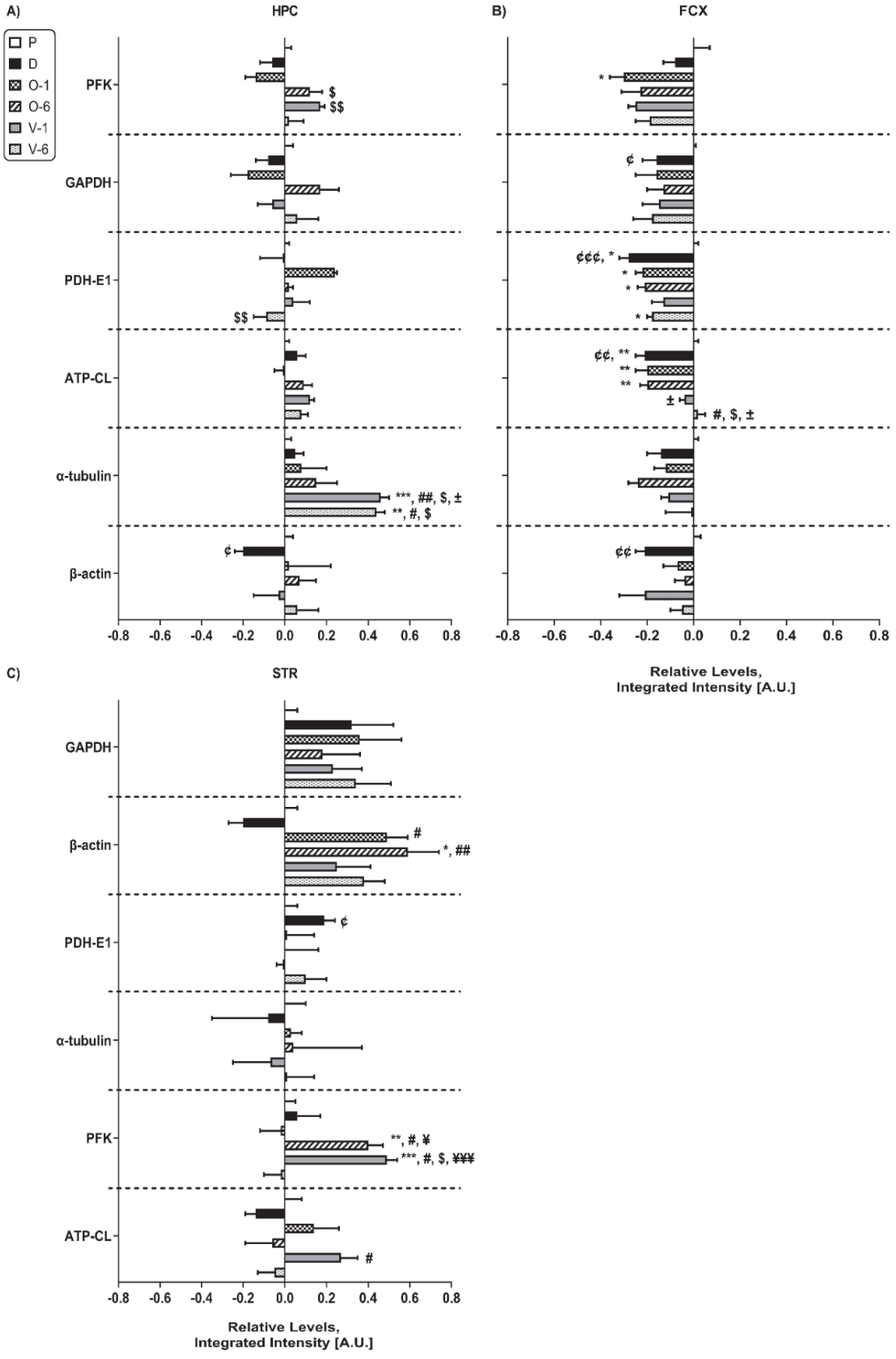
A)
HPC
P
D
O-1
O-6
V-1
V-6
PFK
GAPDH
PDH-E1
ATP-CL
α-tubulin
β-actin
$
$$
$$
***, ##, $, ±
**, #, $
¢
B)
FCX
*
¢
¢¢¢, *
*
*
*
¢¢, **
**
**
±
#, $, ±
¢¢
-0.8 -0.6 -0.4 -0.2 0.0 0.2 0.4 0.6 0.8
Relative Levels,
Integrated Intensity [A.U.]
C)
STR
GAPDH
β-actin
#
*, ##
PDH-E1
¢
α-tubulin
PFK
**, #, ¥
***, #, $, ¥¥¥
ATP-CL
#
-0.8 -0.6 -0.4 -0.2 0.0 0.2 0.4 0.6 0.8
Relative Levels,
Integrated Intensity [A.U.]

Figure 13: Effects of transitional (VCD; V) and surgical (OVX; O) menopause rat models on the expression of cytoskeletal proteins and enzymes involve in glucose metabolism and acetyl-CoA production. Gonadally intact rats at proestros (P) and diestrus (D) are used as controls. Bars shows Mean ± SEM on x-axis represent fractional difference relative to P. Expressios was evaluated in three brain regions: HPC (A), FCX (B) and STR (C) at two post-menopausal time points (1- and 6- weeks following the completion of VCD treatments or OVX surgery). Symbol repetition represents level of significance. One-way ANOVA: * Compare to P with * $p < 0.05$, ** $p < 0.01$, *** $p < 0.001$. Symbols are: * Compare to P, # Compare to D, $ Compare to OVX-1, ± Compare to OVX-6, § Compare to VCD-1, ¥ Compare to VCD-6. T-test between P and D shown by ¢.

Table 5: Serum hormone levels, ChAT activity and protein expression in three brain regions of rats from Experiment 1. Hormone levels are shown in [pg / mL], ChAT activity as [pmol of ACh synthesized / hr / mg protein] and protein expression relative to levels in rats at proestrus. One-way ANOVA analysis is shown with Mean ± SEM, number of animals (n) per group and a connecting-letters report. Levels not connected by same letter are significantly different. ND - Non Detectable (lower than limit of detection).

	Proestrus	Diestrus	OVX-1wk	OVX- 6wk	VCD- 1wk	VCD- 6wk	P-vs-D t-test and p-value	t-test easy sign	1-way ANOVA	1-way ANOVA easy sign
E2	50.57±4.45 A n=8	13.95±2.75 B C n=7	ND C n=7	ND C n=7	20.25±7.89 B n=7	8.3±5.23 B C n=8	t(13)=6.75 p=0.0001	p<0.001	F(5,38)=18.71 p=0.0001	p<0.001
T	186.88±43.22 A n=8	92.23±14.51 B n=7	ND C n=7	ND C n=7	42.62±25.79 B C n=6	57.73±18.98 B C n=8	t(12)=3.1 p<0.01	p<0.01	F(5,37)=6.84 p=0.0001	p<0.001
AD	196.48±42.92 A n=8	67±7.19 B n=7	ND B n=7	ND B n=7	87.27±31.87 B n=7	41.78±15 B n=8	t(13)=2.78 p=0.0156	p<0.05	F(5,38)=9.69 p=0.0001	p<0.001
					HPC					
ChAT	74.48±2.2 A B n=8	80.66±3.2 A n=8	71.33±3.55 A B n=7	74.88±2.15 A B n=7	69.83±3.78 A B n=8	68.13±2.71 B n=8	t(14)=-1.59 p=0.1338	NS	F(5,40)=2.3 p=0.0633	Trend (p<0.1)
ATP-CL	0.99±0.02 A n=8	1.06±0.04 A n=7	0.99±0.04 A n=7	1.09±0.04 A n=7	1.12±0.02 A n=8	1.08±0.03 A n=8	t(13)=-1.51 p=0.1555	NS	F(5,39)=2.41 p=0.0536	Trend (p<0.1)
PFK	0.98±0.03 A B n=8	0.94±0.06 A B n=7	0.86±0.05 B n=7	1.12±0.06 A n=7	1.17±0.02 A n=8	1.02±0.07 A B n=8	t(13)=0.65 p=0.5262	NS	F(5,39)=4.37 p=0.003	p<0.01
α-tubulin	0.99±0.03 C n=5	1.05±0.04 C n=3	1.08±0.12 C n=3	1.15±0.1 B C n=4	1.46±0.04 A n=5	1.44±0.04 A B n=4	t(6)=-1 p=0.3564	NS	F(5,18)=10.08 p=0.0001	p<0.001
PDH-E1	1±0.02 A B n=8	0.99±0.11 A B n=7	1.24±0.01 A n=7	1.02±0.02 A B n=7	1.04±0.08 A B n=8	0.91±0.06 B n=8	t(13)=0.09 p=0.9273	NS	F(5,39)=2.92 p=0.0247	p<0.05
β-actin	1.01±0.04 A n=5	0.8±0.04 A n=3	1.02±0.2 A n=3	1.07±0.08 A n=4	0.97±0.12 A n=5	1.06±0.1 A n=4	t(6)=3.25 p=0.0175	p<0.05	F(5,18)=0.75 p=0.5989	NS
GAPDH	1±0.04 A n=8	0.92±0.06 A n=7	0.82±0.08 A n=7	1.17±0.09 A n=7	0.94±0.07 A n=8	1.06±0.1 A n=8	t(13)=1.07 p=0.3039	NS	F(5,39)=2.1 p=0.0858	Trend (p<0.1)
					FCX					
ChAT	55.97±2.56 A n=8	52.38±2.85 A n=8	59.12±4.5 A n=7	54.3±4.19 A n=7	54.64±4.33 A n=8	55.25±3.23 A n=8	t(14)=0.93 p=0.3663	NS	F(5,40)=0.36 p=0.871	NS
ATP-CL	1±0.02 A n=6	0.79±0.04 B C n=4	0.8±0.05 B C n=5	0.8±0.03 C n=6	0.96±0.02 A B n=5	1.02±0.03 A n=6	t(8)=4.88 p=0.0012	p<0.01	F(5,26)=9.07 p=0.0001	p<0.001
PFK	1±0.07 A n=6	0.92±0.05 A B n=4	0.7±0.06 B n=5	0.77±0.08 A B n=6	0.75±0.03 A B n=5	0.81±0.06 A B n=6	t(8)=0.81 p=0.4415	NS	F(5,26)=2.99 p=0.0291	p<0.05
α-tubulin	1±0.02 A n=5	0.86±0.06 A n=3	0.88±0.05 A n=3	0.76±0.04 A n=4	0.89±0.03 A n=5	0.99±0.11 A n=4	t(6)=2.16 p=0.0737	Trend (p<0.1)	F(5,18)=2.22 p=0.0966	Trend (p<0.1)
PDH-E1	1±0.02 A n=8	0.72±0.04 B n=7	0.78±0.03 B n=7	0.79±0.03 B n=7	0.87±0.05 A B n=8	0.82±0.02 B n=8	t(13)=5.72 p=0.0001	p<0.001	F(5,39)=6.09 p=0.0003	p<0.001
β-actin	1±0.03 A n=5	0.79±0.04 A n=3	0.93±0.06 A n=3	0.96±0.04 A n=4	0.79±0.11 A n=5	0.95±0.05 A n=4	t(6)=4.16 p=0.0059	p<0.01	F(5,18)=1.73 p=0.1786	NS
GAPDH	1±0.01 A n=8	0.84±0.06 A n=7	0.84±0.09 A n=7	0.87±0.07 A n=7	0.85±0.07 A n=8	0.82±0.08 A n=8	t(13)=2.64 p=0.0204	p<0.05	F(5,39)=0.92 p=0.4776	NS
					STR					
ChAT	154.69±4.93 A n=8	169.61±8.26 A n=8	165.35±6.98 A n=7	174.46±6.26 A n=7	154.26±10.4 A n=8	160.29±8.93 A n=8	t(14)=-1.55 p=0.1435	NS	F(5,40)=1.04 p=0.4067	NS
ATP-CL	0.95±0.08 A B n=8	0.86±0.05 B n=7	1.14±0.12 A B n=7	0.94±0.13 A B n=7	1.27±0.08 A n=8	0.95±0.08 A B n=8	t(13)=0.89 p=0.3892	NS	F(5,39)=2.65 p=0.0372	p<0.05
PFK	0.96±0.05 C n=8	1.06±0.11 B C n=7	0.98±0.1 C n=7	1.4±0.07 A B n=7	1.49±0.05 A n=8	0.98±0.08 C n=8	t(13)=-0.84 p=0.4184	NS	F(5,39)=8.2 p=0.0001	p<0.001
α-tubulin	1.02±0.1 A n=5	0.92±0.27 A n=3	1.03±0.05 A n=3	1.04±0.33 A n=4	0.93±0.18 A n=5	1.01±0.13 A n=4	t(6)=0.4 p=0.7059	NS	F(5,18)=0.06 p=0.9967	NS
PDH-E1	0.95±0.06 A n=8	1.19±0.05 A n=7	1.01±0.13 A n=7	1±0.16 A n=7	0.99±0.03 A n=8	1.1±0.1 A n=8	t(13)=-2.66 p=0.0197	p<0.05	F(5,39)=0.77 p=0.5741	NS
β-actin	1.03±0.06 B C n=5	0.8±0.07 C n=3	1.49±0.1 A B n=3	1.59±0.15 A n=4	1.25±0.16 A B C n=5	1.38±0.1 A B C n=4	t(6)=2.27 p=0.0636	Trend (p<0.1)	F(5,18)=4.91 p=0.0052	p<0.01
GAPDH	0.97±0.06 A n=8	1.32±0.2 A n=7	1.36±0.2 A n=7	1.18±0.18 A n=7	1.23±0.14 A n=8	1.34±0.17 A n=8	t(13)=-1.74 p=0.1053	NS	F(5,39)=0.79 p=0.5614	NS

3.5 Discussion

The primary goal of this study was to characterize and compare the effects of two clinically relevant models of surgical (OVX) and transitional (VCD-treated) menopause, as well as treatment with different estrogen receptor agonists, on targets related to glucose utilization and energy production (GAPDH, PDH, PFK), cytoskeletal function and synaptic remodeling (ß-actin, α-tubulin), cytoplasmic acetyl-CoA production (ATP-CL), and choline acetyltransferase (ChAT) activity. Three regions of the brain were examined: the hippocampus because of its critical role in learning and memory consolidation, the frontal cortex because of its role in learning, attention, and cognitive performance, and the striatum because it is a major component of the extrapyramidal motor system and plays an important role in associative and motor learning.

3.5.1 **Experiment 1 (Chapter 3):**

Experiment 1 focused on differences between OVX and VCD models in comparison with gonadally intact rats collected at proestrus (P; i.e., when systemic levels of gonadal hormones are high) and diestrus (D; i.e., when systemic levels of gonadal hormones are low). In the FCX, significantly lower levels of GAPDH, PDH, ß-actin, and ATP-CL were detected at D vs. P, suggesting that in this region of the brain, fluctuations in these endpoints occur in association with the estrous cycle, and are lower at D when gonadal hormones also are low. In contrast, in the HPC only ß-actin was significantly reduced at D vs. P, and in the STR no significant differences between P and D were detected. These data demonstrate that physiological fluctuations in these endpoints occur across the estrous cycle but are brain region specific. In contrast, no significant differences in ChAT activity at P vs. D were detected in any of the three brain regions.

Loss of ovarian function likewise produced brain region-specific effects which varied as a function of time and model. Serum hormone levels were consistent with successful achievement of each of the two models of menopause. As expected, all three hormones were undetectable following OVX. In contrast, rats treated with VCD had low but detectable levels of E2, T and AD comparable to diestrus rats. This is consistent with prior reports (Acosta et al., 2009; Kirshner & Gibbs, 2018; Long et al., 2018, 2019) and with the preservation of androgen-producing stromal cells in the ovaries of VCD-treated rats (Lohff et al., 2005; Mayer et al., 2004; Van Kempen et al., 2011).

In the FCX, lower levels of protein targets were consistently detected at both the 1W and 6W time points following OVX and VCD treatments relative to proestrus rats. Several of these reached statistical significance including effects on PDH, PFK (OVX-1W), and ATP-CL (OVX-1W & OVX-6W). Notably, ATP-CL levels were not significantly lower in VCD-treated rats compared to rats at proestrus which may indicate that cytoplasmic production of acetyl-CoA from citrate is less effected in transitional vs. surgical menopause. Lower levels of PDH in both VCD-treated and OVX rats are consistent with the lower levels detected in the FCX at D vs. P and are consistent with the hypothesis that glycolysis in this region is reduced when gonadal hormone levels are low (Mauvais-Jarvis et al., 2013) (Resnick et al., 2009) (Brinton, 2008).

Very different results were detected in the HPC and STR. In the HPC, no significant effects on PDH or ATP-CL were detected; however, OVX rats had significantly higher levels of PFK at the 6W time point, whereas VCD-treated rats had significantly higher levels of PFK at the 1W time point and higher levels of α-tubulin at both the 1W and 6W time points. In the STR, OVX rats had significantly higher levels of ß-actin at both the 1W and 6W time points and higher levels

of PFK at the 6W time point, whereas VCD-treated rats had significantly higher levels of PFK and ATP-CL at the 1W time point. The higher levels of PFK in VCD-1W rats vs. OVX-6W rats suggests a fundamental difference between the two models in glucose utilization/response, i.e., that in the HPC and STR of VCD-treated rats the capacity to commit glucose to glycolysis is greater at the earlier time-point than in OVX rats.

Notably, neither of the menopausal models were associated with significant reductions in ChAT activity. This was surprising given studies showing fluctuations in ChAT mRNA in the MS and NBM across the estrous cycle (Frick & Berger-Sweeney, 2001; Gibbs, 1996; Kobayashi, Kobayashi, Kato, & Minaguchi, 1963), as well as higher levels of ChAT mRNA in the HPC and FCX of OVX rats following short term estrogen treatment (Gibbs et al., 2002; McMillan, Singer, & Dorsa, 1996). In the case of VCD-treated rats, the low levels of E2, T and AD may contribute to the maintenance of normal levels of ChAT activity. Also, changes in ChAT mRNA and protein may not translate to large changes in enzyme activity. ChAT enzyme activity represents the integrity of cholinergic capacity, but is not a direct measure of cholinergic function, and can be up-regulated or down-regulated by several factors, including cellular levels of acetyl co-A (Contestabile et al., 2008; Tomas Dobransky & Jane Rylett, 2003; T. Dobransky & Rylett, 2005; Rajkumar et al., 2016; Sha, Jin, Kopke, & Wu, 2004; Szutowicz et al., 2013). Chapter 4 contains additional discussions, limitations and summary of findings which are part of a larger context of treating OVX and VCD rats with selective estrogen agonists.

4.0 Impact of Selective Estrogen Agonists and Model of Menopause on the Expression of Enzymes Involve in Brain Metabolism, Acetyl-CoA Production and Integrity of Cholinergic Function

4.1 Introduction

This chapter describes the second of two experiments as continuation to Chapter 3. Here we evaluated the effects of estradiol and of selective estrogen receptor (ER) agonists on surgical (OVX) and transitional (VCD-treated) menopause rat models after 1 week and 6 weeks of continuous treatment. Rats received either vehicle control, E2, PPT (a selective ERα agonist), DPN (a selective ERß agonist), or G-1 (a selective GPR30 agonist) for 1 or 6 weeks following OVX or VCD treatment. These treatments regimen enabled us to provide a detailed description of changes that occurred on pivotal metabolic intersections in specific brain regions and generate a detailed comparison of the effects of selective activation of ERα, ERβ as well as GPER-1 on brain metabolism and neurochemical endpoints. We identify how selective activation of ERs change the expression of these metabolic enzymes and possibly reversing negative effects of menopause. These findings also enhance our understanding of how individual ERs mediate metabolic changes associated with different types of menopause (e.g. surgical Vs transitional) and can be used to create better strategies for estrogen therapy in women.

4.2 Materials and Methods

Most materials and methods for studies involve estrogen-agonist treatments were the same as described in Chapter 4 above. Several difference in the normalization and methodology between the two experiments are described below.

4.2.1 Experiment 2 – Effects of estrogen receptor agonists in OVX and VCD-treated rats

Rats were randomly assigned to either the OVX or VCD treatments as described above. Following surgery rats were provided 1-week recovery before the beginning of treatment with estrogen receptor (ER) agonist. Agonist treatments consisted of continuous subcutaneous (s.c.) administration of 17ß-estradiol (E2), PPT (a selective ERα agonist), DPN (a selective ERß agonist), G-1 (a selective GPR30 agonist), or vehicle. Agonists were dissolved in a vehicle containing 10% DMSO and 20% hydroxypropyl-ß-cyclodextran (HPCD) (Hammond et al., 2011) and were delivered at a dose of 5 µg/day by a miniosmotic pump (Alzet model 2002; Durect, Inc.) implanted s.c. in the dorsal neck region. Following pump implantation, ketofen (3mg/Kg, i.p.) was administrated twice per day for three days to reduce discomfort. Previous studies in our lab found this dose and route of administration to significantly enhance the acquisition of a spatial learning task (Hammond et al., 2009), as well as significant enhancement of potassium-stimulated ACh release in the hippocampus by E2 and G-1 (Hammond et al., 2011). Treatment groups and group sizes in experiment 2 are illustrated in Figure 9 and summarized in Table 7.

4.2.2 Statistical Analysis

Experiment 2:

Hormone levels and ChAT activity were analyzed by 3-way ANOVA with Model, Time, and Agonist Treatment as between factors. Effect of Agonist Treatment on ChAT activity were analyzed by a series of one-way ANOVAs comparing five Agonist Treatment groups per each menopausal model (OVX or VCD) and one of the two time points (1 or 6 weeks). For hormone levels, additional 2-way ANOVA analysis were performed using Agonist Treatment and Time as factors and omitting the data from OVX animals to avoid bias (as levels of E2, T and AD in ovariectomized animals are below detection limit). Significant main effects and interaction effects were further explored using Tukey post-hoc comparisons.

Statistical analysis of the WB data required a different approach. In experiment 2, each gel was organized to include representatives of all agonist treatments and the appropriate controls, using samples from one menopausal model (OVX or VCD) and one of the two time points (1 or 6 weeks). Results were normalized to the respective vehicle-treated controls included on the same gel. Thus, the quantified values represent fold-change relative to the control group for a specific model and time point (e.g., agonist effects for the OVX-1W group reflect fold change relative to OVX-1W controls; agonist effects for the VCD-1W group reflect fold change relative to VCD-1W controls, etc…). These data were each analyzed by one-way ANOVA. The lack of an internal control present on all gels prevents a between gel comparison. Hence this portion of the analysis does not capture potential differences between the four vehicle-treated control groups (OVX-1W-Veh, OVX-6W-Veh, VCD-1W-Veh and VCD-6W-Veh).

To mitigate this limitation a separate set of gels were run, each gel containing samples from the four different control groups. These data were normalized to the OVX-1W controls and reflect

fold differences between the control groups. Each of these blocks of data were then analyzed by 1-way ANOVA either comparing the controls, or comparing effects of agonists within each model and time-point. Post-hoc comparisons were conducted using the Tukey test.

4.3 Results

4.3.1 Experiment 2: Effects of estrogen receptor agonists

4.3.2 Serum hormone levels

Serum levels of E2, T and AD are graphed in Figure 14 and summarized in Table 6. Three-way ANOVAs revealed significant overall effects on E2 ($F[19,72] = 8.155$, $p<0.0001$), T ($F[19,66] = 4.585$, $p<0.0001$) and AD ($F[19,67] = 9.995$, $p<0.0001$) levels.

E2: As expected, E2 levels were significantly elevated in all rats that received E2 treatment. In all E2-treated OVX and VCD animals, levels of E2 after 1-week of treatment were in the physiological range (E2-1W M±SD = 86.5 ± 16.45 pg/mL) whereas levels after 6-weeks of treatment were well above the physiological range (E2-6W M±SD = 225.7 ± 16.45 pg/mL). ANOVA revealed significant main effects of Agonist Treatment ($F[4,72] = 30.16$, $p < 0.001$), Time ($F[1,72] = 7.97$, $p = 0.006$) and an Agonist Treatment * Time interaction ($F[4,72] = 6.2106$, $p = 0.0002$). Post Hoc analysis revealed that levels of E2 were significantly higher in both OVX and VCD rats treated with E2 than in any other groups. As expected, in OVX rats treated with vehicle, PPT, DPN or G-1, serum levels of E2, were extremely low or below the level of detection regardless of time point. E2 levels were higher in all E2-treated animals compared to non-E2 treated rats regardless of time point. Rats treated with E2 for 6-weeks had significantly higher serum E2 levels than all other groups.

T: As expected, levels of T were consistently higher in VCD-treated rats than in OVX rats. A three-way ANOVA analysis of T levels revealed main effects of Model ($F[1,66] = 63.49$, $p <$

0.0001), Agonist Treatment (F[4,66] = 2.67, p = 0.04) and a significant Model * Agonist Treatment interaction (F[4,66] = 2.67, p = 0.04). Post-hoc analysis showed that levels of T were significantly higher in VCD than in OVX rats. In addition, T levels in rats treated with E2 were significantly lower than in animals treated with DPN regardless of Time and Model.

AD: As with T, the three-way ANOVA of AD levels revealed significant main effects of Model (F[1,67] = 97.8, p > 0.0001), Agonist Treatment (F[4,67] = 7.06, p > 0.0001) and Time (F[1,67] = 10.4, p = 0.002), as well as a significant Model * Agonist interaction (F[4,67] = 7.37, p = 0.0001) and a significant Model * Time interaction (F[1,67] = 9.6, p = 0.0029).

Post-hoc analyses show that AD levels were significantly higher in VCD vs OVX rats regardless of Agonist Treatment and Time and higher at 1 week than 6 weeks regardless of Model and Agonist Treatment. Compared to Vehicle, levels of AD were higher in DPN-treated rats and lower in E2-treated rats.

In VCD animals, AD levels were higher at 1-week than at 6-weeks of continuous treatment. In addition, when collapsed across time, E2 treatment produced a significant lower and DPN a significant higher AD levels compare to vehicle-treated VCD rats.

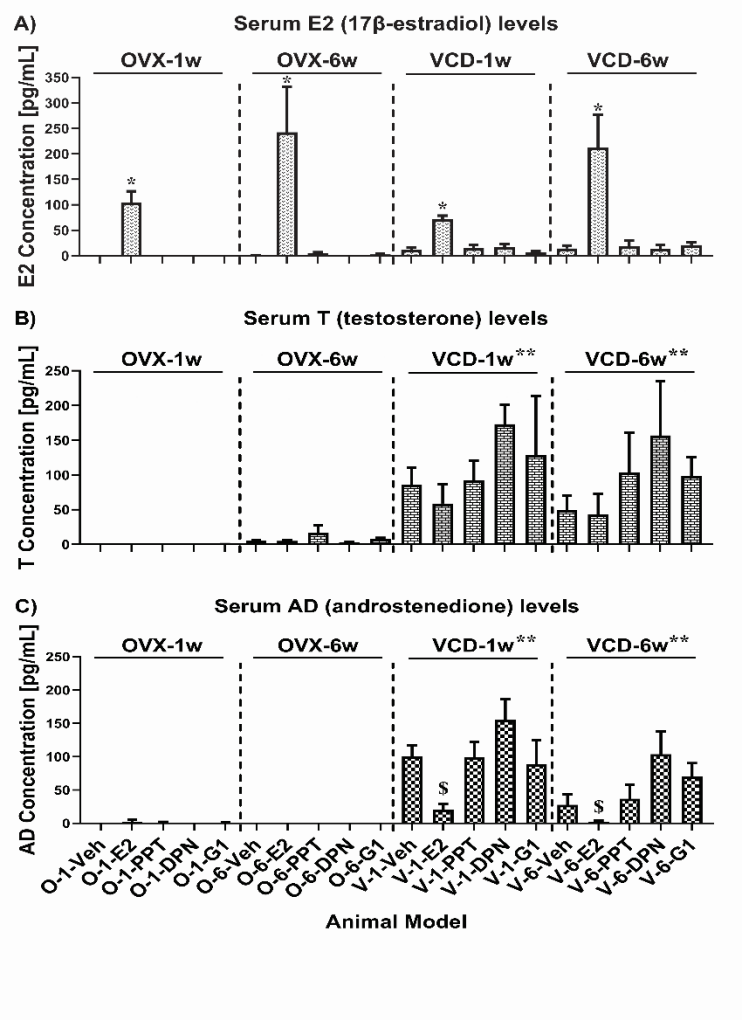

Figure 14: Serum hormone levels of (A) E2 (17β-estradiol), (B) T (testosterone) and (C) AD (androstenedione) in rat models of surgical (OVX; O) or transitional (VCD; V) menopause following treatment with estrogen receptor agonists. Data shown at two time points, following 1- and 6- weeks of continuous treatment with selective agonist: Vehicle, E2, PPT (a selective ERα agonist), DPN (a selective ERß agonist) and G-1 (a selective GPR30 agonist). One-way ANOVA: * $p < 0.0001$. Three-way ANOVA: ** $p < 0.0001$ for the main effect of model, where VCD animals had significantly higher levels of T and AD regardless of treatments and time. Treatment and time had no significant effect on levels T. For AD in VCD rats, E2-treated rats had significantly lower levels of AD than DPN-treated rats, regardless of time. Data shown as Mean ± SEM.

4.3.3 Effects of ER Agonists on ChAT activity in each brain region as a function of model and time

3-way ANOVAs revealed significant overall effects on ChAT activity in the HPC ($F[19,73] = 3.033$, $p = 0.0003$) and FCX ($F[19,73] = 2.921$, $p = 0.0005$), but not the STR ($F[19,73] = 1.099$, $p = 0.3701$). Effects differed among brain regions as well as a function of model and time. The majority of effects on ChAT were detected in the HPC. These data are shown in Figure 15 and summarized in Table 7 and are organized by brain region below.

HPC

ANOVA revealed significant main effects of Model ($F[1,73] = 5.09$, $p = 0.03$, VCD > OVX), and Agonist Treatment ($F[4,73] = 2.64$, $p = 0.04$), as well as a significant Agonist Treatment * Time interaction ($F[4,73] = 3.16$, $p = 0.02$), and a significant 3-way interaction of Model * Time * Agonist Treatment ($F[4,73] = 4.73$, $p = 0.002$). Post-hoc analyses revealed that levels of ChAT were significantly higher in rats treated with, E2, G1 and PPT relative to DPN or vehicle when collapsed across Model and Time. ChAT activity in E2-treated rats was higher after 6-weeks vs. 1-week of treatment when collapsed across Model. ChAT activity in rats treated with PPT was highest after 1-week of treatment.

The effects of Agonist Treatment and Time also differed as a function of Model. For example, in VCD-treated rats ChAT activity in the 1-week controls was significantly higher than at 6-weeks and significantly higher than in OVX controls at both 1-week and 6-weeks. ChAT activity in VCD rats treated with PPT for 1 week were significantly higher than all other agonist treatment groups in both OVX and VCD-treated rats at both the 1- and 6- week time points. In addition, VCD-treated rats treated with G1 for 6-weeks had significantly higher levels of ChAT

activity than OVX-1W-Veh, OVX-6W-Veh, OVX-1W-E2, VCD-6W-Veh and VCD-6W-PPT. (summarized in Figure 15 and Table 7)

FCX

ANOVA revealed a significant main effect of Time ($F[1,73] = 15.7$, $p = 0.0002$, 1W > 6W) and a trend for an effect of Model ($F[1,73] = 3.1$, $p = 0.082$, NS, VCD > OVX). A significant Treatment * Time interaction also was detected ($F[4,73] = 3.9$, $p = 0.006$) where ChAT activity was lower at 6-weeks than at 1-week in vehicle-, PPT- and G-1-treated rats, but not in E2- or DPN-treated rats. No other significant main effects or interactions were detected.

STR

No main effects were detected on ChAT activity; however, the interaction of Agonist Treatment * Time showed a strong trend ($F(4,73) = 2.4098$, $p = 0.057$) where rats treated with PPT for 1-week had higher ChAT activity than vehicle- and DPN-treated rats at 1-week and E2-treated rats at 6-weeks.

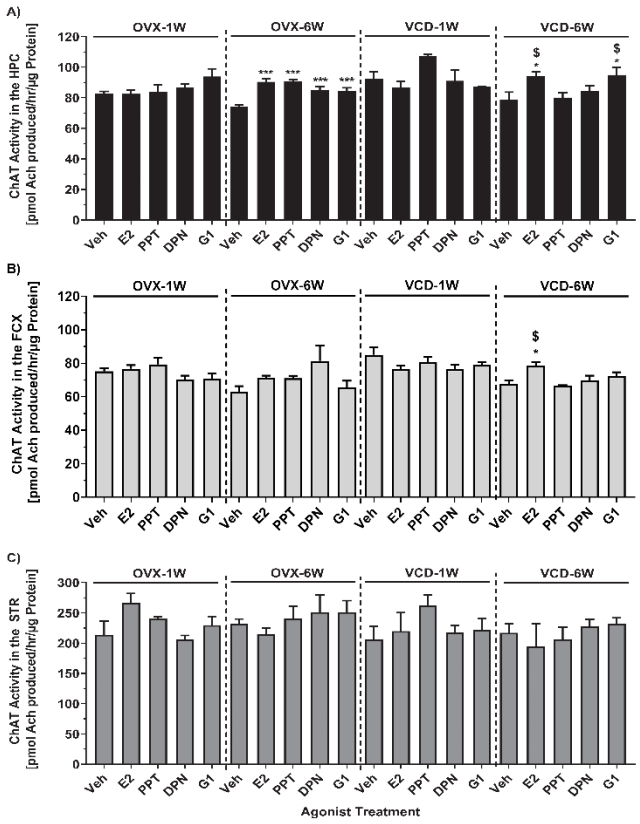

Figure 15: Activity of choline acetyltransferase (ChAT) in HPC, FCX and STR following contentious treatments with selective estrogen agonists for 1- and 6- weeks in rat models of surgical (OVX) and transitional (VCD) menopause. In the HPC, following 6-weeks of treatment in OVX rats, all four treatments resulted in higher ChAT activity than vehicle (OVX-6w-HPC) whereas in VCD only E2 and G1, but not PPT and DPN, had higher ChAT activity than vehicle. Also notable is the menopause model difference in the FCX where following 6-weeks of E2 treatment ChAT activity was higher than vehicles only in VCD animals (VCD-6W-E2) but not OVX (OVX-6W-E2). One-way ANOVA: * $p < 0.05$ and ** $p < 0.001$ compare to Veh; \$ $p < 0.05$ compare to PPT. Data shown as Mean ± SEM.

4.3.4 Effects of agonist treatments on target protein levels in each brain region as a function of model and time point

Treatment with ER agonists produced significant effects on the levels of target proteins in all three brain regions. Effects differed as a function of both model and time-point. These data are summarized in Figures 16, 17and 18 and in Table 7 and are organized by brain region below. Within each region results are organized by analysis of OVX-1W, OVX-6W, VCD-1W, and VCD-6W. Note that analysis of these data are limited to one-way ANOVAs due to limitations in the design and collection of the WB data as described under Methods. Only significant effects and trends are reported.

HPC:

OVX-1W: Significant effects of Agonist Treatments were detected on levels of ATP-CL ($F[4,15] = 15.04$, $p = 0.0001$), PFK ($F[4,15] = 53.32$, $p = 0.0001$) and GAPDH ($F[4,15] = 14.66$, $p = 0.0001$). Post-hoc analyses revealed significantly lower levels of both ATP-CL and PFK, and significantly higher levels of GAPDH in E2-treated rats vs. controls. DPN and G-1 treated rats also had significantly lower levels of ATP-CL and PFK and higher levels of GAPDH than controls. GAPDH levels also were significantly higher in PPT-treated rats vs. controls. With respect to PDH, the overall effect of Agonist Treatment was significant ($F[4,15] = 3.38$, $p = 0.036$). Strong trends for reductions in PDH levels in E2- ($p = 0.08$) and G-1-treated rats ($p = 0.054$) vs. controls were detected.

OVX-6W: Significant effects of Agonist Treatments were detected on levels of α-tubulin ($F[4,19] = 33.89$, $p = 0.0001$), PDH ($F[4,19] = 4.06$, $p = 0.015$) and GAPDH ($F[4,19] = 6.93$, $p =$

0.001). Post-hoc analyses detected no significant effects of E2, however, there was a trend for lower levels of GAPDH in E2-treated rats than in controls ($p = 0.08$). Similarly, G-1 treatment showed a trend for lower GAPDH levels in E2-treated rats than in controls ($p = 0.055$). Rats treated with DPN had significantly higher levels of GAPDH and α-tubulin compared to all other agonist treatments (E2, PPT and G-1). Rats treated with DPN also had higher levels of PDH than rats treated with E2- or G-1.

VCD-1W: A significant effect of Agonist Treatment was detected on α-tubulin levels ($F[4, 19] = 0.28$, $p = 0.0001$), but not the other targets. Levels of α-tubulin in E2 treated rats were significantly lower than in controls or in rats treated with PPT or G-1. PPT-treated rats had significantly lower levels of α-tubulin than controls and rats treated with DPN.

VCD-6W: Significant effects of Agonist Treatments were detected on α-tubulin ($F[4,18] = 21.9$, $p = 0.0001$) and PDH ($F[4,18] = 5.06$, $p = 0.007$). Post-hoc analysis revealed that E2-treated animals had significantly lower levels of α-tubulin than controls and lower levels of PDH then PPT- and DPN- treated rats. Rats treated with PPT had significantly lower levels of α-tubulin than controls and DPN-treated rats.

FCX:

OVX-1W: A significant effect of Agonist Treatment was detected on levels of ATP-CL ($F[4,16] = 6.8$, $p = 0.002$), but not the other targets. Post-hoc analysis revealed significantly lower levels of ATP-CL in E2-treated rats vs. controls. DPN and G-1 treated rats also had significantly lower levels of ATP-CL than controls. Trends for overall effects of Agonist Treatment on PFK

($F[4,16] = 2.58$, $p = 0.08$) and α-tubulin ($F[4,16] = 2.77$, $p = 0.06$) also were detected. Post-hoc analyses revealed that DPN-treated rats had significantly lower levels of PFK vs. controls ($p = 0.04$).

OVX-6W: Significant effects of Agonist Treatments were detected on levels of ATP-CL ($F[4,19] = 3.79$, $p = 0.02$), PFK ($F[4,19] = 4.65$, $p = 0.009$) and α-tubulin ($F[4,19] = 6.5$, $p = 0.002$). No significant differences between E2-treated rats and controls were detected. DPN treated rats had significantly lower levels of ATP-CL and PFK than G-1-treated rats. α-tubulin levels were significantly higher in DPN-treated rats than in E2-, PPT- or G-1 treated rats.

VCD-1W: Significant effects of Agonist Treatments were detected on levels of α-tubulin ($F[4,19] = 7.31$, $p = 0.001$), PDH ($F[4,19] = 15.39$, $p = 0.0001$) and GAPDH ($F[4,19] = 13.09$, $p = 0.0001$). No significant differences between E2-treated rats and controls were detected; however, E2-treated rats had lower levels of PDH and GAPDH than PPT-, DPN- and G-1 treated rats. G-1 treated rats had significantly lower levels of α-tubulin than controls. DPN-treated rats had significantly higher levels of α-tubulin than E2-, PPT- and G-1-treated rats.

VCD-6W: Significant effects of Agonist Treatments were detected on levels of PDH ($F[4,19] = 4.23$, $p = 0.013$) and GAPDH ($F[4,19] = 4.05$, $p = 0.015$). E2-treated rats did not differ significantly from any or the other treatment groups. G-1 treated rats had significantly higher levels of PDH and GAPDH than DPN-treated rats.

STR:

OVX-1W: A significant effect of Agonist Treatment was detected on levels of GAPDH ($F[4,16] = 7.4$, $p = 0.0014$), but not the other targets. E2-treated rats did not differ significantly from controls. G-1 treated rats had higher levels of GAPDH than vehicle- and E2- treated rats. GAPDH levels also were higher in DPN-treated vs. E2-treated rats.

OVX-6W: Significant effects of Agonist Treatments were detected on levels of PFK ($F[4,19] = 5.77$, $p = 0.0032$) and PDH ($F[4,19] = 13.66$, $p = 0.0001$). E2-treated rats did not differ significantly from controls. PPT treated rats had significantly lower levels of PFK than E2-, DPN- and G-1 treated rats. DPN-treated rats had significantly higher levels of PDH than all other groups. PDH levels also were higher in E2- vs. PPT- treated rats.

VCD-1W: Significant effects of Agonist Treatments were detected on levels of ATP-CL ($F[4,20] = 6.08$, $p = 0.002$) and α-tubulin ($F[4,20] = 9.68$, $p = 0.0002$). E2-treated rats did not differ significantly from controls. DPN-treated rats had significantly lower levels of ATP-CL relative to PPT- and G-1 treated rats. PPT- and G-1 treated rats had significantly lower levels of PDH than vehicle- and DPN- treated rats. PDH levels also were lower in G-1- vs. E2-treated rats.

VCD-6W: A significant effect of Agonist Treatment was detected on levels of ATP-CL ($F[4,19] = 3.2$, $p = 0.036$), but not the other targets. E2-treated rats did not differ significantly from controls. DPN treated rats had significantly lower levels of ATP-CL than vehicle-treated controls.

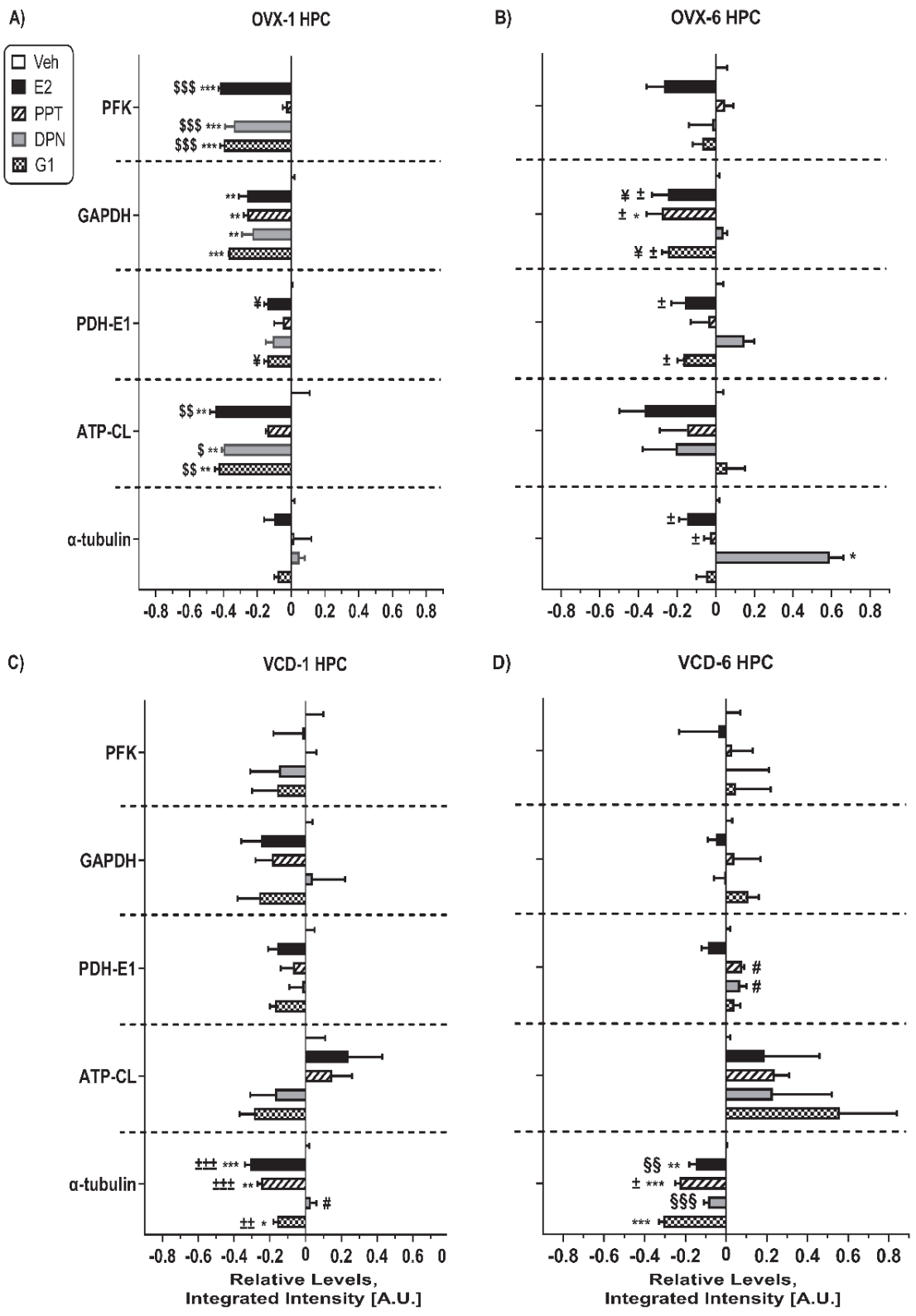
A)
OVX-1 HPC
Veh
E2
PPT
DPN
G1
PFK
GAPDH
PDH-E1
ATP-CL
α-tubulin
-0.8 -0.6 -0.4 -0.2 0 0.2 0.4 0.6 0.8
B)
OVX-6 HPC
-0.8 -0.6 -0.4 -0.2 0 0.2 0.4 0.6 0.8
C)
VCD-1 HPC
PFK
GAPDH
PDH-E1
ATP-CL
α-tubulin
-0.8 -0.6 -0.4 -0.2 0 0.2 0.4 0.6 0
Relative Levels,
Integrated Intensity [A.U.]
D)
VCD-6 HPC
-0.8 -0.6 -0.4 -0.2 0 0.2 0.4 0.6 0.8
Relative Levels,
Integrated Intensity [A.U.]

Figure 16: Effects of 1- and 6- weeks of continuous treatment with selective estrogen agonists on the expression of cytoskeletal proteins and enzymes involve in glucose metabolism and acetyl-CoA production in the HPC of transitional (V) and surgical (O) menopause rat models. Changes in expression were evaluated at two time points representing 1- and 6- weeks of continuous treatments with either Vehicle, E2, PPT (a selective ERα agonist), DPN (a selective ERß agonist) and G-1 (a selective GPR30 agonist). Bars shows Mean ± SEM on x-axis represents fractional difference relative to vehicle treated group. Symbol repetition represents level of significance. One-way ANOVA: * Compared to Vehicle with * $p < 0.05$, ** $p < 0.005$, *** $p < 0.0001$. Symbols are: * compared to Vehicle; # compared to E2; $ compared to PPT; ± compared to DPN; § compared to G1; Dunnett's test: ¥ compared to Vehicle.

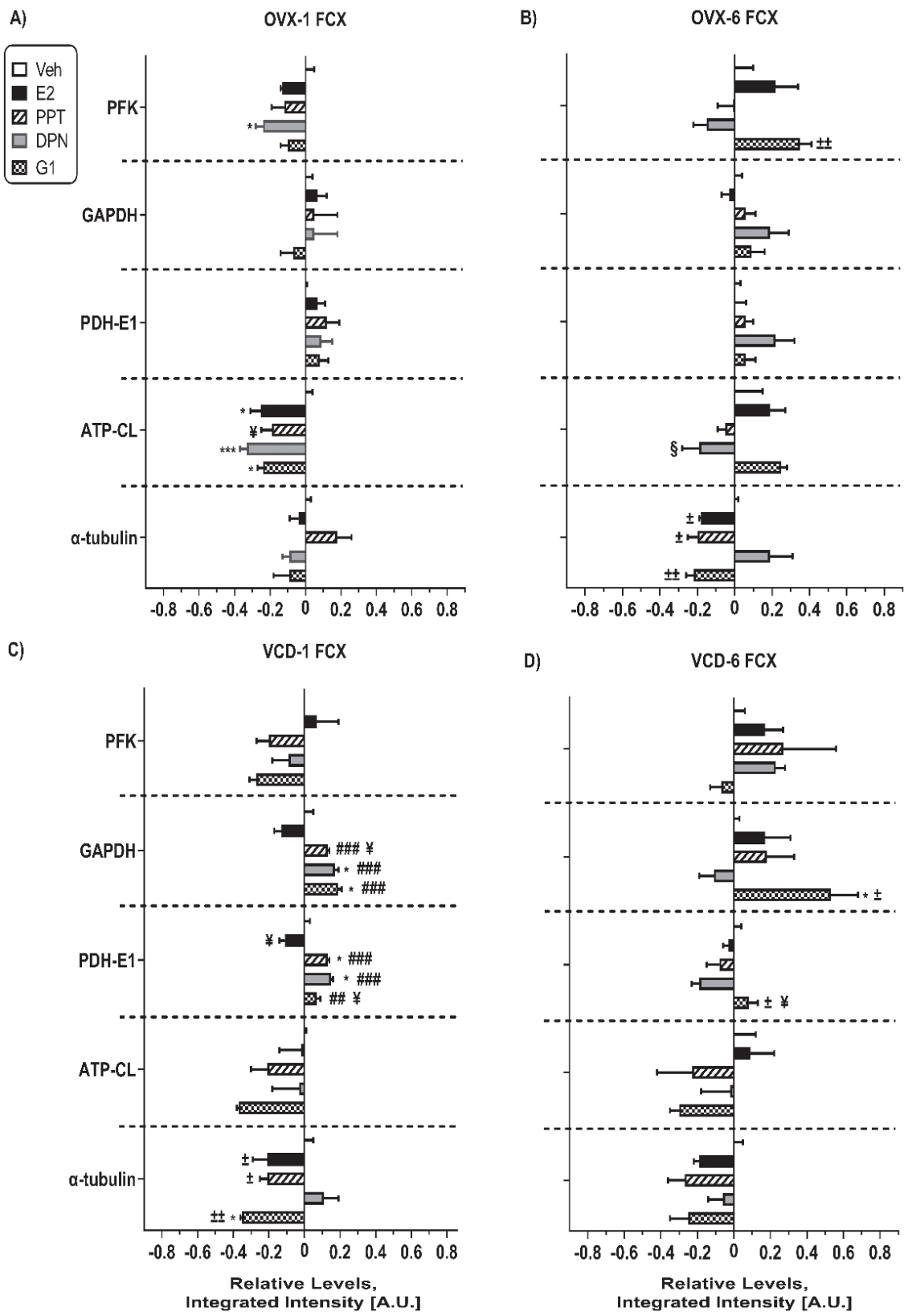
A)
OVX-1 FCX
B)
OVX-6 FCX
Veh
E2
PPT
DPN
G1
PFK
GAPDH
PDH-E1
ATP-CL
α-tubulin
-0.8 -0.6 -0.4 -0.2 0 0.2 0.4 0.6 0.8
C)
VCD-1 FCX
D)
VCD-6 FCX
Relative Levels,
Integrated Intensity [A.U.]

Figure 17: Effects of 1- and 6- weeks of continuous treatment with selective estrogen agonists on the expression of cytoskeletal proteins and enzymes involve in glucose metabolism and acetyl-CoA production in the FCX of transitional (V) and surgical (O) menopause rat models. Changes in expression were evaluated at two time points representing 1- and 6- weeks of continuous treatments with either Vehicle, E2, PPT (a selective ERα agonist), DPN (a selective ERß agonist) and G-1 (a selective GPR30 agonist). Bars shows Mean ± SEM on x-axis represents fractional difference relative to vehicle treated group. Symbol repetition represents level of significance. One-way ANOVA: * Compared to Vehicle with * $p < 0.05$, ** $p < 0.005$, *** $p < 0.0001$. Symbols are: * compared to Vehicle; # compared to E2; $ compared to PPT; ± compared to DPN; § compared to G1; Dunnett's test: ¥ compared to Vehicle.

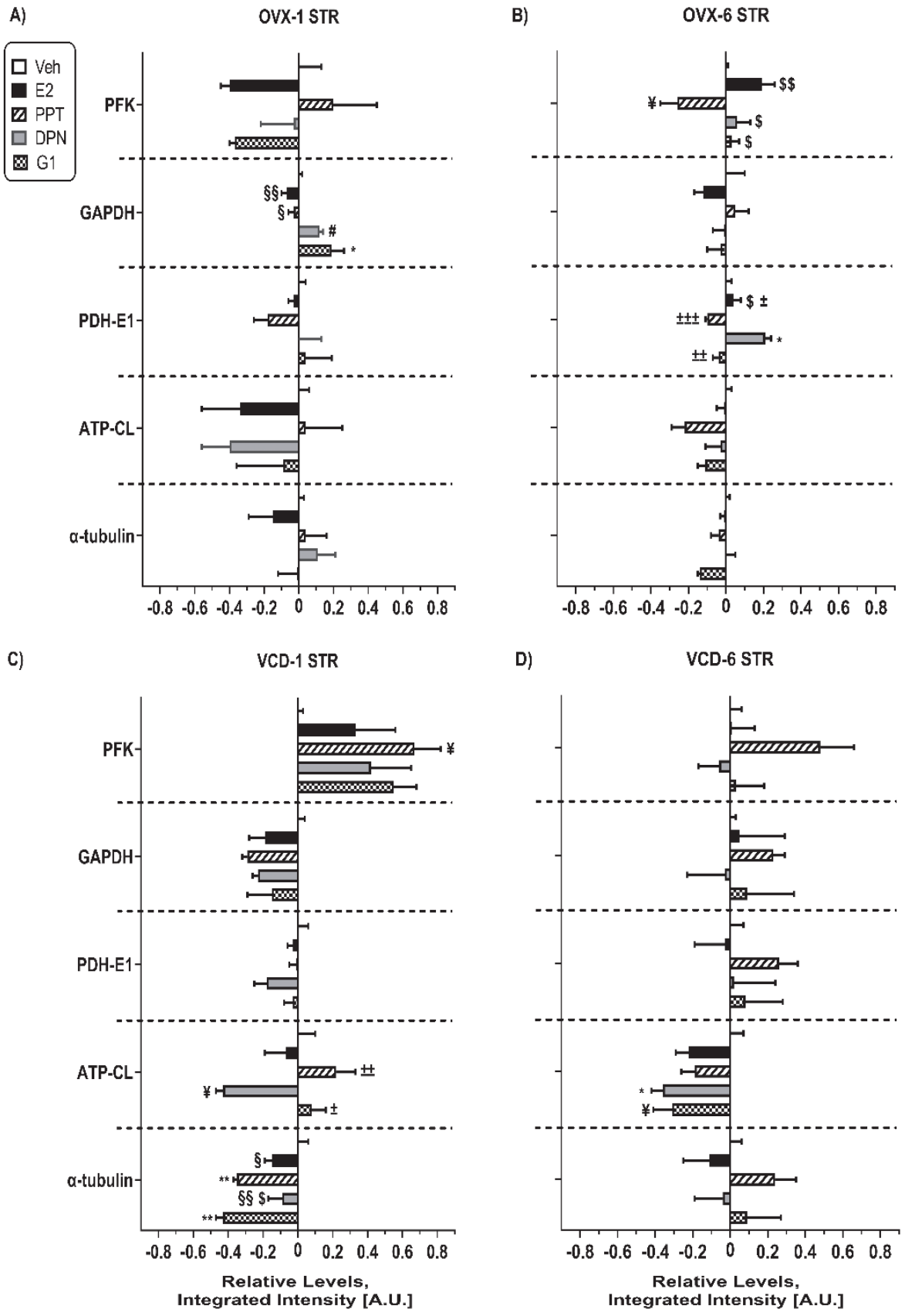
A)
OVX-1 STR
B)
OVX-6 STR
Veh
E2
PPT
DPN
G1
PFK
GAPDH
PDH-E1
ATP-CL
α-tubulin
-0.8 -0.6 -0.4 -0.2 0 0.2 0.4 0.6 0.8
C)
VCD-1 STR
D)
VCD-6 STR
Relative Levels,
Integrated Intensity [A.U.]

Figure 18: Effects of 1- and 6- weeks of continuous treatment with selective estrogen agonists on the expression of cytoskeletal proteins and enzymes involve in glucose metabolism and acetyl-CoA production in the STR of transitional (V) and surgical (O) menopause rat models. Changes in expression were evaluated at two time points representing 1- and 6- weeks of continuous treatments with either Vehicle, E2, PPT (a selective ERα agonist), DPN (a selective ERß agonist) and G-1 (a selective GPR30 agonist). Bars shows Mean ± SEM on x-axis represents fractional difference relative to vehicle treated group. Symbol repetition represents level of significance. One-way ANOVA: * Compared to Vehicle with * $p < 0.05$, ** $p < 0.005$, *** $p < 0.0001$. Symbols are: * compared to Vehicle; # compared to E2; $ compared to PPT; ± compared to DPN; § compared to G1; Dunnett's test: ¥ compared to Vehicle.

4.3.5 **Comparison of vehicle controls as a function of model and time point**

As mentioned under Methods, a separate set of gels were needed to capture potential differences among the four vehicle-treated control groups in Experiment 2. These data are summarized in Figure 19 and Table 8. Several effects of model and time are worth noting. For example, in the HPC levels of GAPDH and ATP-CL were significantly higher at 6 weeks than at 1 week in both models. Levels of PDH at 1 week were lower in VCD-treated rats than in OVX rats. Levels of α-tubulin were lower at 6 weeks than at 1 week in OVX rats, but not in VCD-treated rats, and levels of PFK were higher at 6 weeks than at 1 week in OVX rats, but were higher at 1 week than at 6 weeks in VCD-treated rats. Fewer differences were detected in the FCX and STR. In the FCX levels of ATP-CL were higher in VCD-treated rats than in OVX rats, and were significantly higher in VCD-treated rats at the 6-week time point than in all other groups. In the STR, levels of PFK were substantially higher in VCD-treated rats at the 1-week time point than in all other groups. Levels had declined substantially by 6 weeks. Levels of PFK at the 6-week time point were significantly lower than levels at the 1-week time point for both models. These data demonstrate that the levels of glycolytic enzymes and other target proteins can change significantly

over time following the loss of ovarian function, and that in some cases the changes differ between surgical and transitional models of menopause. These differences need to be considered when comparing effects of agonists across models and time-points.

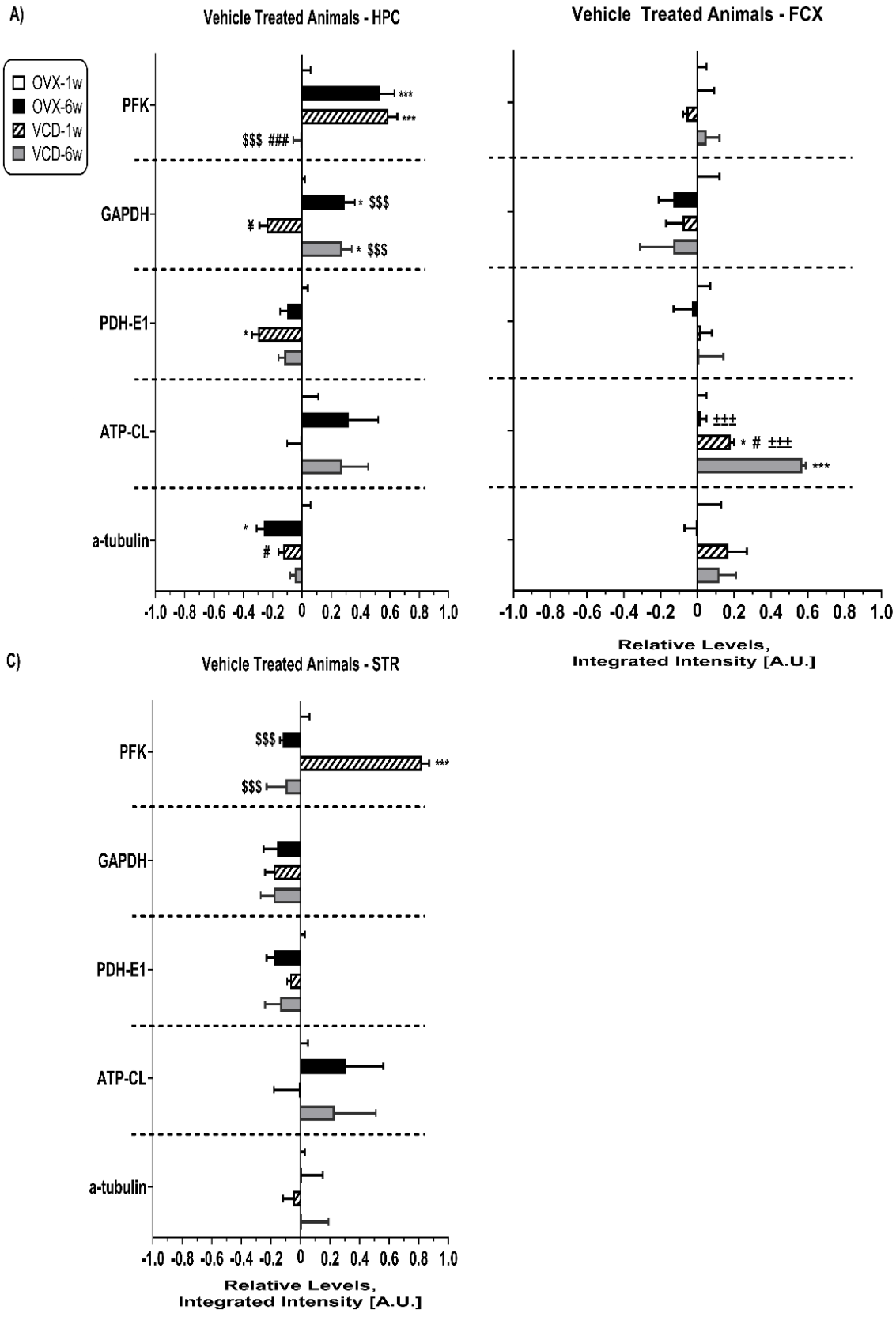
A)
Vehicle Treated Animals - HPC
Vehicle Treated Animals - FCX
OVX-1w
OVX-6w
VCD-1w
VCD-6w
PFK
GAPDH
PDH-E1
ATP-CL
a-tubulin
-1.0 -0.8 -0.6 -0.4 -0.2 0 0.2 0.4 0.6 0.8 1.0
Relative Levels,
Integrated Intensity [A.U.]
C)
Vehicle Treated Animals - STR
PFK
GAPDH
PDH-E1
ATP-CL
a-tubulin
-1.0 -0.8 -0.6 -0.4 -0.2 0 0.2 0.4 0.6 0.8 1.0
Relative Levels,
Integrated Intensity [A.U.]

Figure 19: Effects of menopausal rat models and duration of vehicle treatments on the expression of cytoskeletal proteins and enzymes involve in glucose metabolism and acetyl-CoA production. OVX (O) and VCD (V) animals were implanted with sub cutaneous miniosmotic pump for continuous release of Vehicle solution (10% DMSO and 20% hydroxypropyl-ß-cyclodextran (HPCD)) for 1- or 6- weeks. Bars shows Mean ± SEM on x-axis represents fractional difference relative to OVX-1W-Vehicle group. One-way ANOVA: symbol repetition represents level of significance such that * $p < 0.05$, ** $p < 0.005$ and *** $p < 0.0001$ compared to OVX-1w; # compared to OVX-6w, $ compared to VCD-1w, ± compared to VCD-6w; Dunnett's test: ¥ compared to OVX-1wk.

Table 6: Serum hormone levels of estradiol (E2), testosterone (T) and androstendion (AD) of rats in Experiment 2. Hormone levels are shown in [pg / mL] as Mean ± SEM and number of animals (n), together with connecting-letters report from one-way ANOVA analysis for agonist treatment.

Levels not connected by same letter are significantly different. ND - Non detectable (lower than limit of detection)

Statistics and 1-way ANOVA of Hormones of Aim 2 Animals														
	OVX-1W	OVX-1W-E2	OVX-1W-PPT	OVX-1W-DPN	OVX-1W-G1	F(a,b)=c	p-value	OVX-6W	OVX-6W-E2	OVX-6W-PPT	OVX-6W-DPN	OVX-6W-G1	F(a,b)=c	p-value
E2	ND B n=5	104.44±22.46 A n=4	ND B n=4	ND B n=4	ND B n=4	F(4,16)=23.3334	0.0001	ND B n=5	242.65±88.68 A n=4	4.55±2.28 B n=5	ND B n=5	ND B n=5	F(4,19)=9.6699	0.0002
T	ND A n=5	ND A n=4	ND A n=4	ND A n=3	ND A n=4	N/A	N/A	ND A n=5	ND A n=4	16.46±10.89 A n=5	ND A n=5	ND A n=5	F(4,19)=1.0596	0.4034
AD	ND A n=3	ND A n=4	ND A n=4	ND A n=4	ND A n=5	N/A	N/A	ND 0 n=5	ND 0 n=4	ND 0 n=5	ND 0 n=5	ND 0 n=5	N/A	N/A
	VCD-1W	VCD-1W-E2	VCD-1W-PPT	VCD-1W-DPN	VCD-1W-G1	F(a,b)=c	p-value	VCD-6W	VCD-6W-E2	VCD-6W-PPT	VCD-6W-DPN	VCD-6W-G1	F(a,b)=c	p-value
E2	11.68±4.64 B n=5	72.13±6.58 A n=5	14.66±6.33 B n=5	17.46±5.85 B n=5	6.7±2.41 B n=4	F(4,19)=23.5287	0.0001	14.41±5.82 B n=5	212.27±65.15 A n=5	19.02±11.07 B n=4	13.69±7.44 B n=4	21.09±6.01 B n=5	F(4,18)=7.5905	0.0009
T	85.89±24.66 A n=3	58.75±27.93 A n=5	92.13±28.51 A n=5	173.28±27.51 A n=5	128.79±84.57 A n=3	F(4,16)=1.6009	0.2224	49.45±20.89 A n=5	43.36±29.52 A n=5	103.52±57.9 A n=3	156.87±78.48 A n=3	98.64±27.24 A n=5	F(4,16)=1.3188	0.3053
AD	100.51±16.71 A B n=3	20.21±8.6 B n=5	99.53±22.49 A B n=5	155.16±30.75 A n=5	88.6±36.48 A B n=3	F(4,16)=4.6043	0.0115	27.76±15.37 A B n=5	2.22±1.66 B n=5	36.83±20.84 A B n=3	103.63±34.55 A n=4	70.05±20.17 A B n=5	F(4,17)=3.9382	0.0193

Table 7: Effects of menopause model, agonist treatment and duration of treatment on ChAT activity and protein expressions in three brain regions. Data shown as Mean ± SEM and number of animals (n) together with connecting-letters report of one-way ANOVA analysis for agonist treatments. Post-hoc Tukey analysis are reported in the results section. ChAT activity shown as [pmol of ACh synthesized / hr / mg protein] and for each model and time point group protein expressions are relative to rats treated with oil alone. Levels not connected by same letter are significantly different.

HPC	HPC	HPC	HPC	HPC	HPC	HPC	HPC
	OVX-1W	OVX-1W-E2	OVX-1W-PPT	OVX-1W-DPN	OVX-1W-G1	1-way ANOVA	1-way ANOVA easy sign
ChAT	82.78±1.38 A n=5	82.46±2.56 A n=4	83.81±4.85 A n=4	86.68±2.34 A n=4	93.87±5.08 A n=4	F(4,16)=1.9 p=0.1591	NS
ATP-CL	0.95±0.07 A n=5	0.55±0.03 B n=3	0.86±0.01 A n=4	0.6±0.01 B n=4	0.57±0.02 B n=4	F(4,15)=15.04 p=0.0001	p<0.001
PFK	1±0 A n=5	0.58±0.01 B n=3	0.97±0.02 A n=4	0.66±0.05 B n=4	0.6±0.02 B n=4	F(4,15)=53.32 p=0.0001	p<0.001
α-tubulin	1±0.02 A n=5	0.9±0.06 A n=3	1.02±0.1 A n=4	1.05±0.03 A n=4	0.92±0.02 A n=4	F(4,15)=1.22 p=0.3442	NS
PDH-E1	1±0.01 A n=5	0.86±0.02 A n=3	0.95±0.05 A n=4	0.89±0.04 A n=4	0.86±0.02 A n=4	F(4,15)=3.38 p=0.0368	p<0.05
GAPDH	1±0.02 A n=5	0.74±0.05 B n=3	0.74±0.02 B n=4	0.77±0.06 B n=4	0.63±0 B n=4	F(4,15)=14.66 p=0.0001	p<0.001

HPC	HPC	HPC	HPC	HPC	HPC	HPC	HPC
	OVX-6W	OVX-6W-E2	OVX-6W-PPT	OVX-6W-DPN	OVX-6W-G1	1-way ANOVA	1-way ANOVA easy sign
ChAT	74.37±0.91 B n=5	90.42±2.25 A n=4	90.71±1.06 A n=5	84.95±2.33 A n=5	84.34±2.16 A n=5	F(4,19)=13.29 p=0.0001	p<0.001
ATP-CL	1±0.04 A n=5	0.63±0.13 A n=4	0.85±0.14 A n=5	0.79±0.17 A n=5	1.06±0.09 A n=5	F(4,19)=1.69 p=0.1935	NS
PFK	1.04±0.06 A n=5	0.73±0.09 A n=4	1.05±0.04 A n=5	0.98±0.12 A n=5	0.93±0.05 A n=5	F(4,19)=2.23 p=0.1037	NS
α-tubulin	0.99±0.02 B n=5	0.85±0.04 B n=4	0.97±0.03 B n=5	1.59±0.07 A n=5	0.95±0.05 B n=5	F(4,19)=33.89 p=0.0001	p<0.001
PDH-E1	0.98±0.04 A B n=5	0.84±0.07 B n=4	0.96±0.09 A B n=5	1.15±0.05 A n=5	0.83±0.03 B n=5	F(4,19)=4.06 p=0.0153	p<0.05
GAPDH	0.99±0.02 A B n=5	0.75±0.08 B C n=4	0.72±0.08 C n=5	1.04±0.02 A n=5	0.75±0.03 B C n=5	F(4,19)=6.93 p=0.0013	p<0.01

HPC	HPC	HPC	HPC	HPC	HPC	HPC	HPC
	VCD-1W	VCD-1W-E2	VCD-1W-PPT	VCD-1W-DPN	VCD-1W-G1	1-way ANOVA	1-way ANOVA easy sign
ChAT	92.34±4.83 A n=4	86.82±3.78 A n=5	107.14±1.42 A n=5	91.04±7.06 A n=5	87.2±9.24 A n=5	F(4,19)=1.98 p=0.1392	NS
ATP-CL	0.95±0.11 A n=4	1.24±0.19 A n=5	1.15±0.11 A n=5	0.83±0.14 A n=5	0.71±0.08 A n=5	F(4,19)=2.53 p=0.0748	Trend (p<0.1)
PFK	0.96±0.1 A n=4	0.98±0.16 A n=5	1±0.06 A n=5	0.85±0.16 A n=5	0.84±0.14 A n=5	F(4,19)=0.28 p=0.8901	NS
α-tubulin	0.99±0.02 A n=4	0.69±0.03 C n=5	0.75±0.02 B C n=5	1.03±0.03 A n=5	0.84±0.02 B n=5	F(4,19)=22.93 p=0.0001	p<0.001
PDH-E1	0.97±0.05 A n=4	0.84±0.05 A n=5	0.93±0.07 A n=5	0.98±0.07 A n=5	0.83±0.03 A n=5	F(4,19)=1.24 p=0.3276	NS
GAPDH	0.99±0.04 A n=4	0.75±0.11 A n=5	0.81±0.09 A n=5	1.04±0.18 A n=5	0.74±0.12 A n=5	F(4,19)=1.26 p=0.3197	NS

HPC	HPC	HPC	HPC	HPC	HPC	HPC	HPC
	VCD-6W	VCD-6W-E2	VCD-6W-PPT	VCD-6W-DPN	VCD-6W-G1	1-way ANOVA	1-way ANOVA easy sign
ChAT	78.89±4.76 A n=5	93.9±3.2 A n=5	80.11±3.11 A n=4	84.38±3.68 A n=5	94.94±4.85 A n=5	F(4,19)=3.45 p=0.0278	p<0.05
ATP-CL	1±0.02 A n=5	1.19±0.27 A n=5	1.24±0.07 A n=4	1.23±0.29 A n=5	1.56±0.28 A n=4	F(4,18)=0.76 p=0.566	NS
PFK	1.03±0.07 A n=5	0.96±0.19 A n=5	1.03±0.1 A n=4	1±0.21 A n=5	1.05±0.17 A n=4	F(4,18)=0.04 p=0.9966	NS
α-tubulin	1±0 A n=5	0.85±0.03 B C n=5	0.77±0.02 C D n=4	0.91±0.02 A B n=5	0.69±0.02 D n=4	F(4,18)=21.88 p=0.0001	p<0.001
PDH-E1	1±0.02 A B n=5	0.91±0.03 B n=5	1.08±0.01 A n=4	1.07±0.03 A n=5	1.04±0.03 A B n=4	F(4,18)=5.06 p=0.0066	p<0.01
GAPDH	0.99±0.03 A n=5	0.95±0.04 A n=5	1.04±0.13 A n=4	0.99±0.05 A n=5	1.11±0.05 A n=4	F(4,18)=0.84 p=0.5174	NS

FCX	FCX	FCX	FCX	FCX	FCX	FCX	FCX
	OVX-1W	OVX-1W-E2	OVX-1W-PPT	OVX-1W-DPN	OVX-1W-G1	1-way ANOVA	1-way ANOVA easy sign
ChAT	75.26±1.73 A n=5	76.72±2.15 A n=4	79.41±3.84 A n=4	70.42±2.16 A n=4	70.85±3.23 A n=4	F(4,16)=2.01 p=0.1418	NS
ATP-CL	1.01±0.04 A n=5	0.75±0.06 B n=4	0.81±0.06 A B n=4	0.67±0.04 B n=4	0.76±0.03 B n=4	F(4,16)=6.8 p=0.0021	p<0.01
PFK	0.99±0.05 A n=5	0.87±0.01 A B n=4	0.88±0.07 A B n=4	0.76±0.04 B n=4	0.9±0.04 A B n=4	F(4,16)=2.58 p=0.077	Trend (p<0.1)
α-tubulin	0.99±0.03 A n=5	0.96±0.05 A n=4	1.18±0.08 A n=4	0.91±0.04 A n=4	0.91±0.09 A n=4	F(4,16)=2.77 p=0.0635	Trend (p<0.1)
PDH-E1	1±0.01 A n=5	1.07±0.04 A n=4	1.12±0.07 A n=4	1.09±0.06 A n=4	1.08±0.05 A n=4	F(4,16)=0.72 p=0.5933	NS
GAPDH	1.01±0.04 A n=5	1.07±0.05 A n=4	1.05±0.13 A n=4	1.05±0.13 A n=4	0.93±0.07 A n=4	F(4,16)=0.37 p=0.8233	NS

FCX	FCX	FCX	FCX	FCX	FCX	FCX	FCX
	OVX-6W	OVX-6W-E2	OVX-6W-PPT	OVX-6W-DPN	OVX-6W-G1	1-way ANOVA	1-way ANOVA easy sign
ChAT	63.13±3.21 A n=5	71.26±1.33 A n=4	71.09±1.46 A n=5	81.46±9.09 A n=5	65.56±3.99 A n=5	F(4,19)=2.11 p=0.1189	NS
ATP-CL	1.07±0.15 A B n=5	1.19±0.08 A B n=4	0.95±0.04 A B n=5	0.81±0.09 B n=5	1.25±0.03 A n=5	F(4,19)=3.79 p=0.0198	p<0.05
PFK	1.05±0.1 A B n=5	1.22±0.12 A B n=4	0.99±0.08 A B n=5	0.85±0.07 B n=5	1.35±0.06 A n=5	F(4,19)=4.65 p=0.0087	p<0.01
α-tubulin	1±0.02 A B n=5	0.82±0.01 B n=4	0.8±0.05 B n=5	1.19±0.12 A n=5	0.78±0.04 B n=5	F(4,19)=6.5 p=0.0018	p<0.01
PDH-E1	1.02±0.03 A n=5	1±0.06 A n=4	1.06±0.04 A n=5	1.22±0.1 A n=5	1.06±0.05 A n=5	F(4,19)=1.73 p=0.1843	NS
GAPDH	1±0.04 A n=5	0.97±0.04 A n=4	1.06±0.05 A n=5	1.19±0.1 A n=5	1.09±0.07 A n=5	F(4,19)=1.35 p=0.2898	NS

FCX	FCX	FCX	FCX	FCX	FCX	FCX	FCX
	VCD-1W	VCD-1W-E2	VCD-1W-PPT	VCD-1W-DPN	VCD-1W-G1	1-way ANOVA	1-way ANOVA easy sign
ChAT	85.06±4.55 A n=5	76.47±2.1 A n=5	80.52±3.28 A n=5	76.49±2.51 A n=5	79.03±1.64 A n=4	F(4,19)=1.36 p=0.2843	NS
ATP-CL	1.01±0.01 A n=5	0.98±0.12 A n=5	0.79±0.09 A n=5	0.97±0.15 A n=5	0.63±0.01 A n=4	F(4,19)=2.38 p=0.0883	Trend (p<0.1)
PFK	1±0 A n=5	1.07±0.12 A n=5	0.8±0.07 A n=5	0.91±0.09 A n=5	0.73±0.04 A n=4	F(4,19)=2.73 p=0.06	Trend (p<0.1)
α-tubulin	1.01±0.05 A B n=5	0.79±0.08 B C n=5	0.79±0.04 B C n=5	1.11±0.08 A n=5	0.65±0.01 C n=4	F(4,19)=7.31 p=0.001	p<0.001
PDH-E1	1±0.03 B C n=5	0.89±0.03 C n=5	1.13±0.01 A n=5	1.15±0.01 A n=5	1.07±0.02 A B n=4	F(4,19)=15.39 p=0.0001	p<0.001
GAPDH	0.99±0.05 B C n=5	0.87±0.04 C n=5	1.13±0.01 A B n=5	1.17±0.02 A n=5	1.19±0.02 A n=4	F(4,19)=13.09 p=0.0001	p<0.001

FCX	FCX	FCX	FCX	FCX	FCX	FCX	FCX
	VCD-6W	VCD-6W-E2	VCD-6W-PPT	VCD-6W-DPN	VCD-6W-G1	1-way ANOVA	1-way ANOVA easy sign
ChAT	67.81±1.97 B n=5	78.74±1.99 A n=5	66.7±3.18 B n=4	69.71±2.87 A B n=5	72.35±2.28 A B n=5	F(4,19)=3.81 p=0.0195	p<0.05
ATP-CL	1.06±0.12 A n=5	1.09±0.13 A n=5	0.77±0.19 A n=4	0.98±0.16 A n=5	0.7±0.05 A n=5	F(4,19)=1.66 p=0.2004	NS
PFK	0.99±0.06 A n=5	1.17±0.1 A n=5	1.27±0.29 A n=4	1.23±0.05 A n=5	0.93±0.06 A n=5	F(4,19)=1.37 p=0.2802	NS
α-tubulin	0.97±0.05 A n=5	0.81±0.03 A n=5	0.73±0.09 A n=4	0.94±0.08 A n=5	0.75±0.1 A n=5	F(4,19)=1.83 p=0.1655	NS
PDH-E1	1.01±0.04 A B n=5	0.97±0.03 A B n=5	0.92±0.07 A B n=4	0.81±0.04 B n=5	1.08±0.05 A n=5	F(4,19)=4.23 p=0.0129	p<0.05
GAPDH	0.99±0.03 B n=5	1.17±0.14 A B n=5	1.18±0.15 A B n=4	0.89±0.08 B n=5	1.53±0.15 A n=5	F(4,19)=4.05 p=0.0154	p<0.05

STR	STR	STR	STR	STR	STR	STR	STR
	OVX-1W	OVX-1W-E2	OVX-1W-PPT	OVX-1W-DPN	OVX-1W-G1	1-way ANOVA	1-way ANOVA easy sign
ChAT	213.85±22.1 A n=5	266.09±15.74 A n=4	240.15±3.51 A n=4	205.7±27.02 A n=4	229.86±14.39 A n=4	F(4,16)=1.54 p=0.2386	NS
ATP-CL	1±0.06 A n=5	0.66±0.22 A n=4	1.04±0.21 A n=4	0.6±0.16 A n=4	0.91±0.27 A n=4	F(4,16)=1.07 p=0.403	NS
PFK	1.02±0.13 A n=5	0.6±0.05 A n=4	1.2±0.25 A n=4	0.97±0.19 A n=4	0.63±0.03 A n=4	F(4,16)=2.73 p=0.0661	Trend (p<0.1)
α-tubulin	0.98±0.03 A n=5	0.85±0.14 A n=4	1.04±0.12 A n=4	1.11±0.1 A n=4	0.99±0.11 A n=4	F(4,16)=0.79 p=0.5484	NS
PDH-E1	0.97±0.04 A n=5	0.97±0.03 A n=4	0.82±0.08 A n=4	1±0.13 A n=4	1.04±0.15 A n=4	F(4,16)=0.65 p=0.6336	NS
GAPDH	0.99±0.02 B C n=5	0.93±0.03 C n=4	0.97±0.03 B C n=4	1.12±0.02 A B n=4	1.19±0.07 A n=4	F(4,16)=7.4 p=0.0014	p<0.01

STR	STR	STR	STR	STR	STR	STR	STR
	OVX-6W	OVX-6W-E2	OVX-6W-PPT	OVX-6W-DPN	OVX-6W-G1	1-way ANOVA	1-way ANOVA easy sign
ChAT	231.53±8.49 A n=5	214.95±9.78 A n=4	240.68±19.84 A n=5	251.33±28.4 A n=5	251.32±18.93 A n=5	F(4,19)=0.58 p=0.6805	NS
ATP-CL	0.98±0.03 A n=5	0.99±0.04 A n=4	0.78±0.07 A n=5	0.97±0.08 A n=5	0.89±0.04 A n=5	F(4,19)=2.11 p=0.1197	NS
PFK	1±0.01 A B n=5	1.19±0.07 A n=4	0.74±0.09 B n=5	1.06±0.07 A n=5	1.03±0.04 A n=5	F(4,19)=5.77 p=0.0032	p<0.01
α-tubulin	0.98±0.02 A n=5	0.99±0.02 A n=4	0.96±0.04 A n=5	1±0.05 A n=5	0.86±0.01 A n=5	F(4,19)=2.28 p=0.0988	Trend (p<0.1)
PDH-E1	0.98±0.03 B C n=5	1.04±0.04 B n=4	0.9±0.01 C n=5	1.21±0.03 A n=5	0.96±0.03 B C n=5	F(4,19)=13.66 p=0.0001	p<0.001
GAPDH	0.93±0.1 A n=5	0.88±0.05 A n=4	1.05±0.07 A n=5	0.99±0.06 A n=5	0.97±0.07 A n=5	F(4,19)=0.58 p=0.6783	NS

STR	STR	STR	STR	STR	STR	STR	STR
	VCD-1W	VCD-1W-E2	VCD-1W-PPT	VCD-1W-DPN	VCD-1W-G1	1-way ANOVA	1-way ANOVA easy sign
ChAT	205.99±21.6 A n=5	219.82±30.39 A n=5	262.66±16.53 A n=5	217.97±11.09 A n=5	222.32±17.89 A n=4	F(4,19)=1.11 p=0.3788	NS
ATP-CL	0.95±0.1 A B n=5	0.93±0.12 A B n=5	1.22±0.11 A n=5	0.57±0.04 B n=5	1.08±0.08 A n=5	F(4,20)=6.08 p=0.0023	p<0.01
PFK	0.98±0.03 A n=5	1.33±0.23 A n=5	1.67±0.15 A n=5	1.42±0.23 A n=5	1.55±0.13 A n=5	F(4,20)=2.2 p=0.1058	NS
α-tubulin	1±0.06 A n=5	0.85±0.04 A B n=5	0.65±0.02 B C n=5	0.91±0.08 A n=5	0.57±0.04 C n=5	F(4,20)=9.68 p=0.0002	p<0.001
PDH-E1	1±0.06 A n=5	0.97±0.03 A n=5	0.99±0.04 A n=5	0.82±0.07 A n=5	0.97±0.05 A n=5	F(4,20)=1.72 p=0.1848	NS
GAPDH	1±0.04 A n=5	0.81±0.09 A n=5	0.71±0.03 A n=5	0.77±0.03 A n=5	0.85±0.14 A n=5	F(4,20)=1.66 p=0.1976	NS

STR	STR	STR	STR	STR	STR	STR	STR
	VCD-6W	VCD-6W-E2	VCD-6W-PPT	VCD-6W-DPN	VCD-6W-G1	1-way ANOVA	1-way ANOVA easy sign
ChAT	216.87±15.6 A n=5	194.93±6.7 A n=5	206.61±19.38 A n=4	228.06±11.81 A n=5	232.2±19.37 A n=5	F(4,19)=1.07 p=0.4009	NS
ATP-CL	1.01±0.07 A n=5	0.78±0.07 A B n=5	0.81±0.07 A B n=4	0.64±0.06 B n=5	0.69±0.1 A B n=5	F(4,19)=3.2 p=0.036	p<0.05
PFK	0.99±0.06 A n=5	1.01±0.12 A n=5	1.48±0.18 A n=4	0.94±0.11 A n=5	1.03±0.15 A n=5	F(4,19)=2.59 p=0.0696	Trend (p<0.1)
α-tubulin	0.97±0.06 A n=5	0.89±0.14 A n=5	1.24±0.11 A n=4	0.96±0.15 A n=5	1.09±0.18 A n=5	F(4,19)=0.83 p=0.5242	NS
PDH-E1	0.96±0.07 A n=5	0.97±0.16 A n=5	1.26±0.1 A n=4	1.02±0.22 A n=5	1.08±0.2 A n=5	F(4,19)=0.45 p=0.7702	NS
GAPDH	0.99±0.03 A n=5	1.05±0.24 A n=5	1.23±0.06 A n=4	0.97±0.2 A n=5	1.09±0.25 A n=5	F(4,19)=0.25 p=0.9087	NS

Table 8: Effects of menopause model and duration of Vehicle treatment on ChAT activity and protein expressions in three brain regions. Data shown as Mean ± SEM and number of animals (n) together with connecting-letters report of one-way ANOVA analysis for agonist treatments. Post-hoc Tukey analysis are reported in the results section. ChAT activity shown as [pmol of ACh synthesized / hr / mg protein] and for each model and time point group protein expressions are relative to OVX-1W-Vehicle rats. Levels not connected by same letter are significantly different.

		Statistics				1-way ANOVA	
Region	Measurment	OVX-1w	OVX-6w	VCD-1w	VCD-6w	1-way ANOVA	1-way ANOVA easy sign
HPC	ChAT	82.78±1.38 A B n=5	74.37±0.91 B n=5	92.34±4.83 A n=4	78.89±4.76 A B n=5	F(3,15)=4.85 p=0.0148	p<0.05
HPC	ATP-CL	1±0.11 A n=5	1.32±0.2 A n=5	0.99±0.09 A n=4	1.27±0.18 A n=5	F(3,15)=1.16 p=0.356	NS
HPC	PFK	1±0.06 B n=5	1.53±0.1 A n=5	1.59±0.06 A n=4	0.99±0.05 B n=5	F(3,15)=19.27 p=0.0001	p<0.001
HPC	α-tubulin	1±0.06 A n=5	0.74±0.05 B n=5	0.87±0.03 A B n=4	0.95±0.03 A n=5	F(3,15)=4.83 p=0.0151	p<0.05
HPC	PDH-E1	1±0.04 A n=5	0.9±0.05 A B n=5	0.7±0.04 B n=4	0.88±0.04 A B n=5	F(3,15)=6.18 p=0.006	p<0.01
HPC	GAPDH	1±0.02 B n=5	1.29±0.07 A n=5	0.76±0.05 B n=4	1.27±0.07 A n=5	F(3,15)=16.51 p=0.0001	p<0.001
FCX	ChAT	75.26±1.73 A B n=5	63.13±3.21 B n=5	85.06±4.55 A n=5	67.81±1.97 B n=5	F(3,16)=9.66 p=0.0007	p<0.001
FCX	ATP-CL	0.98±0.05 C n=5	1.02±0.03 C n=5	1.18±0.02 B n=5	1.57±0.02 A n=5	F(3,16)=53.22 p=0.0001	p<0.001
FCX	PFK	1±0.05 A n=5	1±0.09 A n=5	0.94±0.02 A n=5	1.05±0.07 A n=5	F(3,16)=0.42 p=0.7441	NS
FCX	α-tubulin	0.96±0.13 A n=5	0.99±0.06 A n=5	1.17±0.1 A n=5	1.12±0.09 A n=5	F(3,16)=0.91 p=0.4574	NS
FCX	PDH-E1	0.99±0.07 A n=5	0.97±0.1 A n=5	1.02±0.06 A n=5	1.01±0.13 A n=5	F(3,16)=0.06 p=0.9821	NS
FCX	GAPDH	0.99±0.12 A n=5	0.87±0.08 A n=5	0.92±0.09 A n=5	0.87±0.18 A n=5	F(3,16)=0.21 p=0.8903	NS
STR	ChAT	213.85±22.1 A n=5	231.53±8.49 A n=5	205.99±21.6 A n=5	216.87±15.6 A n=5	F(3,16)=0.36 p=0.7833	NS
STR	ATP-CL	1±0.05 A n=5	1.31±0.25 A n=5	0.99±0.17 A n=5	1.23±0.28 A n=5	F(3,16)=0.59 p=0.6274	NS
STR	PFK	1±0.06 B n=5	0.88±0.02 B n=5	1.82±0.05 A n=5	0.9±0.13 B n=5	F(3,16)=31.29 p=0.0001	p<0.001
STR	α-tubulin	1±0.03 A n=5	1.01±0.14 A n=5	0.95±0.07 A n=5	1.01±0.18 A n=5	F(3,16)=0.07 p=0.9759	NS
STR	PDH-E1	1±0.03 A n=5	0.82±0.05 A n=5	0.93±0.02 A n=5	0.86±0.1 A n=5	F(3,16)=1.56 p=0.2385	NS
STR	GAPDH	1±0.01 A n=5	0.84±0.09 A n=5	0.82±0.06 A n=5	0.82±0.09 A n=5	F(3,16)=1.27 p=0.3183	NS

4.4 Discussion

4.4.1 Experiment 2:

Experiment 2 focused on characterizing the effects of E2 and of selective ER agonists on neurochemical endpoints, at two time points in each of the two menopausal models. Again, serum hormone levels in the vehicle-treated controls confirmed successful representation of systemic hormones levels in the two menopausal models. As expected, rats receiving E2 had significantly higher plasma E2 levels relative to other groups. Continuous administration of E2 at a dose of 3 μg/day resulted in physiological levels after 1 week of treatment and supra-physiological levels after 6 weeks of treatment as recently reported (J. Li & Gibbs, 2019). Notably, 6 weeks treatment with DPN led to significant elevations in T and a strong trend for elevation of AD in VCD-treated rats. The exact mechanism of this is currently unknown. ERβ is expressed by both thecal and granulosa cells (Drummond & Fuller, 2012). It may be that activation of ERβ by DPN stimulates thecal cells to increase biosynthesis of androgens, or may inhibit the transformation of androgens to estrogens in the granulosa cells causing levels of androgens to increase. This needs to be investigated.

Effects of Agonist Treatments:

Agonist treatments produced numerous effects on multiple endpoints that were both model and time dependent as well as brain region specific. For clarity, we have organized the discussion of these effects by brain region below.

HPC

Effects of agonists in the HPC were both model- and time-dependent. Several effects are particularly notable. For example, in OVX rats, E2 treatment initiated immediately following OVX resulted in significant lower levels of glycolytic enzymes and ATP-CL at the 1W time point (Figure 16A). Similar effects were produced by DPN and G-1. PPT treatment resulted in reductions in GAPDH, but not the other targets. These data suggest that most of the effects of E2 on these endpoints are mediated by activation of ERß and/or GPR30, with effects on GAPDH also mediated by ERα. The effects are consistent with significantly reduced metabolic activity in the HPC at this early time point, corresponding with reductions in glycolysis, ATP production, cytosolic acetyl-CoA. The data also may indicate decreased demands for the synthesis of cholesterol and triglycerides as well as decreases in glucose-induce insulin secretion, protein isoprenoid-based modifications, and histone acetylation (Beigneux et al., 2004; Chypre, Zaidi, & Smans, 2012). Such ATP-CL associated changes can lead to a condition of energy deficit by affecting intermediates of the TCA cycle and glucose metabolism (Mochel, 2017). These findings are consistent with our recent results showing significant reductions in the levels of tryptophan and tyrosine in the HPC 1W after OVX (Long et al., 2018), and further reductions in these amino acids after 1W treatment with ER agonists (Long et al., 2019). Note that no effects of agonist treatments on ChAT activity were detected in the HPC at the 1W time point, despite the significant reductions in glycolytic enzymes and ATP-CL.

After 1W of treatment many of the effects were reduced or even reversed after 6W of treatment (Figure 16B). For example, the lower levels of PFK and ATP-CL were no longer statistically significant, and the negative effects of DPN on levels of GAPDH and PDH were no longer observed after 6W of treatment. In contrast, a significant higher levels of α -tubulin were detected in response to 6W treatment with DPN relative to all other groups. These data

demonstrate that some of the negative effects of ER agonist treatment on glycolytic enzymes and ATP-CL lessen with time despite continued treatment, whereas effects on tubulin emerge and appear to be ERß-specific. Hence, in this brain region, sustained treatment with ER agonists following OVX has negative effects on metabolic activity which recover over time and may be followed by higher levels of specific cytoskeletal proteins. Note that ChAT activity also was significantly higher at the 6W time point in response to treatment with each of the four ER agonists. This suggests that continued activation of any of the three ERs is sufficient to produce higher ChAT activity in the HPC of OVX rats. These data are consistent with the increases in high affinity choline uptake and acetylcholine release that have been reported in OVX rats following sustained or repeated treatment with E2 or G-1 (Hammond et al., 2011; O'Malley, Dean Hautamaki, Kelley, & Meyer, 1987; J. L. Pongrac, Gibbs, & Defranco, 2004).

Effects of agonists in the HPC of VCD-treated rats were quite different from those in OVX rats. For example, Figure 16C shows that in VCD-treated rats, 1W of agonist treatment produced no statistically significant changes in the levels of glycolytic enzymes or ATP-CL relative to controls. In contrast, significant reductions in α -tubulin were detected in rats treated with E2, PPT, or G-1. After 6W of treatment reductions in tubulin continued to be detected. No other significant differences relative to controls were detected. Likewise, no significant effects of ER agonists on ChAT activity were detected in VCD-treated rats at the 1W time point. Significant higher levels were detected after 6W treatment with E2 or G1, but not PPT or DPN. Collectively, these findings demonstrate that the effects of ER agonists on the levels of glycolytic enzymes, ATP-CL, and tubulin in the hippocampus are fundamentally different in VCD-treated vs. OVX rats. In addition, unlike OVX rats, the data suggest that effects of E2 on ChAT activity in VCD-treated rats requires activation of GPR30.

FCX

Effects of agonists in the FCX also were model- and time-dependent, and were different from those detected in the HPC. Figure 17A shows that in OVX rats, 1W of E2 treatment had no significant effects on glycolytic enzymes, but did produce a significant lower levels of ATP-CL. Similar effects were produced by PPT, DPN and G-1, suggesting that activation of any of the three ERs is sufficient to lower the levels of ATP-CL. Lower levels of PFK were detected in rats treated with DPN, but not in response to E2, PPT, or G-1. Hence short-term agonist treatment following OVX appears to have relatively little effect on glycolytic enzymes and related metabolic activity in the FCX. This is consistent with results showing no significant reductions in TRP or TYR in the FCX in response to OVX or agonist treatments (Long et al., 2018). The lower levels of ATP-CL were similar to effects in the HPC and suggest that this is one effect that is consistent between the two brain regions. Note that by 6W no statistically significant effects of agonist treatments were detected relative to controls. Lower levels of in α -tubulin were observed in response to E2, PPT and G-1 as in the HPC, but were not statistically significant. This suggests some consistency in the effects of ER agonists administered immediately following OVX on α -tubulin in these two brain regions. No significant effects of agonist treatments on ChAT activity were detected in the FCX of OVX rats.

Effects in VCD-treated rats again were different from those in OVX rats. In VCD-treated rats, 1W of E2 treatment resulted in lower levels of PDH relative to controls, but did not significantly affect other targets. Significant lower levels of α ER-tubulin were detected in rats treated with G-1, as well as a similar trend in rats treated with E2 and PPT which have not reach statistical significance. Surprisingly, treatment with PPT, DPN or G-1 resulted in significant higher levels of GAPDH and PDH, suggesting that selective activation of ERα, ERß, or GPR30 alone

may increase glycolytic enzymes in the FCX of VCD-treated rats at this early time-point. Since E2 did not have the same effect, this suggests that under specific circumstances, activation of multiple ERs can diminish or reverse regional effects associated with activation of any single ER (Korol & Pisani, 2015; Sheppard, Choleris, & Galea, 2019). After 6W of treatment, many of the effects on GAPDH, PFK and α-tubulin were no longer observed. Exceptions were the significantly higher levels of GAPDH and PDH in rats treated with G-1, suggesting that continuous activation of GPR30 can elevate the expression of these glycolytic enzymes in the FCX of VCD-treated rats. As in OVX rats, agonist treatments had no significant effect on ChAT activity at the 1W time point. E2 produced slight higher levels of ChAT activity at the 6W time point, but overall there was very little evidence of ER agonist effects on ChAT in the FCX.

STR

Effects of agonists in the STR were diverse and, as in the other brain regions, were both model- and time dependent. Notably, treatment with E2 produced no statistically significant effects relative to controls in either OVX or VCD-treated rats at either time-point. Hence in contrast to HPC and FCX, treatment with E2 has comparatively little effect on the levels of glycolytic enzymes, α -tubulin, and ATP-CL in the STR. In OVX rats, 1W treatment with G1 resulted in a significantly higher levels of GAPDH relative to controls and other treatment groups. No other significant differences from controls were detected, suggesting the effect was specific to activation of GPR30. After 6W of treatment, the higher levels of GAPDH were no longer detected; however, there were significantly higher levels of PDH in rats treated with DPN. There also were significant lower levels of PFK in rats treated with PPT, demonstrating selective changes in different stages of glucose metabolism by ERα and ERβ. No other significant effects of agonist treatments were

detected at 6W relative to controls. In VCD-treated rats, significant lower levels of α -tubulin were detected after 1W treatment with PPT or G-1, as well as significantly higher levels of PFK in rats treated with PPT. After 6W treatment, the effects on α -tubulin were no longer detected and a lower levels of ATP-CL were now observed in rats treated with DPN or G-1. No significant effects on ChAT activity were detected in the STR in either OVX or VCD-treated rats at either time point.

Collectively, these results indicate that ER agonists have much more limited effects on the levels of glycolytic enzymes, α-tubulin, ATP-CL, and ChAT in the STR than in the HPC and FCX. This would suggest more limited effects on metabolic activity, ATP production, and the demands for cytosolic acetyl-CoA. Effects of selective ER agonists were detected; however different agonists often had different or opposite effects, which is consistent with the fact there were no significant effects of E2. This also is consistent with the low levels of ERα and ERß in the STR in comparison with HPC and FCX, and with our prior results showing very limited effects on amino acid levels and neurotransmitter endpoints in the STR of OVX and VCD-treated rats (Long et al., 2019). The lack of effects on ChAT activity was surprising given that the majority of cholinergic neurons in the STR contain GPR30, not unlike cholinergic neurons in the MS, DBB, and NBM. Since GPR30 is a membrane receptor, it is possible that effects associated with GPR30 activation occur much more rapidly and transiently than effects associated with activation of nuclear ERα or ERß. Hence effects of E2 and G-1 on ChAT may have occurred prior to the 1W and 6W time-points. This needs to be investigated.

4.4.2 **Limitations of Studies (Chapters 3 and 4)**

Our data provide a relative comparison of differences in metabolic, cytoskeletal and cholinergic markers between cycling, OVX and VCD animals as well as their response to selective

estrogen agonists. However, some limitations of this study should be noted. Data from our regional brain homogenates represents an averaged regional protein expression from all types of cells present in a specific brain region (rather than changes in cell-specific populations). For agonist effects in experiment 2, our methodological approach prevented us from directly capturing potential differences between the four vehicle-treated control groups. This was mitigated by either comparing the vehicle-treated controls, or comparing effects of agonists within each model and time-point (relative to corresponding vehicle control). Activity of ChAT served as a specific marker for the integrity of cholinergic system and the capacity to produce acetylcholine (Contestabile et al., 2008; Gibbs, 1998, 2010). Yet, specific changes in regional metabolic needs (e.g. to preserve region-specific functions) as well as changes in metabolism of cholinergic neurons and the impact on cholinergic functions needs to be studied directly. Measurements of metabolic enzymes and skeletal proteins were limited to relative protein expression and does not account for changes in enzymatic activity and in the regulation of such activity by sex hormones (Gaignard et al., 2015; Irwin et al., 2011; Irwin et al., 2012; Joe & Ramirez, 2001; Nilsen et al., 2007; Ramirez et al., 2001) (Butler et al., 2001; Chen, Brown, et al., 2009; Joe et al., 2005; Jurasek et al., 2018; A. Kostanyan & K. Nazaryan, 1992; Robertson et al., 1998; Szutowicz et al., 2005). Several differences between OVX and VCD animals still needs to be investigated. Agonist treatments have been shown to affect the directionality of regional effects mediated by specific ERs. Yet, we have not identified specific mechanisms of actions. Also, differences in the distribution, expression and responsiveness of estrogen receptors with respect to time needs to be further characterized between the models. Differences in the response of central regulation of energy may also change the availability of metabolites to different brain regions (e.g. glucose and ketones) and need to be evaluated. The levels of local estrogen production were considered to have no significant potency

and were not evaluated. Despite these limitations, data from this study are of great value for understanding core differences between P, D, OVX and VCD animals as well as their response to estrogen. We evaluated different variables (model, time and agonist treatments) and charted a protein network across several pathways to better understand systemic regional changes across estrogenic treatments.

Existing literature suggests a relationship between glycolytic enzymes in the brain to the integrity of cholinergic neurons. Transient effects on glycolytic enzymes been demonstrated in several rat models of neuronal lesions and particularly with lesions specific to cholinergic neurons. Selective neurotoxin-induced immune-lesions of the basal forebrain cholinergic neurons lead to higher levels of PFK expression and activity in the hippocampus and frontal cortex at 3 and 7 days after lesions (Zeitschel et al., 2002). This was consist with other studies showing higher PFK activity following mechanical deafferentation of the cholinergic septo-hippocampal pathway (Krügel, Bigl, Eschrich, & Bigl, 2001). While specific mechanisms are still unknown, in the HPC lower integrity of cholinergic markers impact the levels of PFK and correlated with higher density of glucose transporters in cortical regions (Mehlhorn et al., 1998). PDH function may also be related to cholinergic integrity. In rat brains, regions expressing cholinergic markers are highly abounded in PDH expression relative to regions with minimal to no cholinergic neurons (Lefresne, Beaujouan, & Glowinski, 1978; Milner, Aoki, Sheu, Blass, & Pickel, 1987). In Alzheimer's disease and other neurodegenerative diseases, the extent of cholinergic defects corresponds to reductions in PDH activity, expression and to the loss of cognitive functions (Perry, Perry, Tomlinson, Blessed, & Gibson, 1980; Szutowicz et al., 2013). Despite this evidence, our data have not identified a correlation between ChAT activity to any of those glycolytic enzymes (PFK, ATP-CL, GAPDH and PDH). Significantly lower expression of glycolytic enzymes was observed in the

FCX of OVX and VCD rats (e.g. Figure 13, FCX region) as well as in specific brain regions of certain agonist treated rats (e.g. Figure 15, OVX-1W-HPC; Figure 17, VCD and OVX animals). In those cases, cholinergic function may still been impaired in endpoints that are not detectable by regional levels of ChAT activity. Whether or not cholinergic functions correlates with glycolytic function in OVX and VCD models needs to be directly evaluated.

Current literature supports the general notion that loss of ovarian function, and particularly ovarian estrogens, leads to lower glucose utilization and higher ketone consumption in the brain (Brinton, 2008; Mauvais-Jarvis et al., 2013; Resnick et al., 2009). The ability of estrogen treatments to restore or protect glycolytic function was demonstrated in OVX rats (Shi & Simpkins, 1997), in ovariectomized non-human primates (Cheng, Cohen, Wang, & Bondy, 2001) and in postemenopausal women (Eberling, Reed, Coleman, & Jagust, 2000) where all E2-treated groups showing higher glycolytic metabolism compare to non-treated controls. Our results differentiate the effects of E2 and specific agonists between OVX to VCD models as well as between 1- and 6- weeks of treatments. Most agonists caused lower expression of glycolytic enzymes in the HPC of OVX rats following 1- but not 6- weeks of treatment whereas agonist treatments resulted in lower α-tubulin in the HPC of VCD animals regardless of time. This may represent a fundamental difference in response to estrogen agonists where agonist impact on glycolytic metabolism is shorter in VCD (not detected at 1-week) while agonists lower structural markers (e.g. α-tubulin) (e.g. Figure 15). In the FCX, specific agonist treatments increase the expression of certain glycolytic enzymes in VCD but not OVX rats at both time points. This represents another difference in response to agonist treatments which can still be observed at 6-weeks.

4.4.3 Summary of Studies (Chapters 3 and 4)

Overall, we identified distinct differences in the expression of key metabolic enzymes capable of modulating glycolytic, acetyle-CoA and cholinergic pathways. These differences were described between cycling animals and models of surgical (OVX) and transitional (VCD) menopause. The effects were region-, model- and time- dependent as well as distinguished in the response to estrogen receptor agonists. Following the loss of ovarian function, the frontal cortex was especially sensitive with lower expression of all enzymes in both VCD and OVX models, whereas the striatum showed higher expression of structural protein (β-actin) and enzymes committing glucose to the glycolytic pathway (PFK and GAPDH). In rats treated with estrogen receptor agonists, the hippocampus of OVX rats was shown to be more sensitive to agonist treatments than VCD rats. In the FCX, agonist treatments increased expression of enzymes related to glycolytic flux (GAPDH and PDH) at the 1-week time-point where treatment with G1 (a GPER1 agonists) showed higher levels of those enzymes at both 1- and 6-weeks. This may contribute to differences in the effects of estrogen treatments on cognition and age-related cognitive decline in women that have experienced surgical vs. transitional menopause.

5.0 Indirect Actions of Estradiol on Cholinergic Neurons are Mediated Via Orexin Neurons in the Latheral Hypothalamus

5.1 Introduction

In the orexin studies, my goal was to elucidate mechanisms by which estradiol (E2) and G-1 (a GPER-1 agonist) affects basal forebrain cholinergic neurons to influence cognitive performance. Projections of cholinergic neurons from the septum, diagonal band of Broca, and nucleus basalis magnocellularis to the hippocampus and frontal cortex affect cognitive performance (Gibbs, 2010). Evidence suggests that these effects are mediated, at least in part, by the novel G protein-coupled estrogen receptor GPER-1.

This cholinergic system also receives projections from orexin-containing neurons of the lateral hypothalamus. Studies show that orexin signaling to these areas in response to food leads to increased acetylcholine release in the hippocampus and cortex, particularly in association with physiologically relevant cues such as food reward (Fadel & Burk, 2010). Previously, *Hammond et al.* shown that GPER-1 mediates an increase in potassium-stimulated ACh release in the hippocampus with corresponding effects on spatial learning (Hammond et al., 2011; Hammond, Nelson, Kline, & Gibbs, 2012). It is possible that E2 and G-1 have indirect effect on cholinergic function through orexinergic projections to influence cognitive performance.

To begin investigating these possibilities we investigated whether orexin-containing neurons in the lateral hypothalamus contain GPER-1 and/or ERα. We also investigated the effects of E2 and G1 on relative levels of orexin mRNA in the lateral hypothalamus.

Ovariectomized rats received E2 or G-1 at 5µg/day for 7 days using miniosmotic pumps implanted s.c. Controls included ovariectomized rats and gonadally intact rats treated with vehicle. Tissues were dissected and processed for qRT-PCR quantification of relative levels of orexin mRNAs relative to mRNA for GAPDH.

5.2 Methods

All procedures were carried out in accordance with PHHS policies on the use of animals in research, and with the approval of the University of Pittsburgh's Institutional Animal Care and Use Committee.

Animals:

Young adult (~3 months of age) Sprague-Dawley rats were purchased from Hilltop Laboratories, Inc. Rats were ovariectomized by the supplier, shipped, and then individually housed in our facility on a 12 hour:12 hour light/dark schedule with unrestricted access to food and water. Rats were housed for at least two weeks prior to treatment.

Drug Treatments:

E2 and G-1 were dissolved first in DMSO and then in 20% ß-hydroxypropyl cyclodextran and then administered by miniosmotic pump (Alzet model 2002) implanted s.c.in the dorsal neck region. Controls received pumps containing vehicle. Young ovariectomized rats were treated continuously for one week with 5ug/day E2, G1 or vehicle administrated subcutaneously. An additional group of gonadally intact rats were treated with vehicle.

Tissue dissection for RNA isolation:

Rats were anesthetized, euthanized by decapitation and brains were dissected. Trunk blood was collected , serum was processed from blood and stored at –200C until assayed for E2. Using a brain matrix, the hypothalamic area was dissected (Bregma -1.80 to -3.30) and the lateral and medial hypothalamic regions were collected. Tissue samples were kept frozen in -800c until RNA isolation.

Immunohistochemistry:

For co-localization studies, four ovariectomized rats were processed for immunohistochemical detection of orexin and co-localization with GPR30 or ERα. Rats were perfused with 4% paraformaldehyde. Brains were removed, post-fixed with 4% paraformaldehyde for 24 hours, and sunk in 20% sucrose. Adjacent series of 40 micron coronal sections through the lateral hypothalamus were cut and were incubated with an antibody against orexin (mouse monoclonal anti-orexin mAB763; R&D Systems; diluted 1:800). Sections were then incubated with antibodies against GPR30 (rabbit anti-GPR30, a gift from Edward Filardo, Brown University, diluted1:200) or ERα, (Santa Cruz, Inc., rabbit anti-ERα (H-184) sc-7207, diluted 1:500). Co-localization of orexin and GPR30 was conducted using a donkey-anti-mouse antibody labeled with Alexa-488 (Molecular Probes, Inc.) and a donkey-anti-rabbit IgG labeled with Cy3 (Jackson Immunoresearch, Inc.). Staining was photographed using an Olympus FV1000 confocal microscope. Co-localization of orexin and ERα was conducted using biotin-labeled secondary antibodies and avidin-biotin-HRP technology with DAB as the chromagen.

For ERα staining, cobalt chloride was included in the reaction solution to produce a dark blue-black reaction product. Orexin staining was conducted without cobalt chloride and produced a reddish-brown reaction product. To quantify double-staining, the hypothalamus was divided

into medial and lateral portions as shown below. Matched sections were analyzed and the mean number of orexin-positive cells ± s.e.m. was determined for the medial and lateral regions for each rat. The percentage of orexin-positive cells that also contained GPR30 or ERα also was analyzed and is presented as the mean ± s.e.m. percentage of double-labeled cells.

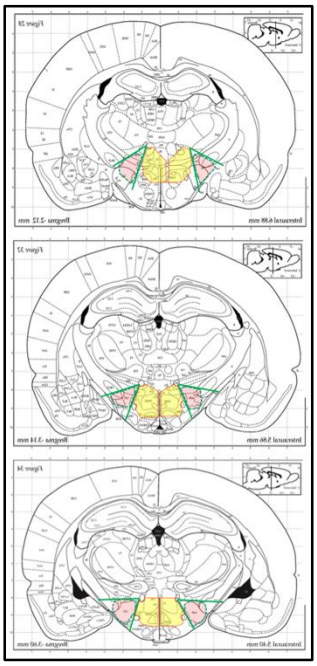

Figure 20: Drawings indicating the medial (yellow) and lateral (pink) locations of the hypothalamus where orexin cells were identified and analyzed for co-localization with GPER-1 or ERα. Drawings are from Paxinos and Watson (1986) The Rat Brain in Stereotaxic Atlas, Academic Press, London.

qRT-PCR:

qRT-PCR was used to verify the presence and to evaluate relative levels of prepro orexin in the hypothalamus. Total RNA was extracted from frozen tissue by adding TRIzol (Invitrogen, Inc.) and homogenization of tissue according to manufacture instructions. SuperScript III kit (Invitrogen, Inc.) was used for reverse transcription of mRNA. Real-time PCR was performed using SYBR green fluorescence dye and an ABI 7300 Sequence Detection System (ABI). All samples were run in duplicate, and glyceraldehyde 3-phosphate dehydrogenase (GAPDH) was used as reference gene. Negative controls for RT and PCR reactions included no template and no enzyme and also were performed in duplicate. The following sequences were used (listed in

5'—3' direction): Prepro-orexin sense: GCCGTCTCTACGAACTGTTG. Prepro-orexin antisense: CGAGGAGAGGGGAAAGTTAG. GAPDH sense: TGCCACTCAGAAGACTGTGG. GAPDH antisense: GGATGCAGGGATGATGTTCT. Products size is 303bp for prepro-orexin and 85bp for GAPDH. Product purity was confirmed by analyzing the dissociation curve and agarose gel electrophoresis. Each treatment group included four animals. For all treatment groups, effects of treatment on relative prepro-orexin were calculated according to *Pfaffl* model (Pfaffl, 2001) .Calculated fold change in orexin mRNA was normalized to mean change of OVX group. One-way ANOVA was used to determine significant differences in expression between treatment groups. Differences in the GAPDH mRNA levels between treatment groups were not significant ($p<0.05$). These qPCR studies were limited to n = 3.

5.2.1 **Results and Discussion**

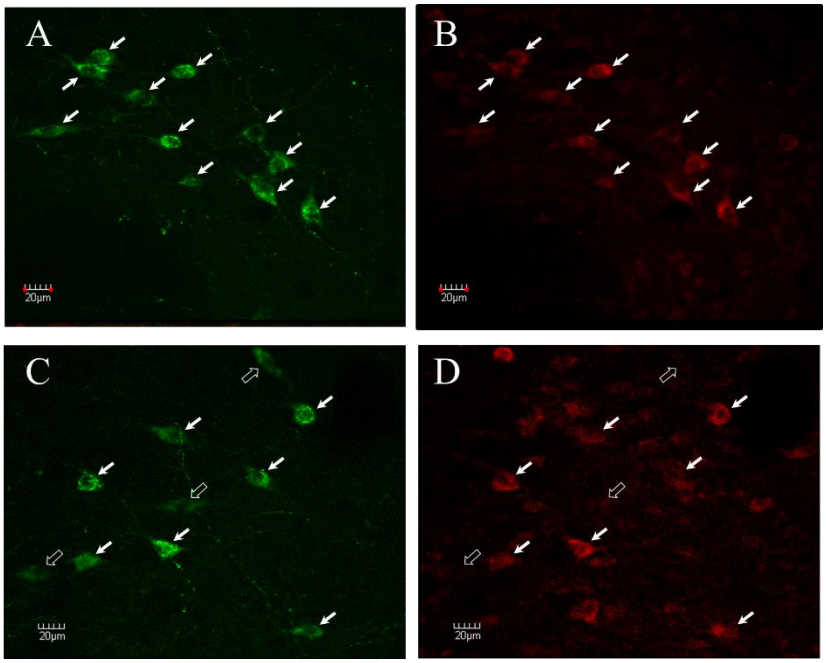

Figure 21: Many Orexin Cells Express GPER-1. Orexin (A & C) and GPER-1 (B & D) immunoreactive cells detected in the lateral hypothalamus. Solid arrows indicate double-labeled cells. Open arrows indicate orexin-positive

cells that were judged to be GPER-1 negative (lack of signal). Note that many of the orexin-positive cells also contain GPER-1.

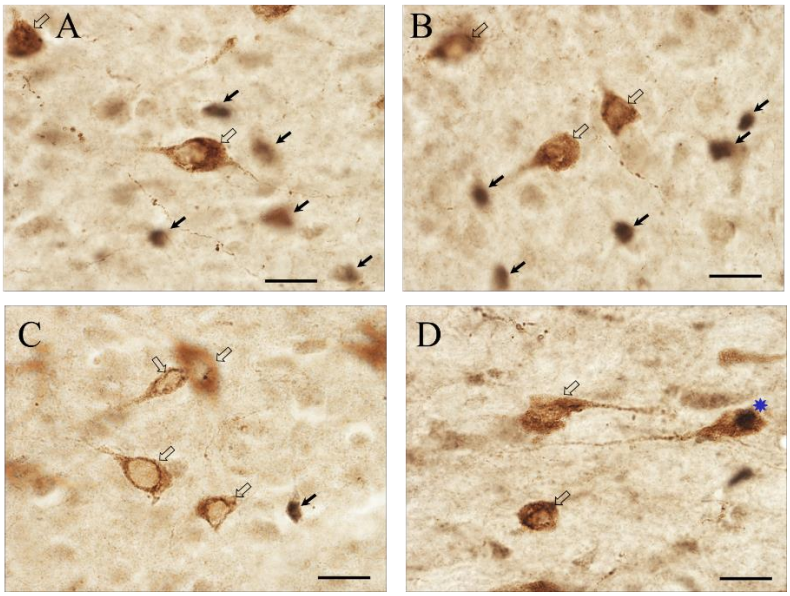

Figure 22: Very few orexin cells express ERα in the LH region. Localization of orexin-positive cells (large reddish-brown profiles) and ERα-positive nuclei (small dark profiles) detected in the lateral hypothalamus. Open arrows indicate orexin-positive cells that lack ERα staining. Solid arrows indicate ERα-positive profiles. One double-labeled cell is shown in panel D (*). Most of the orexin-positive cells did not contain ERα staining. Scale bar = 20 µm.

Table 9: Summary of Orexin/GPER-1 Co-localization

Rat	Measure	Medial	Lateral
1	Mean No. Orexin Cells/Sxn % Double-Labeled	95.6 ± 25.8 49.2% ± 3.6%	83.9 ± 16.9 53.1% ± 3.1%
2	Mean No. Orexin Cells/Sxn % Double-Labeled	85.8 ± 22.5 46.5% ± 5.0%	73.9 ± 13.3 63.7% ± 4.7%
3	Mean No. Orexin Cells/Sxn % Double-Labeled	87.1 ± 26.7 49.0% ± 2.5%	81.0 ± 19.6 57.6% ± 3.5%
4	Mean No. Orexin Cells/Sxn % Double-Labeled	93.4 ± 20.6 47.0% ± 4.46%	70.2 ± 11.7 51.3% ± 3.2%
	MEANS ± SEM	**90.5 ± 2.4** **46.7% ± 1.0%**	**77.2 ± 3.1** **56.5% ± 2.8%**

Table 10: Summary of Orexin/ERα Co-localization

Rat	Measure	Medial	Lateral
1	Mean No. Orexin Cells/Sxn % Double-Labeled	99.0 ± 26.1 1.7% ± 0.6%	92.8 ± 17.4 2.2% ± 0.4%
2	Mean No. Orexin Cells/Sxn % Double-Labeled	89.6 ± 19.9 0.8% ± 0.4%	75.7 ± 10.8 1.0% ± 0.5%
3	Mean No. Orexin Cells/Sxn % Double-Labeled	83.3 ± 32.7 1.0% ± 0.6%	74.8 ± 17.6 2.0% ± 0.9%
4	Mean No. Orexin Cells/Sxn % Double-Labeled	96.7 ± 18.2 0.4% ± 0.3%	81.8 ± 11.3 1.0% ± 0.4%
	MEANS ± SEM	**92.1 ± 3.6** **1.0% ± 0.3%**	**81.3 ± 4.1** **1.5% ± 0.3%**

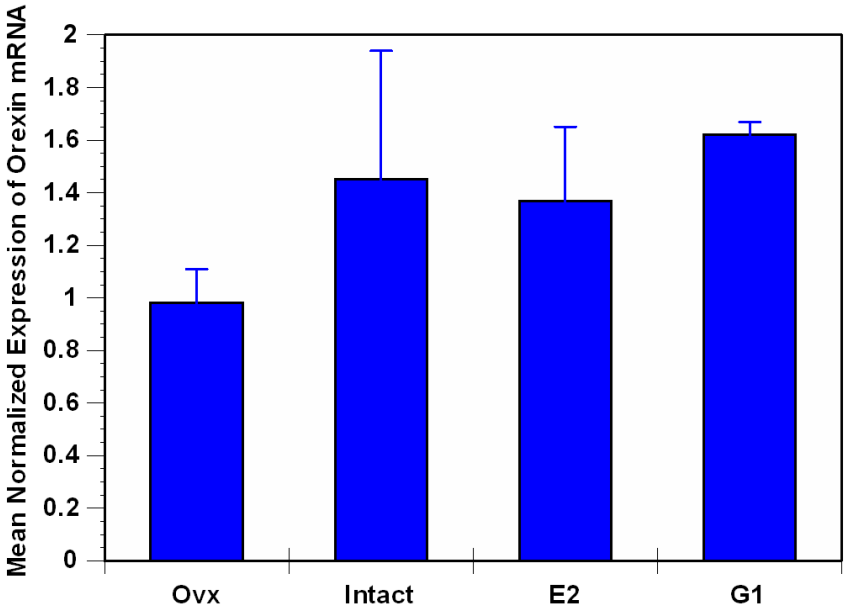

Figure 23: G-1 restored hypothalamic Orexin mRNA levels after ovariectomy. Relative mean mRNA expression of orexin in the hypothalamus as determined by two qRT-PCR reactions (each with n = 3 animals). Results were normalized to the mean GAPDH levels in vehicle treated ovariectomized rats. Treatment with E2 increased orexin mRNA in similar trend as intact animals. The GPR30 agonist, G1, was sufficient to increase hypothalamic mRNA orexin levels. Treatment groups: Intact- gonadally intact with vehicle; OVX- ovariectomized with vehicle; E2- OVX with E2 and G1- OVX with selective GPR30 agonist.

Results demonstrated that approximately 50% of orexin-positive cells also contain GPER-1 (Figure 21), whereas > 1% contain ERα (Figure 22), suggesting that E2 may regulate orexin signaling via GPER-1. In limited qPCR results, ovariectomy appeared to decrease relative levels of orexin mRNA in the hypothalamus; however, both E2 and G1 appeared to restore levels of orexin mRNA. These results suggest that selective activation of GPR30 may be sufficient to increase hypothalamic Orexin mRNA levels. The fact that G1 produced a similar effect as E2 and the greater abundance of GPR30 in orexinergic neurons suggests that GPR30 has a significant role

in mediating the effects of estrogen on orexin mRNA in the hypothalamus. Whether these are biologically significant and/or translate into differential effects on cholinergic function needs to be determined.

Orexin (hypocretins) play significant role in the regulation of energy homeostasis, arousal, and vigilance (Tsujino & Sakurai, 2009). Orexinergic neurons provide a network of connections by projecting from the lateral hypothalamus to the forebrain, thalamus, hippocampus, septum, basal ganglia, dopaminergic nuclei, dorsal raphe nuclei, and the amygdala (Nambu et al., 1999). These projections enable orexin to play significant role in memory consolidation, attention, metabolism, sleep and stimulus-reward processing (Aston-Jones, Smith, Moorman, & Richardson, 2009; Kessler, Stanley, Frederick-Duus, & Fadel, 2011; Sakurai & Mieda, 2011). Interestingly, estrogens also have been shown to influence the same functions, behaviors and cognitive pathways as orexinergic neurons. *Hammond et al.* demonstrated that E2 and G-1 increase acetylcholine release in the HPC in response to food-stimuli similar to the effect of orexin on acetylcholine release and food intake (Hammond et al., 2011; Hammond et al., 2012). Those studies raised the possibility that certain estrogenic effects, on acetylcholine release into the HPC, may be mediated by estrogen actions on orexin neurons. The co-localization of GPER-1 in orexin neurons, but not ERα, positioning GPER-1 to mediate estrogenic actions on orexin neurons. Our attempt to detect changes in levels of orexin mRNA following E2 or G1 treatments showed limited effect with higher orexin mRNA levels in treated ovariectomized rats versus untreated rats. Revealing the projections from GPER1-containg orexin neurons as well as how estrogens influence those projections may provide an indirect mechanism for estrogen effects on cognition.

6.0 Summary and Perspective

6.1 Scope of Studies and Key Findings

The broader goal of these studies was to identify mechanisms by which circulating 17β-estradiol affects different brain regions involved in cognitive processes. A large multi-omics study was performed, aiming to characterize and compare the effects of transitional and surgical menopause on neurochemical endpoints in the brain. A sensitive and robust multiplex method was developed to allow accurate quantification. A rat model for VCD-induced transitional menopause was established and compared with normally cycling rats and bi-lateral ovariectomized rats as model of surgical menopause. These studies were further extended to evaluate the effects of treatment with different estrogen receptor agonists. Additional studies evaluated the direct and indirect effects of estrogens on cholinergic neurons. Overall this work demonstrated a robust methodology for reliable quantification of proteins in rat brain homogenates, a direct characterization comparing differences in pivotal neurochemical endpoints between OVX, VCD and normally cycling rats, and differences in response to continuous treatment with ER-agonists at two time points (1- and 6- weeks) and three brain regions (HPC, FCX and STR).

First, a normalization method based on total-protein stain was developed (Chapter 2) to enable an accurate, sensitive and robust multiplex quantification of proteins in brain homogenates, as well as to overcome the challenge of hormonal effects on the expression of housekeeping proteins. The use of REVERT total protein stain (TP) had many advantages over normalization to housekeeping proteins (HKPs) with few limitations as discussed in section 2.5.3. TP had greater linear range of detection and less variability than individual HKPs. TP also produced a stable,

reversible and easy to use staining that did not interfere with immunodetection and enabled fluorescence multiplexing of at least six targets on the same PVDF membrane. Data collected using TP normalization revealed that TP reduced variability and improved reliability of quantification across gels as compare to HKPs. This methodology enabled me to process large number of samples and generate a proteomics-scale data sets.

A comparison between surgical (OVX) and transitional (VCD) menopausal models, as well as normally cycling rats at proestrus (P) and diestrus (D), was conducted (Chapter 3). Several endpoints were chosen to represent changes in expression of pivotal enzymes involve in glucose utilization (PFK and GAPDH), mitochondrial energy production (PDH), cytoskeleton (β-actin and α-tubulin), acetyle-CoA production (ATP-CL) and the activity of choline acetyltransferase (ChAT ; responsible for the synthesis of the acetylcholine) (see Chapter 3.3.3.1 for selection criteria of targets). Data demonstrated that physiological fluctuations in expression of these proteins occur across the estrous cycle but are time and brain region specific. In the FCX, ATP-CL levels were lowered in OVX, but not VCD-treated rats, compared to P. This may indicate a fundamental difference in the availability of citrate with impact on the cytoplasmic capacity for acetyl-CoA production. PDH expression was lower in D, VCD and OVX compare to rats in P. This is consistent with the hypothesis that glycolysis in this region is reduced when gonadal hormone levels are low (Brinton, 2008; Mauvais-Jarvis et al., 2013; Resnick et al., 2009). Notably, activity of ChAT remained stable at both P and D stages despite changes in ChAT mRNA levels in previous studies (Frick & Berger-Sweeney, 2001; Gibbs, 1996; Kobayashi et al., 1963). In both the HPC and STR, higher PFK levels were detected in VCD-treated rats at early time point of 1-week, while in OVX rats PFK was higher at 6-weeks, demonstrating a time-dependent difference in the capacity to commit glucose in glycolytic pathways.

This study was extended to characterize the effects of different estrogen receptor agonists on neurochemical endpoints, at two time points in each of the two menopausal models (Chapter 4). Agonist treatments produced numerous effects on multiple endpoints that were both model and time dependent as well as brain region specific. In the HPC, most of the effects on ATP-CL and GAPDH were mediated by activation of ERß and/or GPR30 and were consistent with significantly reduced metabolic activity in the HPC at early time point of 1-week, corresponding with reductions in glycolysis, ATP production, cytosolic acetyl-CoA. In the FCX, many agonist effects in VCD-treated rats were different from those in OVX rats. Differences in effects of E2 suggests that under specific circumstances, activation of multiple ERs can diminish or reverse effects associated with activation of any single ER. Further implications of these findings were discussed in more detail in Chapter 4. Collectively, these results indicate that ER agonists have much more limited effects on the levels of glycolytic enzymes, α-tubulin, ATP-CL, and ChAT in the STR than in the HPC and FCX.

Chapter 5 described efforts to identify indirect mechanisms of E2 on cholinergic neurons in the rat brain. These studies used immunohistochemistry approach to co-localized GPER1 expression in orexin cells in the lateral hypothalamus. These orexinergic neurons project to cholinergic neurons in different regions of the basal forebrain. Orexins also are known to mediate physiological, energy homeostasis and cognitive effects which correspond with effects of estrogen treatments. Localizing GPER1 on ~50% of orexin neurons, and not ERα (< 1%), contributes to our understanding of how GPER1-containing orexin neurons may mediate estrogenic effects on cholinergic neurons.

6.2 Overall Impact and Limitations

Our studies demonstrated three major principles: (1) Chapter 2 shows that changes in hormone levels affect the expression of common HKP and that using TP stain is a reliable alternative for protein normalization, (2) Chapter 3 shows that there are time- and brain region-dependent differences in the expression of metabolic and cytoskeletal proteins between rat models of surgical menopause (OVX), transitional menopause (VCD) and cycling rats at proestrus and diestrus, and (3) Chapter 4 shows that effects of selective estrogen agonists are also dependent on the menopause model, duration of contentious treatment and are region specific.

While these conclusions are highly important to understand the selective actions of hormones on the brain, our studies had some limitations. Methodological limitations of the TP staining were discussed in section 2.5.3 and for experiments comparing menopause models in section 4.4.2. Several additional limitations are worth mentioning. First, our ChAT activity assay is an *in-vitro* assay conducted under saturating conditions where choline is available in excess. Current literature suggests that synaptic choline-reuptake is the rate limiting step for ACh production; however, more studies are needed to identify whether acetyl-coA or other co-factors may also limit the reaction (see section 3.3.3). In-tube enzymatic reactions do not capture the actions of biological regulatory mechanisms and availability of substrate in synaptic compartments as well as in the cell or brain region. These differences may result in ChAT activity in our assay being higher than what might exist *in-vivo*. Such differences may limit our ability to detect effects that occur *in-vivo*.

Our scope of measurements was also limited to protein expression levels in regional homogenates. As mentioned in section 4.4.1, additional studies in these samples measured regional levels of amino acids and metabolites of several neurotransmitter pathways. For example, we

measured levels of amino acids tryptophan (TRP) and tyrosine (TYR) were lower in the HPC of OVX and E2-treated OVX rats (Long et al., 2018, 2019). This is in agreement with the lower levels of glycolytic enzymes we observed in the HPC of E2-treated OVX rats (Chapter 4). This is important as amino acids can be converted into glucose through gluconeogenesis or into ketone bodies (e.g. TRP and TYR are ketogenic amino acids). There are also metabolic pathways connecting amino acids, glycolysis and production of neurotransmitters (Hertz & Chen, 2017) which may have differed across our models and played a role in metabolic adaptation or compensatory response to the menopause model, time or agonist treatment in a brain region-dependent manner. Additionally, we have not quantified regional changes in precursors for glycolytic, ketosis or beta-oxidation pathways to compare availability of these energy-producing pathways (e.g. levels of glucose, ketone bodies and fatty acids). Differences in metabolic precursors may explain changes in enzyme expression as different brain regions have limited glucose availability and can shift to rely on non-glycolytic metabolic pathways (in model-, time- and region- dependent manners). We also have not measured any regional metabolic pool or reserves which may affect functional outcomes. Additionally, we included two time points in our studies (1- and 6- weeks) to represent shorter and longer periods of time following the loss of ovarian function (Chapter 3) or of continuous agonist treatment (Chapter 4).

In some cases we observed significant differences between menopausal models and agonist treatments. Future experiments should evaluate the broader impact of these changes on neurological endpoints and cognitive functions. For example, in OVX rats, the lower expression of glycolytic enzymes in the FCX as well as increase in those enzymes in the STR detected in Chapter 3 were not observed following treatment with E2 in Chapter 4. This seems to correlate with lower reliance on central learning in OVX rats (e.g. less utilization of FCX function may

correlate with lower glycolytic enzymes) and higher reliance on striatal learning (e.g. which may require more glycolytic capacity). Treatment of OVX rats with E2 appears to reverse or prevent these effects. This paradigm can be tested using spatial memory tasks comparing performance on task acquisition and in spatial challenges between OVX and VCD rats, as well as with agonist treatments. Brains of these animals can be further analyzed post-task to identify if successful spatial performance correlates with glycolytic or metabolic endpoints. With respect to neuroanatomical changes, immunohistochemistry can be used to identify regional changes in neuronal spine density and markers of neuronal activation (e.g. c-Fos, FosB and Arc) when co-localized with specific neuronal population (e.g. ChAT-containing cholinergic neurons). Similar studies have demonstrated that different estrogen agonists can lead to opposing effects on learning and memory by activation of different memory systems (Korol & Pisani, 2015). Such studies can further elucidate how the metabolic changes and agonist treatments impact neuronal function and cognition.

6.3 Conclusions and Future Directions

Our goal is to understand mechanisms by which estrogens affect the brain. These studies aimed to create a comprehensive analysis of simultaneous changes both within and across pathways. Our collective studies generated new data to describe the expression of multiple proteins, enzyme activity, metabolites with interacting neurotransmitter pathways and free amino acids.

These data, as well as previous datasets, can be integrated into network analysis tools such as QIAGEN's ingenuity pathway analysis (IPA) or NetworkAnalyst

(https://www.networkanalyst.ca/). These tools enable the analysis, integration and interpretation of different types of data (e.g. RNA, proteins, omics data, and individual data), and taking into account specific study designs and experimental conditions (e.g. time, age, model, clinical vs pre-clinical). Such analysis can generate interaction maps, canonical pathways, subnetworks, clustering data sorting by functional relevance and more advanced outputs.

In these studies, we resolved some variables to better explain the complex effects of estrogen of several endpoints. Differences detected between OVX and VCD models may explain clinical differences observed in the effects of estrogen replacement therapies between women who undergo surgical versus transitional menopause. The differences in response to estrogen treatment and selective ER agonists providing a pre-clinical metabolic map for the development of more specific estrogen therapies.

A large body of knowledge related to the effects of sex hormones on the brain already exists. Thus, a dedicated database can be established with high degree of neuroanatomical segregation and strong emphasis on neuronal function and outcomes on cognition. This large-data approach, together with the use of animal models that better translate effects to human menopause, can yield an enhanced evidence-based approach for customized and selective hormonal therapies. In such approach optimal hormonal therapy may emerge based on multiple parameters such as the mechanism and time-frame in which loss of ovarian function occurs (age, transational menopause, bilateral or unilateral ovariectomy etc.) as well as based on the effects on brain metabolism, functionality and cognitive performance. This approach can help guide the neuro-endocrinology field into the personalized medicine era.

Focused studies can validate and identify functional impact of specific differences between OVX and VCD rat models and their response to treatment with estrogen agonists. For example,

the difference in response to G-1 (GPER1 agonist) treatment lead to higher levels of ATP-CL in the FCX of OVX rats but not VCD rats should be further investigated (Figure 17). Activation of GPER1 may maintain levels of ATP-CL in OVX animals with outcomes on energy production (e.g. ATP/ADP levels), lipogenesis, cholesterol metabolism, neuronal functions (e.g. ntr release and capability for memory formation) as well as on cognitive performance (e.g. attention, learning and memory). While G-1 may mediate these effects in one region, a different ER may mediate them in other brain regions. These differences may also be investigated to customize and target hormonal therapy to specific brain regions. Some of the future goals should be to identify how these effects differ across models of menopause, time from loss of ovarian functions and whether ER agonist treatments can reverse undesired effects on brain function and cognition.

Bibliography

Abraham, I. M., Koszegi, Z., Tolod-Kemp, E., & Szego, E. M. (2009). Action of estrogen on survival of basal forebrain cholinergic neurons: promoting amelioration. *Psychoneuroendocrinology, 34 Suppl 1*, S104-112. doi: 10.1016/j.psyneuen.2009.05.024

Acosta, J. I., Mayer, L., Talboom, J. S., Tsang, C. W., Smith, C. J., Enders, C. K., & Bimonte-Nelson, H. A. (2009). Transitional versus surgical menopause in a rodent model: etiology of ovarian hormone loss impacts memory and the acetylcholine system. *Endocrinology, 150*(9), 4248-4259. doi: 10.1210/en.2008-1802

Akram, M. (2013). Mini-review on glycolysis and cancer. *J Cancer Educ, 28*(3), 454-457. doi: 10.1007/s13187-013-0486-9

Albanito, L., Madeo, A., Lappano, R., Vivacqua, A., Rago, V., Carpino, A., . . . Maggiolini, M. (2007). G protein-coupled receptor 30 (GPR30) mediates gene expression changes and growth response to 17beta-estradiol and selective GPR30 ligand G-1 in ovarian cancer cells. *Cancer Res, 67*(4), 1859-1866. doi: 10.1158/0008-5472.CAN-06-2909

Alenazi, F. S., Ibrahim, B. A., & Briski, K. P. (2015). Re-purposing of histological tissue sections for corroborative western blot analysis of hypothalamic metabolic neuropeptide expression following delineation of transactivated structures by Fos immuno-mapping. *Neuropeptides, 50*, 29-33. doi: 10.1016/j.npep.2015.02.001

Alexander, A., Irving, A. J., & Harvey, J. (2017). Emerging roles for the novel estrogen-sensing receptor GPER1 in the CNS. *Neuropharmacology, 113*(Pt B), 652-660. doi: 10.1016/j.neuropharm.2016.07.003

Alwine, J. C., Kemp, D. J., & Stark, G. R. (1977). Method for detection of specific RNAs in agarose gels by transfer to diazobenzyloxymethyl-paper and hybridization with DNA probes. *Proc Natl Acad Sci U S A, 74*(12), 5350-5354.

Argente-Arizon, P., Guerra-Cantera, S., Garcia-Segura, L. M., Argente, J., & Chowen, J. A. (2017). Glial cells and energy balance. *J Mol Endocrinol, 58*(1), R59-R71. doi: 10.1530/JME-16-0182

Arnal, J. F., Lenfant, F., Metivier, R., Flouriot, G., Henrion, D., Adlanmerini, M., . . . Katzenellenbogen, J. (2017). Membrane and Nuclear Estrogen Receptor Alpha Actions: From Tissue Specificity to Medical Implications. *Physiol Rev, 97*(3), 1045-1087. doi: 10.1152/physrev.00024.2016

Aston-Jones, G., Smith, R. J., Moorman, D. E., & Richardson, K. A. (2009). Role of lateral hypothalamic orexin neurons in reward processing and addiction. *Neuropharmacology, 56 Suppl 1*, 112-121. doi: 10.1016/j.neuropharm.2008.06.060

Babayan, A. H., & Kramar, E. A. (2013). Rapid effects of oestrogen on synaptic plasticity: interactions with actin and its signalling proteins. *J Neuroendocrinol, 25*(11), 1163-1172. doi: 10.1111/jne.12108

Baez-Jurado, E., Rincon-Benavides, M. A., Hidalgo-Lanussa, O., Guio-Vega, G., Ashraf, G. M., Sahebkar, A., . . . Barreto, G. E. (2019). Molecular mechanisms involved in the protective actions of Selective Estrogen Receptor Modulators in brain cells. *Front Neuroendocrinol, 52*, 44-64. doi: 10.1016/j.yfrne.2018.09.001

Bartella, V., Rizza, P., Barone, I., Zito, D., Giordano, F., Giordano, C., . . . Ando, S. (2012). Estrogen receptor beta binds Sp1 and recruits a corepressor complex to the estrogen receptor alpha gene promoter. *Breast Cancer Res Treat, 134*(2), 569-581. doi: 10.1007/s10549-012-2090-9

Barth, C., Villringer, A., & Sacher, J. (2015). Sex hormones affect neurotransmitters and shape the adult female brain during hormonal transition periods. *Front Neurosci, 9*, 37. doi: 10.3389/fnins.2015.00037

Beigneux, A. P., Kosinski, C., Gavino, B., Horton, J. D., Skarnes, W. C., & Young, S. G. (2004). ATP-citrate lyase deficiency in the mouse. *J Biol Chem, 279*(10), 9557-9564. doi: 10.1074/jbc.M310512200

Benmansour, S., Adeniji, O. S., Privratsky, A. A., & Frazer, A. (2016). Effects of Long-Term Treatment with Estradiol and Estrogen Receptor Subtype Agonists on Serotonergic Function in Ovariectomized Rats. *Neuroendocrinology, 103*(3-4), 269-281. doi: 10.1159/000437268

Berggren, K., Steinberg, T. H., Lauber, W. M., Carroll, J. A., Lopez, M. F., Chernokalskaya, E., . . . Patton, W. F. (1999). A luminescent ruthenium complex for ultrasensitive detection of proteins immobilized on membrane supports. *Anal Biochem, 276*(2), 129-143. doi: 10.1006/abio.1999.4364

Bernal-Mondragon, C., Arriaga-Avila, V., Martinez-Abundis, E., Barrera-Mera, B., Mercado-Gomez, O., & Guevara-Guzman, R. (2017). Effects of repeated 9 and 30-day exposure to extremely low-frequency electromagnetic fields on social recognition behavior and estrogen receptors expression in olfactory bulb of Wistar female rats. *Neurol Res, 39*(2), 165-175. doi: 10.1080/01616412.2016.1252875

Bernal-Mondragon, C., Rivas-Arancibia, S., Kendrick, K. M., & Guevara-Guzman, R. (2013). Estradiol prevents olfactory dysfunction induced by A-beta 25-35 injection in hippocampus. *BMC Neurosci, 14*, 104. doi: 10.1186/1471-2202-14-104

Black, K. L., Witty, C. F., & Daniel, J. M. (2016). Previous Midlife Oestradiol Treatment Results in Long-Term Maintenance of Hippocampal Oestrogen Receptor alpha Levels in Ovariectomised Rats: Mechanisms and Implications for Memory. *J Neuroendocrinol, 28*(10). doi: 10.1111/jne.12429

Boulware, M. I., Weick, J. P., Becklund, B. R., Kuo, S. P., Groth, R. D., & Mermelstein, P. G. (2005). Estradiol activates group I and II metabotropic glutamate receptor signaling, leading to opposing influences on cAMP response element-binding protein. *J Neurosci, 25*(20), 5066-5078. doi: 10.1523/JNEUROSCI.1427-05.2005

Bradford, M. M. (1976). A rapid and sensitive method for the quantitation of microgram quantities of protein utilizing the principle of protein-dye binding. *Analytical biochemistry, 72*(1-2), 248-254. doi: 10.1016/0003-2697(76)90527-3

Brailoiu, E., Dun, S. L., Brailoiu, G. C., Mizuo, K., Sklar, L. A., Oprea, T. I., . . . Dun, N. J. (2007). Distribution and characterization of estrogen receptor G protein-coupled receptor 30 in the rat central nervous system. *J Endocrinol, 193*(2), 311-321. doi: 10.1677/JOE-07-0017

Brill, M. S., Kleele, T., Ruschkies, L., Wang, M., Marahori, N. A., Reuter, M. S., . . . Misgeld, T. (2016). Branch-Specific Microtubule Destabilization Mediates Axon Branch Loss during Neuromuscular Synapse Elimination. *Neuron, 92*(4), 845-856. doi: 10.1016/j.neuron.2016.09.049

Brinton, R. D. (2008). Estrogen regulation of glucose metabolism and mitochondrial function: therapeutic implications for prevention of Alzheimer's disease. *Adv Drug Deliv Rev, 60*(13-14), 1504-1511. doi: 10.1016/j.addr.2008.06.003

Brinton, R. D., Yao, J., Yin, F., Mack, W. J., & Cadenas, E. (2015). Perimenopause as a neurological transition state. *Nat Rev Endocrinol, 11*(7), 393-405. doi: 10.1038/nrendo.2015.82

Briz, V., & Baudry, M. (2014). Estrogen Regulates Protein Synthesis and Actin Polymerization in Hippocampal Neurons through Different Molecular Mechanisms. *Front Endocrinol (Lausanne), 5*, 22. doi: 10.3389/fendo.2014.00022

Broughton, B. R., Brait, V. H., Kim, H. A., Lee, S., Chu, H. X., Gardiner-Mann, C. V., . . . Sobey, C. G. (2014). Sex-dependent effects of G protein-coupled estrogen receptor activity on outcome after ischemic stroke. *Stroke, 45*(3), 835-841. doi: 10.1161/STROKEAHA.113.001499

Butler, R., Leigh, P. N., & Gallo, J.-M. (2001). Androgen-induced up-regulation of tubulin isoforms in neuroblastoma cells. *Journal of Neurochemistry, 78*(4), 854-861. doi: 10.1046/j.1471-4159.2001.00475.x

Cai, M., Ma, Y. L., Qin, P., Li, Y., Zhang, L. X., Nie, H., . . . Xiong, L. Z. (2014). The loss of estrogen efficacy against cerebral ischemia in aged postmenopausal female mice. *Neurosci Lett, 558*, 115-119. doi: 10.1016/j.neulet.2013.11.007

Camp, B. W., Gerson, J. E., Tsang, C. W., Villa, S. R., Acosta, J. I., Blair Braden, B., . . . Bimonte-Nelson, H. A. (2012). High serum androstenedione levels correlate with impaired memory in the surgically menopausal rat: a replication and new findings. *Eur J Neurosci, 36*(8), 3086-3095. doi: 10.1111/j.1460-9568.2012.08194.x

Candeias, E., Duarte, A. I., Sebastiao, I., Fernandes, M. A., Placido, A. I., Carvalho, C., . . . Moreira, P. I. (2016). Middle-Aged Diabetic Females and Males Present Distinct Susceptibility to Alzheimer Disease-like Pathology. *Mol Neurobiol*. doi: 10.1007/s12035-016-0155-1

Catalina-Rodriguez, O., Kolukula, V. K., Tomita, Y., Preet, A., Palmieri, F., Wellstein, A., . . . Avantaggiati, M. L. (2012). The mitochondrial citrate transporter, CIC, is essential for mitochondrial homeostasis. *Oncotarget, 3*(10), 1220-1235. doi: 10.18632/oncotarget.714

Cawood, M. L., Field, H. P., Ford, C. G., Gillingwater, S., Kicman, A., Cowan, D., & Barth, J. H. (2005). Testosterone measurement by isotope-dilution liquid chromatography-tandem mass spectrometry: validation of a method for routine clinical practice. *Clin Chem, 51*(8), 1472-1479. doi: 10.1373/clinchem.2004.044503

Cersosimo, M. G., & Benarroch, E. E. (2015). Estrogen actions in the nervous system: Complexity and clinical implications. *Neurology, 85*(3), 263-273. doi: 10.1212/WNL.0000000000001776

Cha, Y., Lee, S. H., Jang, S. K., Guo, H., Ban, Y. H., Park, D., . . . Kim, Y. B. (2016). A silk peptide fraction restores cognitive function in AF64A-induced Alzheimer disease model rats by increasing expression of choline acetyltransferase gene. *Toxicol Appl Pharmacol, 314*, 48-54. doi: 10.1016/j.taap.2016.11.008

Chen, J. Q., Brown, T. R., & Russo, J. (2009). Regulation of energy metabolism pathways by estrogens and estrogenic chemicals and potential implications in obesity associated with increased exposure to endocrine disruptors. *Biochim Biophys Acta, 1793*(7), 1128-1143. doi: 10.1016/j.bbamcr.2009.03.009

Chen, J. Q., Cammarata, P. R., Baines, C. P., & Yager, J. D. (2009). Regulation of mitochondrial respiratory chain biogenesis by estrogens/estrogen receptors and physiological, pathological and pharmacological implications. *Biochim Biophys Acta, 1793*(10), 1540-1570. doi: 10.1016/j.bbamcr.2009.06.001

Cheng, C. M., Cohen, M., Wang, J. I. E., & Bondy, C. A. (2001). Estrogen augments glucose transporter and IGF1 expression in primate cerebral cortex. *The FASEB Journal, 15*(6), 907-915. doi: 10.1096/fj.00-0398com

Chuang, D.-M., & Ishitani, R. (1996). A role for GAPDH in apoptosis and neurodegeneration. *Nature Medicine, 2*(6), 609-610. doi: 10.1038/nm0696-609

Chypre, M., Zaidi, N., & Smans, K. (2012). ATP-citrate lyase: a mini-review. *Biochem Biophys Res Commun, 422*(1), 1-4. doi: 10.1016/j.bbrc.2012.04.144

Colciago, A., Casati, L., Negri-Cesi, P., & Celotti, F. (2015). Learning and memory: Steroids and epigenetics. *J Steroid Biochem Mol Biol, 150*, 64-85. doi: 10.1016/j.jsbmb.2015.02.008

Collins, M. A., An, J., Peller, D., & Bowser, R. (2015). Total protein is an effective loading control for cerebrospinal fluid western blots. *J Neurosci Methods, 251*, 72-82. doi: 10.1016/j.jneumeth.2015.05.011

Contestabile, A., Ciani, E., & Contestabile, A. (2008). The place of choline acetyltransferase activity measurement in the "cholinergic hypothesis" of neurodegenerative diseases. *Neurochem Res, 33*(2), 318-327. doi: 10.1007/s11064-007-9497-4

Coyoy, A., Guerra-Araiza, C., & Camacho-Arroyo, I. (2016). Metabolism Regulation by Estrogens and Their Receptors in the Central Nervous System Before and After Menopause. *Horm Metab Res, 48*(8), 489-496. doi: 10.1055/s-0042-110320

Cruz, G., Fernandois, D., & Paredes, A. H. (2017). Ovarian function and reproductive senescence in the rat: role of ovarian sympathetic innervation. *Reproduction, 153*(2), R59-R68. doi: 10.1530/REP-16-0117

Cui, J., Shen, Y., & Li, R. (2013). Estrogen synthesis and signaling pathways during aging: from periphery to brain. *Trends Mol Med, 19*(3), 197-209. doi: 10.1016/j.molmed.2012.12.007

Cunningham, M. A., Wirth, J. R., Freeman, L. R., Boger, H. A., Granholm, A. C., & Gilkeson, G. S. (2014). Estrogen receptor alpha deficiency protects against development of cognitive impairment in murine lupus. *J Neuroinflammation, 11*, 171. doi: 10.1186/s12974-014-0171-x

D'Souza, G. X., & Waldvogel, H. J. (2016). Targeting the Cholinergic System to Develop a Novel Therapy for Huntington's Disease. *J Huntingtons Dis, 5*(4), 333-342. doi: 10.3233/JHD-160200

Dalal, P. K., & Agarwal, M. (2015). Postmenopausal syndrome. *Indian J Psychiatry, 57*(Suppl 2), S222-232. doi: 10.4103/0019-5545.161483

Daniel, J. M. (2006). Effects of oestrogen on cognition: what have we learned from basic research? *J Neuroendocrinol, 18*(10), 787-795. doi: 10.1111/j.1365-2826.2006.01471.x

Davis, S. R., Lambrinoudaki, I., Lumsden, M., Mishra, G. D., Pal, L., Rees, M., . . . Simoncini, T. (2015). Menopause. *Nat Rev Dis Primers, 1*, 15004. doi: 10.1038/nrdp.2015.4

De Jesus-Burgos, M. I., Gonzalez-Garcia, S., Cruz-Santa, Y., & Perez-Acevedo, N. L. (2016). Amygdalar activation of group I metabotropic glutamate receptors produces anti- and pro-conflict effects depending upon animal sex in a sexually dimorphic conditioned conflict-based anxiety model. *Behav Brain Res, 302*, 200-212. doi: 10.1016/j.bbr.2016.01.009

de Jesus, L. W., Bogerd, J., Vieceli, F. M., Branco, G. S., Camargo, M. P., Cassel, M., . . . Borella, M. I. (2017). Gonadotropin subunits of the characiform Astyanax altiparanae: Molecular

characterization, spatiotemporal expression and their possible role on female reproductive dysfunction in captivity. *Gen Comp Endocrinol, 246*, 150-163. doi: 10.1016/j.ygcen.2016.12.004

Del Bianco-Borges, B., & Franci, C. R. (2015). Estrogen-dependent post-translational change in the nitric oxide system may mediate the leptin action on LH and prolactin secretion. *Brain Res, 1604*, 62-73. doi: 10.1016/j.brainres.2015.02.001

Diedenhofen, B., & Musch, J. (2016). cocron: A Web Interface and R Package for the Statistical Comparison of Cronbach's Alpha Coefficients. *International Journal of Internet Science., 11*, 51-60.

Dietrich, A. K., Humphreys, G. I., & Nardulli, A. M. (2013). 17beta-estradiol increases expression of the oxidative stress response and DNA repair protein apurinic endonuclease (Ape1) in the cerebral cortex of female mice following hypoxia. *J Steroid Biochem Mol Biol, 138*, 410-420. doi: 10.1016/j.jsbmb.2013.07.007

Dobransky, T., & Jane Rylett, R. (2003). Functional Regulation of Choline Acetyltransferase by Phosphorylation. *Neurochemical Research, 28*(3/4), 537-542. doi: 10.1023/a:1022873323561

Dobransky, T., & Rylett, R. J. (2005). A model for dynamic regulation of choline acetyltransferase by phosphorylation. *J Neurochem, 95*(2), 305-313. doi: 10.1111/j.1471-4159.2005.03367.x

Dominguez, R., & Micevych, P. (2010). Estradiol rapidly regulates membrane estrogen receptor alpha levels in hypothalamic neurons. *J Neurosci, 30*(38), 12589-12596. doi: 10.1523/JNEUROSCI.1038-10.2010

Donner, A., & Zou, G. (2002). Testing the Equality of Dependent Intraclass Correlation Coefficients. *Journal of the Royal Statistical Society. Series D (The Statistician), 51*(3), 367-379.

Drummond, A. E., & Fuller, P. J. (2012). Ovarian actions of estrogen receptor-beta: an update. *Semin Reprod Med, 30*(1), 32-38. doi: 10.1055/s-0031-1299595

Eaton, S. L., Roche, S. L., Llavero Hurtado, M., Oldknow, K. J., Farquharson, C., Gillingwater, T. H., & Wishart, T. M. (2013). Total protein analysis as a reliable loading control for quantitative fluorescent Western blotting. *PLoS One, 8*(8), e72457. doi: 10.1371/journal.pone.0072457

Eberling, J. L., Reed, B. R., Coleman, J. E., & Jagust, W. J. (2000). Effect of estrogen on cerebral glucose metabolism in postmenopausal women. *Neurology, 55*(6), 875-877. doi: 10.1212/wnl.55.6.875

Fadel, J., & Burk, J. A. (2010). Orexin/hypocretin modulation of the basal forebrain cholinergic system: Role in attention. *Brain Res, 1314*, 112-123. doi: 10.1016/j.brainres.2009.08.046

Fan, J., Li, B. J., Wang, X. F., Zhong, L. L., & Cui, R. J. (2017). Ghrelin produces antidepressant-like effect in the estrogen deficient mice. *Oncotarget, 8*(35), 58964-58973. doi: 10.18632/oncotarget.19768

Filardo, E. J. (2002). Epidermal growth factor receptor (EGFR) transactivation by estrogen via the G-protein-coupled receptor, GPR30: a novel signaling pathway with potential significance for breast cancer. *J Steroid Biochem Mol Biol, 80*(2), 231-238.

Flamini, M. I., Sanchez, A. M., Goglia, L., Tosi, V., Genazzani, A. R., & Simoncini, T. (2009). Differential actions of estrogen and SERMs in regulation of the actin cytoskeleton of endometrial cells. *Mol Hum Reprod, 15*(10), 675-685. doi: 10.1093/molehr/gap045

Flanagan-Cato, L. M. (2011). Sex differences in the neural circuit that mediates female sexual receptivity. *Front Neuroendocrinol, 32*(2), 124-136. doi: 10.1016/j.yfrne.2011.02.008

Fortress, A. M., Fan, L., Orr, P. T., Zhao, Z., & Frick, K. M. (2013). Estradiol-induced object recognition memory consolidation is dependent on activation of mTOR signaling in the dorsal hippocampus. *Learn Mem, 20*(3), 147-155. doi: 10.1101/lm.026732.112

Frank, A., Brown, L. M., & Clegg, D. J. (2014). The role of hypothalamic estrogen receptors in metabolic regulation. *Front Neuroendocrinol, 35*(4), 550-557. doi: 10.1016/j.yfrne.2014.05.002

Frick, K. M. (2009). Estrogens and age-related memory decline in rodents: what have we learned and where do we go from here? *Horm Behav, 55*(1), 2-23. doi: 10.1016/j.yhbeh.2008.08.015

Frick, K. M., & Berger-Sweeney, J. (2001). Spatial reference memory and neocortical neurochemistry vary with the estrous cycle in C57BL/6 mice. *Behav Neurosci, 115*(1), 229-237.

Frick, K. M., Kim, J., Tuscher, J. J., & Fortress, A. M. (2015). Sex steroid hormones matter for learning and memory: estrogenic regulation of hippocampal function in male and female rodents. *Learn Mem, 22*(9), 472-493. doi: 10.1101/lm.037267.114

Fuente-Martin, E., Garcia-Caceres, C., Morselli, E., Clegg, D. J., Chowen, J. A., Finan, B., . . . Tschop, M. H. (2013). Estrogen, astrocytes and the neuroendocrine control of metabolism. *Rev Endocr Metab Disord, 14*(4), 331-338. doi: 10.1007/s11154-013-9263-7

Funabashi, T., Kleopoulos, S. P., Brooks, P. J., Kimura, F., Pfaff, D. W., Shinohara, K., & Mobbs, C. V. (2000). Changes in estrogenic regulation of estrogen receptor α mRNA and progesterone receptor mRNA in the female rat hypothalamus during aging: an in situ hybridization study. *Neuroscience Research, 38*(1), 85-92. doi: 10.1016/s0168-0102(00)00150-4

Funakoshi, T., Yanai, A., Shinoda, K., Kawano, M. M., & Mizukami, Y. (2006). G protein-coupled receptor 30 is an estrogen receptor in the plasma membrane. *Biochem Biophys Res Commun, 346*(3), 904-910. doi: 10.1016/j.bbrc.2006.05.191

Gaignard, P., Savouroux, S., Liere, P., Pianos, A., Therond, P., Schumacher, M., . . . Guennoun, R. (2015). Effect of Sex Differences on Brain Mitochondrial Function and Its Suppression by Ovariectomy and in Aged Mice. *Endocrinology, 156*(8), 2893-2904. doi: 10.1210/en.2014-1913

Gao, Q.-G., Zhou, L.-P., Lee, V. H.-Y., Chan, H.-Y., Man, C. W.-Y., & Wong, M.-S. (2018). Ginsenoside Rg1 activates ligand-independent estrogenic effects via rapid estrogen receptor signaling pathway. *Journal of Ginseng Research*. doi: 10.1016/j.jgr.2018.03.004

Garcia-Caceres, C., Quarta, C., Varela, L., Gao, Y., Gruber, T., Legutko, B., . . . Tschop, M. H. (2016). Astrocytic Insulin Signaling Couples Brain Glucose Uptake with Nutrient Availability. *Cell, 166*(4), 867-880. doi: 10.1016/j.cell.2016.07.028

Gazit, N., Vertkin, I., Shapira, I., Helm, M., Slomowitz, E., Sheiba, M., . . . Slutsky, I. (2016). IGF-1 Receptor Differentially Regulates Spontaneous and Evoked Transmission via Mitochondria at Hippocampal Synapses. *Neuron, 89*(3), 583-597. doi: 10.1016/j.neuron.2015.12.034

Gibbons, A., & Dean, B. (2016). The Cholinergic System: An Emerging Drug Target for Schizophrenia. *Current Pharmaceutical Design, 22*(14), 2124-2133. doi: 10.2174/1381612822666160127114010

Gibbs, R. B. (1996). Fluctuations in relative levels of choline acetyltransferase mRNA in different regions of the rat basal forebrain across the estrous cycle: effects of estrogen and progesterone. *J Neurosci, 16*(3), 1049-1055.

Gibbs, R. B. (1998). Impairment of basal forebrain cholinergic neurons associated with aging and long-term loss of ovarian function. *Exp Neurol, 151*(2), 289-302. doi: 10.1006/exnr.1998.6789

Gibbs, R. B. (1999). Estrogen replacement enhances acquisition of a spatial memory task and reduces deficits associated with hippocampal muscarinic receptor inhibition. *Horm Behav, 36*(3), 222-233. doi: 10.1006/hbeh.1999.1541

Gibbs, R. B. (2000). Effects of gonadal hormone replacement on measures of basal forebrain cholinergic function. *Neuroscience, 101*(4), 931-938.

Gibbs, R. B. (2010). Estrogen therapy and cognition: a review of the cholinergic hypothesis. *Endocr Rev, 31*(2), 224-253. doi: 10.1210/er.2009-0036

Gibbs, R. B., & Gabor, R. (2003). Estrogen and cognition: applying preclinical findings to clinical perspectives. *J Neurosci Res, 74*(5), 637-643. doi: 10.1002/jnr.10811

Gibbs, R. B., & Johnson, D. A. (2007). Cholinergic lesions produce task-selective effects on delayed matching to position and configural association learning related to response pattern and strategy. *Neurobiol Learn Mem, 88*(1), 19-32. doi: 10.1016/j.nlm.2007.03.007

Gibbs, R. B., Nelson, D., Anthony, M. S., & Clarkson, T. B. (2002). Effects of long-term hormone replacement and of tibolone on choline acetyltransferase and acetylcholinesterase activities in the brains of ovariectomized, cynomologous monkeys. *Neuroscience, 113*(4), 907-914. doi: 10.1016/s0306-4522(02)00239-7

Gilda, J. E., & Gomes, A. V. (2013). Stain-Free total protein staining is a superior loading control to beta-actin for Western blots. *Anal Biochem, 440*(2), 186-188. doi: 10.1016/j.ab.2013.05.027

Gnoni, G. V., Priore, P., Geelen, M. J., & Siculella, L. (2009). The mitochondrial citrate carrier: metabolic role and regulation of its activity and expression. *IUBMB Life, 61*(10), 987-994. doi: 10.1002/iub.249

Goldman, J. M., Murr, A. S., & Cooper, R. L. (2007). The rodent estrous cycle: characterization of vaginal cytology and its utility in toxicological studies. *Birth Defects Res B Dev Reprod Toxicol, 80*(2), 84-97. doi: 10.1002/bdrb.20106

Govindaraj, V., & Rao, A. J. (2016). Proteomic identification of non-erythrocytic alpha-spectrin-1 down-regulation in the pre-optic area of neonatally estradiol-17beta treated female adult rats. *Horm Mol Biol Clin Investig, 26*(3), 165-172. doi: 10.1515/hmbci-2016-0008

Graham, M. D., Gardner Gregory, J., Hussain, D., Brake, W. G., & Pfaus, J. G. (2015). Ovarian steroids alter dopamine receptor populations in the medial preoptic area of female rats: implications for sexual motivation, desire, and behaviour. *Eur J Neurosci, 42*(12), 3138-3148. doi: 10.1111/ejn.13121

Grimm, A., Mensah-Nyagan, A. G., & Eckert, A. (2016). Alzheimer, mitochondria and gender. *Neurosci Biobehav Rev, 67*, 89-101. doi: 10.1016/j.neubiorev.2016.04.012

Grissom, E. M., & Daniel, J. M. (2016). Evidence for Ligand-Independent Activation of Hippocampal Estrogen Receptor-alpha by IGF-1 in Hippocampus of Ovariectomized Rats. *Endocrinology, 157*(8), 3149-3156. doi: 10.1210/en.2016-1197

Gros, R., Ding, Q., Sklar, L. A., Prossnitz, E. E., Arterburn, J. B., Chorazyczewski, J., & Feldman, R. D. (2011). GPR30 expression is required for the mineralocorticoid receptor-independent

rapid vascular effects of aldosterone. *Hypertension, 57*(3), 442-451. doi: 10.1161/HYPERTENSIONAHA.110.161653

Grove-Strawser, D., Boulware, M. I., & Mermelstein, P. G. (2010). Membrane estrogen receptors activate the metabotropic glutamate receptors mGluR5 and mGluR3 to bidirectionally regulate CREB phosphorylation in female rat striatal neurons. *Neuroscience, 170*(4), 1045-1055. doi: 10.1016/j.neuroscience.2010.08.012

Guo, J. Q., Deng, H. H., Bo, X., & Yang, X. S. (2017). Involvement of BDNF/TrkB and ERK/CREB axes in nitroglycerin-induced rat migraine and effects of estrogen on these signals in the migraine. *Biol Open, 6*(1), 8-16. doi: 10.1242/bio.021022

Gupta, G., Srivastava, A., & Setty, B. S. (2012). Androgen-Estrogen Synergy in the Regulation of Energy Metabolism in Epididymis and Vas Deferens of Rhesus Monkey. *Endocrine Research, 17*(3-4), 383-394. doi: 10.1080/07435809109106815

Hadjimarkou, M. M., & Vasudevan, N. (2018). GPER1/GPR30 in the brain: Crosstalk with classical estrogen receptors and implications for behavior. *J Steroid Biochem Mol Biol, 176*, 57-64. doi: 10.1016/j.jsbmb.2017.04.012

Hammond, R., Mauk, R., Ninaci, D., Nelson, D., & Gibbs, R. B. (2009). Chronic treatment with estrogen receptor agonists restores acquisition of a spatial learning task in young ovariectomized rats. *Horm Behav, 56*(3), 309-314. doi: 10.1016/j.yhbeh.2009.06.008

Hammond, R., Nelson, D., & Gibbs, R. B. (2011). GPR30 co-localizes with cholinergic neurons in the basal forebrain and enhances potassium-stimulated acetylcholine release in the hippocampus. *Psychoneuroendocrinology, 36*(2), 182-192. doi: 10.1016/j.psyneuen.2010.07.007

Hammond, R., Nelson, D., Kline, E., & Gibbs, R. B. (2012). Chronic treatment with a GPR30 antagonist impairs acquisition of a spatial learning task in young female rats. *Horm Behav, 62*(4), 367-374. doi: 10.1016/j.yhbeh.2012.07.004

Hansberg-Pastor, V., Gonzalez-Arenas, A., Pina-Medina, A. G., & Camacho-Arroyo, I. (2015). Sex Hormones Regulate Cytoskeletal Proteins Involved in Brain Plasticity. *Front Psychiatry, 6*, 165. doi: 10.3389/fpsyt.2015.00165

Hara, M. R., Cascio, M. B., & Sawa, A. (2006). GAPDH as a sensor of NO stress. *Biochim Biophys Acta, 1762*(5), 502-509. doi: 10.1016/j.bbadis.2006.01.012

Hara, Y., Waters, E. M., McEwen, B. S., & Morrison, J. H. (2015). Estrogen Effects on Cognitive and Synaptic Health Over the Lifecourse. *Physiol Rev, 95*(3), 785-807. doi: 10.1152/physrev.00036.2014

Harper, S., & Speicher, D. W. (2001). Detection of proteins on blot membranes. *Curr Protoc Protein Sci, Chapter 10*, Unit 10 18. doi: 10.1002/0471140864.ps1008s00

Hassel, B., Solyga, V., & Lossius, A. (2008). High-affinity choline uptake and acetylcholine-metabolizing enzymes in CNS white matter. A quantitative study. *Neurochemistry international, 53*(6-8), 193-198.

Heberden, C. (2017). Sex steroids and neurogenesis. *Biochem Pharmacol, 141*, 56-62. doi: 10.1016/j.bcp.2017.05.019

Heldring, N., Pike, A., Andersson, S., Matthews, J., Cheng, G., Hartman, J., . . . Gustafsson, J. A. (2007). Estrogen receptors: how do they signal and what are their targets. *Physiol Rev, 87*(3), 905-931. doi: 10.1152/physrev.00026.2006

Hertz, L., & Chen, Y. (2017). Integration between Glycolysis and Glutamate-Glutamine Cycle Flux May Explain Preferential Glycolytic Increase during Brain Activation, Requiring Glutamate. *Front Integr Neurosci, 11*, 18. doi: 10.3389/fnint.2017.00018

Higdon, R., & Kolker, E. (2015). Can "normal" protein expression ranges be estimated with high-throughput proteomics? *J Proteome Res, 14*(6), 2398-2407. doi: 10.1021/acs.jproteome.5b00176

Hinckelmann, M. V., Virlogeux, A., Niehage, C., Poujol, C., Choquet, D., Hoflack, B., . . . Saudou, F. (2016). Self-propelling vesicles define glycolysis as the minimal energy machinery for neuronal transport. *Nat Commun, 7*, 13233. doi: 10.1038/ncomms13233

Hoga, L., Rodolpho, J., Goncalves, B., & Quirino, B. (2015). Women's experience of menopause: a systematic review of qualitative evidence. *JBI Database System Rev Implement Rep, 13*(8), 250-337. doi: 10.11124/jbisrir-2015-1948

Hoshi, M., Takashima, A., Noguchi, K., Murayama, M., Sato, M., Kondo, S., . . . Imahori, K. (1996). Regulation of mitochondrial pyruvate dehydrogenase activity by tau protein kinase I/glycogen synthase kinase 3beta in brain. *Proc Natl Acad Sci U S A, 93*(7), 2719-2723.

Hoyer, P. B., Devine, P. J., Hu, X., Thompson, K. E., & Sipes, I. G. (2001). Ovarian toxicity of 4-vinylcyclohexene diepoxide: a mechanistic model. *Toxicol Pathol, 29*(1), 91-99. doi: 10.1080/019262301301418892

Hwang, C. J., Park, M. H., Choi, M. K., Choi, J. S., Oh, K. W., Hwang, D. Y., . . . Hong, J. T. (2016). Acceleration of amyloidogenesis and memory impairment by estrogen deficiency through NF-kappaB dependent beta-secretase activation in presenilin 2 mutant mice. *Brain Behav Immun, 53*, 113-122. doi: 10.1016/j.bbi.2015.11.013

Iacobazzi, V., & Infantino, V. (2014). Citrate--new functions for an old metabolite. *Biol Chem, 395*(4), 387-399. doi: 10.1515/hsz-2013-0271

Ikeda, H., Taira, N., Hara, F., Fujita, T., Yamamoto, H., Soh, J., . . . Miyoshi, S. (2010). The estrogen receptor influences microtubule-associated protein tau (MAPT) expression and the selective estrogen receptor inhibitor fulvestrant downregulates MAPT and increases the sensitivity to taxane in breast cancer cells. *Breast Cancer Res, 12*(3), R43. doi: 10.1186/bcr2598

Irwin, R. W., Yao, J., Ahmed, S. S., Hamilton, R. T., Cadenas, E., & Brinton, R. D. (2011). Medroxyprogesterone acetate antagonizes estrogen up-regulation of brain mitochondrial function. *Endocrinology, 152*(2), 556-567. doi: 10.1210/en.2010-1061

Irwin, R. W., Yao, J., To, J., Hamilton, R. T., Cadenas, E., & Brinton, R. D. (2012). Selective oestrogen receptor modulators differentially potentiate brain mitochondrial function. *J Neuroendocrinol, 24*(1), 236-248. doi: 10.1111/j.1365-2826.2011.02251.x

Janes, K. A. (2015). An analysis of critical factors for quantitative immunoblotting. *Sci Signal, 8*(371), rs2. doi: 10.1126/scisignal.2005966

Jha, M. K., Jeon, S., & Suk, K. (2012). Pyruvate Dehydrogenase Kinases in the Nervous System: Their Principal Functions in Neuronal-glial Metabolic Interaction and Neuro-metabolic Disorders. *Curr Neuropharmacol, 10*(4), 393-403. doi: 10.2174/157015912804143586

Joe, I., Kipp, J. L., & Ramirez, V. D. (2005). The non-genomic Action of Sex Steroids. 61-72. doi: 10.1007/3-540-26940-1_4

Joe, I., & Ramirez, V. D. (2001). Binding of estrogen and progesterone-BSA conjugates to glyceraldehyde-3-phosphate dehydrogenase (GAPDH) and the effects of the free steroids on GAPDH enzyme activity: physiological implications. *Steroids, 66*(6), 529-538.

Johnson, D. A., Zambon, N. J., & Gibbs, R. B. (2002). Selective lesion of cholinergic neurons in the medial septum by 192 IgG-saporin impairs learning in a delayed matching to position T-maze paradigm. *Brain Research, 943*(1), 132-141. doi: 10.1016/s0006-8993(02)02623-9

Jover-Mengual, T., Castello-Ruiz, M., Burguete, M. C., Jorques, M., Lopez-Morales, M. A., Aliena-Valero, A., . . . Salom, J. B. (2017). Molecular mechanisms mediating the neuroprotective role of the selective estrogen receptor modulator, bazedoxifene, in acute ischemic stroke: A comparative study with 17beta-estradiol. *J Steroid Biochem Mol Biol, 171*, 296-304. doi: 10.1016/j.jsbmb.2017.05.001

Jurasek, M., Cernohorska, M., Rehulka, J., Spiwok, V., Sulimenko, T., Draberova, E., . . . Sedlak, D. (2018). Estradiol dimer inhibits tubulin polymerization and microtubule dynamics. *J Steroid Biochem Mol Biol, 183*, 68-79. doi: 10.1016/j.jsbmb.2018.05.008

Kasten, T. P., Mhaskar, Y., & Dunaway, G. A. (1993). Regulation of brain 6-phosphofructo-1-kinase: effects of aging, fructose-2,6-bisphosphate, and regional subunit distribution. *Mol Cell Biochem, 120*(1), 61-68. doi: 10.1007/bf00925985

Kessler, B. A., Stanley, E. M., Frederick-Duus, D., & Fadel, J. (2011). Age-related loss of orexin/hypocretin neurons. *Neuroscience, 178*, 82-88. doi: 10.1016/j.neuroscience.2011.01.031

Kirshner, Z. Z., & Gibbs, R. B. (2018). Use of the REVERT((R)) total protein stain as a loading control demonstrates significant benefits over the use of housekeeping proteins when analyzing brain homogenates by Western blot: An analysis of samples representing different gonadal hormone states. *Mol Cell Endocrinol*. doi: 10.1016/j.mce.2018.01.015

Kobayashi, T., Kobayashi, T., Kato, J., & Minaguchi, H. (1963). Fluctuations in Choline Acetylase Activity in Hypothalamus of Rat during Estrous Cycle and after Castration. *Endocrinol Jpn, 10*, 175-182. doi: https://doi.org/10.1507/endocrj1954.10.175

Koebele, S. V., Mennenga, S. E., Hiroi, R., Quihuis, A. M., Hewitt, L. T., Poisson, M. L., . . . Bimonte-Nelson, H. A. (2017). Cognitive changes across the menopause transition: A longitudinal evaluation of the impact of age and ovarian status on spatial memory. *Horm Behav, 87*, 96-114. doi: 10.1016/j.yhbeh.2016.10.010

Koh, P. O. (2014a). Estradiol alleviates the ischemic brain injury-induced decrease of neuronal calcium sensor protein hippocalcin. *Neurosci Lett, 582*, 32-37. doi: 10.1016/j.neulet.2014.08.045

Koh, P. O. (2014b). Estradiol ameliorates the reduction in parvalbumin expression induced by ischemic brain injury. *Neurosci Lett, 574*, 36-40. doi: 10.1016/j.neulet.2014.05.006

Konishi, S. (1985). Normalizing and variance stabilizing transformations for intraclass correlations. *Annals of the Institute of Statistical Mathematics, 37*(1), 87-94.

Konishi, S., & Gupta, A. (1987). Inferences about interclass and intraclass correlations from familial data. *Advances in the statistical sciences, 4*, 225-233.

Korol, D. L., & Pisani, S. L. (2015). Estrogens and cognition: Friends or foes?: An evaluation of the opposing effects of estrogens on learning and memory. *Horm Behav, 74*, 105-115. doi: 10.1016/j.yhbeh.2015.06.017

Korol, D. L., & Wang, W. (2018). Using a memory systems lens to view the effects of estrogens on cognition: Implications for human health. *Physiol Behav, 187*, 67-78. doi: 10.1016/j.physbeh.2017.11.022

Kostanyan, A., & Nazaryan, K. (1992). Rat brain glycolysis regulation by estradiol-17 beta. *Biochim Biophys Acta, 1133*(3), 301-306.

Kostanyan, A., & Nazaryan, K. (1992). Rat brain glycolysis regulation by estradiol-17β. *Biochimica et Biophysica Acta (BBA) - Molecular Cell Research, 1133*(3), 301-306. doi: 10.1016/0167-4889(92)90051-c

Krügel, U., Bigl, V., Eschrich, K., & Bigl, M. (2001). Deafferentation of the septo-hippocampal pathway in rats as a model of the metabolic events in Alzheimer's disease. *International Journal of Developmental Neuroscience, 19*(3), 263-277. doi: 10.1016/s0736-5748(01)00010-7

Kumar, A., Dumasia, K., Gaonkar, R., Sonawane, S., Kadam, L., & Balasinor, N. H. (2015). Estrogen and androgen regulate actin-remodeling and endocytosis-related genes during rat spermiation. *Mol Cell Endocrinol, 404*, 91-101. doi: 10.1016/j.mce.2014.12.029

Kumar, S., Singh, U., Singh, O., Goswami, C., & Singru, P. S. (2017). Transient receptor potential vanilloid 6 (TRPV6) in the mouse brain: Distribution and estrous cycle-related changes in the hypothalamus. *Neuroscience, 344*, 204-216. doi: 10.1016/j.neuroscience.2016.12.025

Laschet, J. J., Minier, F., Kurcewicz, I., Bureau, M. H., Trottier, S., Jeanneteau, F., . . . Pumain, R. (2004). Glyceraldehyde-3-phosphate dehydrogenase is a GABAA receptor kinase linking glycolysis to neuronal inhibition. *J Neurosci, 24*(35), 7614-7622. doi: 10.1523/JNEUROSCI.0868-04.2004

Lau, W. S., Chan, R. Y., Guo, D. A., & Wong, M. S. (2008). Ginsenoside Rg1 exerts estrogen-like activities via ligand-independent activation of ERalpha pathway. *J Steroid Biochem Mol Biol, 108*(1-2), 64-71. doi: 10.1016/j.jsbmb.2007.06.005

Lee, H. G., Jo, J., Hong, H. H., Kim, K. K., Park, J. K., Cho, S. J., & Park, C. (2016). State-of-the-art housekeeping proteins for quantitative western blotting: Revisiting the first draft of the human proteome. *Proteomics, 16*(13), 1863-1867. doi: 10.1002/pmic.201500344

Lee, M. N., Ha, S. H., Kim, J., Koh, A., Lee, C. S., Kim, J. H., . . . Ryu, S. H. (2009). Glycolytic flux signals to mTOR through glyceraldehyde-3-phosphate dehydrogenase-mediated regulation of Rheb. *Mol Cell Biol, 29*(14), 3991-4001. doi: 10.1128/MCB.00165-09

LeFevre, J., & McClintock, M. K. (1988). Reproductive senescence in female rats: a longitudinal study of individual differences in estrous cycles and behavior. *Biol Reprod, 38*(4), 780-789.

Lefresne, P., Beaujouan, J. C., & Glowinski, J. (1978). Evidence for extramitochondrial pyruvate dehydrogenase involved in acetylcholine synthesis in nerve endings. *Nature, 274*(5670), 497-500. doi: 10.1038/274497a0

Lejri, I., Grimm, A., & Eckert, A. (2018). Mitochondria, Estrogen and Female Brain Aging. *Front Aging Neurosci, 10*, 124. doi: 10.3389/fnagi.2018.00124

Levin, E. R. (2009). Plasma membrane estrogen receptors. *Trends Endocrinol Metab, 20*(10), 477-482. doi: 10.1016/j.tem.2009.06.009

Li, B., Matter, E. K., Hoppert, H. T., Grayson, B. E., Seeley, R. J., & Sandoval, D. A. (2014). Identification of optimal reference genes for RT-qPCR in the rat hypothalamus and intestine for the study of obesity. *Int J Obes (Lond), 38*(2), 192-197. doi: 10.1038/ijo.2013.86

Li, C., Brake, W. G., Romeo, R. D., Dunlop, J. C., Gordon, M., Buzescu, R., . . . McEwen, B. S. (2004). Estrogen alters hippocampal dendritic spine shape and enhances synaptic protein immunoreactivity and spatial memory in female mice. *Proc Natl Acad Sci U S A, 101*(7), 2185-2190. doi: 10.1073/pnas.0307313101

Li, J., & Gibbs, R. B. (2019). Detection of estradiol in rat brain tissues: Contribution of local versus systemic production. *Psychoneuroendocrinology, 102*, 84-94. doi: 10.1016/j.psyneuen.2018.11.037

Li, J., Oberly, P. J., Poloyac, S. M., & Gibbs, R. B. (2016). A microsomal based method to detect aromatase activity in different brain regions of the rat using ultra performance liquid

chromatography-mass spectrometry. *J Steroid Biochem Mol Biol, 163*, 113-120. doi: 10.1016/j.jsbmb.2016.04.013

Li, J., Rao, D., & Gibbs, R. B. (2018). Effects of Cholinergic Lesions and Cholinesterase Inhibitors on Aromatase and Estrogen Receptor Expression in Different Regions of the Rat Brain. *Neuroscience, 384*, 203-213. doi: 10.1016/j.neuroscience.2018.05.033

Li, J., Wang, B., Wu, H., Yu, Y., Xue, G., & Hou, Y. (2014). 17beta-estradiol attenuates ketamine-induced neuroapoptosis and persistent cognitive deficits in the developing brain. *Brain Res, 1593*, 30-39. doi: 10.1016/j.brainres.2014.09.013

Li, L., Chen, J., Sun, S., Zhao, J., Dong, X., & Wang, J. (2017). Effects of Estradiol on Autophagy and Nrf-2/ARE Signals after Cerebral Ischemia. *Cell Physiol Biochem, 41*(5), 2027-2036. doi: 10.1159/000475433

Lima, F. B., Ota, F. H., Cabral, F. J., Del Bianco Borges, B., & Franci, C. R. (2014). Estrogen, but not progesterone, induces the activity of nitric oxide synthase within the medial preoptic area in female rats. *Brain Res, 1578*, 23-29. doi: 10.1016/j.brainres.2014.07.003

Liu, N. K., & Xu, X. M. (2006). beta-tubulin is a more suitable internal control than beta-actin in western blot analysis of spinal cord tissues after traumatic injury. *J Neurotrauma, 23*(12), 1794-1801. doi: 10.1089/neu.2006.23.1794

Lohff, J. C., Christian, P. J., Marion, S. L., Arrandale, A., & Hoyer, P. B. (2005). Characterization of cyclicity and hormonal profile with impending ovarian failure in a novel chemical-induced mouse model of perimenopause. *Comp Med, 55*(6), 523-527.

Lohff, J. C., Christian, P. J., Marion, S. L., & Hoyer, P. B. (2006). Effect of duration of dosing on onset of ovarian failure in a chemical-induced mouse model of perimenopause. *Menopause, 13*(3), 482-488. doi: 10.1097/01.gme.0000191883.59799.2e

Long, T., Yao, J. K., Li, J., Kirshner, Z. Z., Nelson, D., Dougherty, G. G., & Gibbs, R. B. (2018). Comparison of transitional vs surgical menopause on monoamine and amino acid levels in the rat brain. *Mol Cell Endocrinol, 476*, 139-147. doi: 10.1016/j.mce.2018.05.003

Long, T., Yao, J. K., Li, J., Kirshner, Z. Z., Nelson, D., Dougherty, G. G., & Gibbs, R. B. (2019). Estradiol and selective estrogen receptor agonists differentially affect brain monoamines and amino acids levels in transitional and surgical menopausal rat models. *Mol Cell Endocrinol, 496*, 110533. doi: 10.1016/j.mce.2019.110533

Lopez, M., & Tena-Sempere, M. (2015). Estrogens and the control of energy homeostasis: a brain perspective. *Trends Endocrinol Metab, 26*(8), 411-421. doi: 10.1016/j.tem.2015.06.003

Lu, H., Ma, K., Jin, L., Zhu, H., & Cao, R. (2018). 17beta-estradiol rescues damages following traumatic brain injury from molecule to behavior in mice. *J Cell Physiol, 233*(2), 1712-1722. doi: 10.1002/jcp.26083

Luine, V. N. (1985). Estradiol increases choline acetyltransferase activity in specific basal forebrain nuclei and projection areas of female rats. *Exp Neurol, 89*(2), 484-490.

Luine, V. N. (2014). Estradiol and cognitive function: past, present and future. *Horm Behav, 66*(4), 602-618. doi: 10.1016/j.yhbeh.2014.08.011

Lynch, J. F., 3rd, Winiecki, P., Vanderhoof, T., Riccio, D. C., & Jasnow, A. M. (2016). Hippocampal cytosolic estrogen receptors regulate fear generalization in females. *Neurobiol Learn Mem, 130*, 83-92. doi: 10.1016/j.nlm.2016.01.010

Mahavongtrakul, M., Kanjiya, M. P., Maciel, M., Kanjiya, S., & Sinchak, K. (2013). Estradiol dose-dependent regulation of membrane estrogen receptor-alpha, metabotropic glutamate receptor-1a, and their complexes in the arcuate nucleus of the hypothalamus in female rats. *Endocrinology, 154*(9), 3251-3260. doi: 10.1210/en.2013-1235

Manavathi, B., & Kumar, R. (2006). Steering estrogen signals from the plasma membrane to the nucleus: two sides of the coin. *J Cell Physiol, 207*(3), 594-604. doi: 10.1002/jcp.20551

Martinez-Beamonte, R., Navarro, M. A., Larraga, A., Strunk, M., Barranquero, C., Acin, S., . . . Osada, J. (2011). Selection of reference genes for gene expression studies in rats. *J Biotechnol, 151*(4), 325-334. doi: 10.1016/j.jbiotec.2010.12.017

Mauvais-Jarvis, F., Clegg, D. J., & Hevener, A. L. (2013). The role of estrogens in control of energy balance and glucose homeostasis. *Endocr Rev, 34*(3), 309-338. doi: 10.1210/er.2012-1055

Mayer, L. P., Devine, P. J., Dyer, C. A., & Hoyer, P. B. (2004). The follicle-deplete mouse ovary produces androgen. *Biol Reprod, 71*(1), 130-138. doi: 10.1095/biolreprod.103.016113

Mayer, L. P., Dyer, C. A., Eastgard, R. L., Hoyer, P. B., & Banka, C. L. (2005). Atherosclerotic lesion development in a novel ovary-intact mouse model of perimenopause. *Arterioscler Thromb Vasc Biol, 25*(9), 1910-1916. doi: 10.1161/01.ATV.0000175767.46520.6a

McCarrey, A. C., & Resnick, S. M. (2015). Postmenopausal hormone therapy and cognition. *Horm Behav, 74*, 167-172. doi: 10.1016/j.yhbeh.2015.04.018

McEwen, B. (2002). Estrogen actions throughout the brain. *Recent Prog Horm Res, 57*, 357-384.

McEwen, B. S. (2014). Sex, stress and the brain: interactive actions of hormones on the developing and adult brain. *Climacteric, 17 Suppl 2*, 18-25. doi: 10.3109/13697137.2014.949662

McEwen, B. S., Akama, K. T., Spencer-Segal, J. L., Milner, T. A., & Waters, E. M. (2012). Estrogen effects on the brain: actions beyond the hypothalamus via novel mechanisms. *Behav Neurosci, 126*(1), 4-16. doi: 10.1037/a0026708

McKenna, M. C., Dienel, G. A., Sonnewald, U., Waagepetersen, H. S., & Schousboe, A. (2012). Energy Metabolism of the Brain. 200-231. doi: 10.1016/b978-0-12-374947-5.00011-0

McMillan, P. J., Singer, C. A., & Dorsa, D. M. (1996). The effects of ovariectomy and estrogen replacement on trkA and choline acetyltransferase mRNA expression in the basal forebrain of the adult female Sprague-Dawley rat. *J Neurosci, 16*(5), 1860-1865.

Mehlhorn, G., Löffler, T., Apelt, J., Robner, S., Urabe, T., Hattori, N., . . . Schliebs, R. (1998). Glucose metabolism in cholinoceptive cortical ratbrain regions after basal forebrain cholinergic lesion. *International Journal of Developmental Neuroscience, 16*(7-8), 675-690. doi: 10.1016/s0736-5748(98)00078-1

Meitzen, J., & Mermelstein, P. G. (2011). Estrogen receptors stimulate brain region specific metabotropic glutamate receptors to rapidly initiate signal transduction pathways. *J Chem Neuroanat, 42*(4), 236-241. doi: 10.1016/j.jchemneu.2011.02.002

Mergenthaler, P., Lindauer, U., Dienel, G. A., & Meisel, A. (2013). Sugar for the brain: the role of glucose in physiological and pathological brain function. *Trends Neurosci, 36*(10), 587-597. doi: 10.1016/j.tins.2013.07.001

Mesulam, M. M. (1996). The systems-level organization of cholinergic innervation in the human cerebral cortex and its alterations in Alzheimer's disease. *Prog Brain Res, 109*, 285-297.

Metcalfe, K., Lynch, H. T., Foulkes, W. D., Tung, N., Kim-Sing, C., Olopade, O. I., . . . Narod, S. A. (2015). Effect of Oophorectomy on Survival After Breast Cancer in BRCA1 and BRCA2 Mutation Carriers. *JAMA Oncol, 1*(3), 306-313. doi: 10.1001/jamaoncol.2015.0658

Micevych, P. E., Mermelstein, P. G., & Sinchak, K. (2017). Estradiol Membrane-Initiated Signaling in the Brain Mediates Reproduction. *Trends Neurosci, 40*(11), 654-666. doi: 10.1016/j.tins.2017.09.001

Milner, T. A., Aoki, C., Sheu, K. F., Blass, J. P., & Pickel, V. M. (1987). Light microscopic immunocytochemical localization of pyruvate dehydrogenase complex in rat brain: topographical distribution and relation to cholinergic and catecholaminergic nuclei. *J Neurosci, 7*(10), 3171-3190.

Milner, T. A., Ayoola, K., Drake, C. T., Herrick, S. P., Tabori, N. E., McEwen, B. S., . . . Alves, S. E. (2005). Ultrastructural localization of estrogen receptor beta immunoreactivity in the rat hippocampal formation. *J Comp Neurol, 491*(2), 81-95. doi: 10.1002/cne.20724

Milner, T. A., McEwen, B. S., Hayashi, S., Li, C. J., Reagan, L. P., & Alves, S. E. (2001). Ultrastructural evidence that hippocampal alpha estrogen receptors are located at extranuclear sites. *J Comp Neurol, 429*(3), 355-371.

Mitra, S. W., Hoskin, E., Yudkovitz, J., Pear, L., Wilkinson, H. A., Hayashi, S., . . . Alves, S. E. (2003). Immunolocalization of estrogen receptor beta in the mouse brain: comparison with estrogen receptor alpha. *Endocrinology, 144*(5), 2055-2067. doi: 10.1210/en.2002-221069

Mochel, F. (2017). Triheptanoin for the treatment of brain energy deficit: A 14-year experience. *J Neurosci Res, 95*(11), 2236-2243. doi: 10.1002/jnr.24111

Moran, J., Garrido, P., Alonso, A., Cabello, E., & Gonzalez, C. (2013). 17beta-Estradiol and genistein acute treatments improve some cerebral cortex homeostasis aspects deteriorated by aging in female rats. *Exp Gerontol, 48*(4), 414-421. doi: 10.1016/j.exger.2013.02.010

Moran, J., Garrido, P., Cabello, E., Alonso, A., & Gonzalez, C. (2014). Effects of estradiol and genistein on the insulin signaling pathway in the cerebral cortex of aged female rats. *Exp Gerontol, 58*, 104-112. doi: 10.1016/j.exger.2014.07.018

Mori, H., Matsuda, K., Yamawaki, M., & Kawata, M. (2014). Estrogenic regulation of histamine receptor subtype H1 expression in the ventromedial nucleus of the hypothalamus in female rats. *PLoS One, 9*(5), e96232. doi: 10.1371/journal.pone.0096232

Moritz, C. P. (2017). Tubulin or Not Tubulin: Heading Toward Total Protein Staining as Loading Control in Western Blots. *Proteomics, 17*(20). doi: 10.1002/pmic.201600189

Moritz, C. P., Marz, S. X., Reiss, R., Schulenborg, T., & Friauf, E. (2014). Epicocconone staining: a powerful loading control for Western blots. *Proteomics, 14*(2-3), 162-168. doi: 10.1002/pmic.201300089

Morseman, J. P., Moss, M. W., Zoha, S. J., & Allnutt, F. C. (1999). PBXL-1: a new fluorochrome applied to detection of proteins on membranes. *Biotechniques, 26*(3), 559-563.

Mosconi, L., Berti, V., Quinn, C., McHugh, P., Petrongolo, G., Osorio, R. S., . . . Brinton, R. D. (2017). Perimenopause and emergence of an Alzheimer's bioenergetic phenotype in brain and periphery. *PLoS One, 12*(10), e0185926. doi: 10.1371/journal.pone.0185926

Mosconi, L., Mistur, R., Switalski, R., Tsui, W. H., Glodzik, L., Li, Y., . . . de Leon, M. J. (2009). FDG-PET changes in brain glucose metabolism from normal cognition to pathologically verified Alzheimer's disease. *Eur J Nucl Med Mol Imaging, 36*(5), 811-822. doi: 10.1007/s00259-008-1039-z

Mott, N. N., & Pak, T. R. (2013). Estrogen signaling and the aging brain: context-dependent considerations for postmenopausal hormone therapy. *ISRN Endocrinol, 2013*, 814690. doi: 10.1155/2013/814690

Moura, P. J., & Petersen, S. L. (2010). Estradiol Acts through Nuclear- and Membrane-Initiated Mechanisms to Maintain a Balance between GABAergic and Glutamatergic Signaling in the Brain: Implications for Hormone Replacement Therapy. *Reviews in the Neurosciences, 21*(5). doi: 10.1515/revneuro.2010.21.5.363

Muhammad, F. S., Goode, A. K., Kock, N. D., Arifin, E. A., Cline, J. M., Adams, M. R., . . . Appt, S. E. (2009). Effects of 4-vinylcyclohexene diepoxide on peripubertal and adult Sprague-Dawley rats: ovarian, clinical, and pathologic outcomes. *Comp Med, 59*(1), 46-59.

Nambu, T., Sakurai, T., Mizukami, K., Hosoya, Y., Yanagisawa, M., & Goto, K. (1999). Distribution of orexin neurons in the adult rat brain1Published on the World Wide Web on 17 March 1999.1. *Brain Research, 827*(1-2), 243-260. doi: 10.1016/s0006-8993(99)01336-0

Nelson, B. S., Springer, R. C., & Daniel, J. M. (2014). Antagonism of brain insulin-like growth factor-1 receptors blocks estradiol effects on memory and levels of hippocampal synaptic proteins in ovariectomized rats. *Psychopharmacology (Berl), 231*(5), 899-907. doi: 10.1007/s00213-013-3310-7

Newhouse, P., & Dumas, J. (2015). Estrogen-cholinergic interactions: Implications for cognitive aging. *Horm Behav, 74*, 173-185. doi: 10.1016/j.yhbeh.2015.06.022

Nguyen, T. V., Ducharme, S., & Karama, S. (2016). Effects of Sex Steroids in the Human Brain. *Mol Neurobiol*. doi: 10.1007/s12035-016-0198-3

Nicholls, C., Li, H., & Liu, J. P. (2012). GAPDH: a common enzyme with uncommon functions. *Clin Exp Pharmacol Physiol, 39*(8), 674-679. doi: 10.1111/j.1440-1681.2011.05599.x

Nilsen, J., Irwin, R. W., Gallaher, T. K., & Brinton, R. D. (2007). Estradiol in vivo regulation of brain mitochondrial proteome. *J Neurosci, 27*(51), 14069-14077. doi: 10.1523/JNEUROSCI.4391-07.2007

O'Malley, C. A., Dean Hautamaki, R., Kelley, M., & Meyer, E. M. (1987). Effects of ovariectomy and estradiol benzoate on high affinity choline uptake, ACh synthesis, and release from rat cerebral cortical synaptosomes. *Brain Research, 403*(2), 389-392. doi: 10.1016/0006-8993(87)90082-5

Oda, Y. (1999). Choline acetyltransferase: the structure, distribution and pathologic changes in the central nervous system. *Pathol Int, 49*(11), 921-937.

Park, S., Jeon, J. H., Min, B. K., Ha, C. M., Thoudam, T., Park, B. Y., & Lee, I. K. (2018). Role of the Pyruvate Dehydrogenase Complex in Metabolic Remodeling: Differential Pyruvate Dehydrogenase Complex Functions in Metabolism. *Diabetes Metab J, 42*(4), 270-281. doi: 10.4093/dmj.2018.0101

Perry, E. K., Perry, R. H., Tomlinson, B. E., Blessed, G., & Gibson, P. H. (1980). Coenzyme A-acetylating enzymes in Alzheimer's disease: possible cholinergic 'compartment' of pyruvate dehydrogenase. *Neurosci Lett, 18*(1), 105-110.

Pfaffl, M. W. (2001). A new mathematical model for relative quantification in real-time RT-PCR. *Nucleic Acids Res, 29*(9), e45. doi: 10.1093/nar/29.9.e45

Pongrac, J. L., Gibbs, R. B., & Defranco, D. B. (2004). Estrogen-mediated regulation of cholinergic expression in basal forebrain neurons requires extracellular-signal-regulated kinase activity. *Neuroscience, 124*(4), 809-816. doi: 10.1016/j.neuroscience.2004.01.013

Pongrac, J. L., & Rylett, R. J. (2002). Differential Effects of Nerve Growth Factor on Expression of Choline Acetyltransferase and Sodium-Coupled Choline Transport in Basal Forebrain Cholinergic Neurons in Culture. *Journal of Neurochemistry, 66*(2), 804-810. doi: 10.1046/j.1471-4159.1996.66020804.x

Poor, M. L., Santa, P. F., & Sittampalam, G. S. (1988). Visualization of multiple protein bands on the same nitrocellulose membrane by double immunoblotting. *Anal Biochem, 175*(1), 191-195.

Prasad, C., Rupar, T., & Prasad, A. N. (2011). Pyruvate dehydrogenase deficiency and epilepsy. *Brain Dev, 33*(10), 856-865. doi: 10.1016/j.braindev.2011.08.003

Radhika, N. S., Govindaraj, V., Sarangi, S. K., & Rao, A. J. (2015). Neonatal exposure to 17beta-estradiol down-regulates the expression of synaptogenesis related genes in selected brain regions of adult female rats. *Life Sci, 141*, 1-7. doi: 10.1016/j.lfs.2015.09.013

Rajkumar, K., Nichita, A., Anoor, P. K., Raju, S., Singh, S. S., & Burgula, S. (2016). Understanding perspectives of signalling mechanisms regulating PEBP1 function. *Cell Biochem Funct, 34*(6), 394-403. doi: 10.1002/cbf.3198

Ramirez, V. D., Kipp, J. L., & Joe, I. (2001). Estradiol, in the CNS, targets several physiologically relevant membrane-associated proteins. *Brain Research Reviews, 37*(1-3), 141-152. doi: 10.1016/s0165-0173(01)00114-x

Rao, Y. S., Shults, C. L., Pinceti, E., & Pak, T. R. (2015). Prolonged ovarian hormone deprivation alters the effects of 17beta-estradiol on microRNA expression in the aged female rat hypothalamus. *Oncotarget, 6*(35), 36965-36983. doi: 10.18632/oncotarget.5433

Ray, B., Bailey, J. A., Simon, J. R., & Lahiri, D. K. (2012). High-affinity choline uptake (HACU) and choline acetyltransferase (ChAT) activity in neuronal cultures for mechanistic and drug discovery studies. *Curr Protoc Neurosci, Chapter 7*, Unit 7 23. doi: 10.1002/0471142301.ns0723s60

Renart, J., Reiser, J., & Stark, G. R. (1979). Transfer of proteins from gels to diazobenzyloxymethyl-paper and detection with antisera: a method for studying antibody specificity and antigen structure. *Proc Natl Acad Sci U S A, 76*(7), 3116-3120.

Resnick, S. M., Espeland, M. A., Jaramillo, S. A., Hirsch, C., Stefanick, M. L., Murray, A. M., . . . Davatzikos, C. (2009). Postmenopausal hormone therapy and regional brain volumes: the WHIMS-MRI Study. *Neurology, 72*(2), 135-142. doi: 10.1212/01.wnl.0000339037.76336.cf

Rettberg, J. R., Yao, J., & Brinton, R. D. (2014). Estrogen: a master regulator of bioenergetic systems in the brain and body. *Front Neuroendocrinol, 35*(1), 8-30. doi: 10.1016/j.yfrne.2013.08.001

Revankar, C. M., Cimino, D. F., Sklar, L. A., Arterburn, J. B., & Prossnitz, E. R. (2005). A transmembrane intracellular estrogen receptor mediates rapid cell signaling. *Science, 307*(5715), 1625-1630. doi: 10.1126/science.1106943

Richter, N., Allendorf, I., Onur, O. A., Kracht, L., Dietlein, M., Tittgemeyer, M., . . . Kukolja, J. (2014). The integrity of the cholinergic system determines memory performance in healthy elderly. *Neuroimage, 100*, 481-488. doi: 10.1016/j.neuroimage.2014.06.031

Rivero-Gutierrez, B., Anzola, A., Martinez-Augustin, O., & de Medina, F. S. (2014). Stain-free detection as loading control alternative to Ponceau and housekeeping protein immunodetection in Western blotting. *Anal Biochem, 467*, 1-3. doi: 10.1016/j.ab.2014.08.027

Robertson, J. A., Bhattacharyya, S., & Ing, N. H. (1998). Tamoxifen up-regulates oestrogen receptor-alpha, c-fos and glyceraldehyde 3-phosphate-dehydrogenase mRNAs in ovine endometrium. *J Steroid Biochem Mol Biol, 67*(4), 285-292.

Rocca, W. A., Grossardt, B. R., & Shuster, L. T. (2014). Oophorectomy, estrogen, and dementia: a 2014 update. *Mol Cell Endocrinol, 389*(1-2), 7-12. doi: 10.1016/j.mce.2014.01.020

Rocca, W. A., Grossardt, B. R., Shuster, L. T., & Stewart, E. A. (2012). Hysterectomy, oophorectomy, estrogen, and the risk of dementia. *Neurodegener Dis, 10*(1-4), 175-178. doi: 10.1159/000334764

Romero-Calvo, I., Ocon, B., Martinez-Moya, P., Suarez, M. D., Zarzuelo, A., Martinez-Augustin, O., & de Medina, F. S. (2010). Reversible Ponceau staining as a loading control alternative to actin in Western blots. *Anal Biochem, 401*(2), 318-320. doi: 10.1016/j.ab.2010.02.036

Rubin, B. S., Fox, T. O., & Bridges, R. S. (1986). Estrogen binding in nuclear and cytosolic extracts from brain and pituitary of middle-aged female rats. *Brain Research, 383*(1-2), 60-67. doi: 10.1016/0006-8993(86)90008-9

Russell, J. K., Jones, C. K., & Newhouse, P. A. (2019). The Role of Estrogen in Brain and Cognitive Aging. *Neurotherapeutics, 16*(3), 649-665. doi: 10.1007/s13311-019-00766-9

Sa, S. I., Fonseca, B. M., Teixeira, N., & Madeira, M. D. (2015). Estrogen receptors alpha and beta have different roles in the induction and trafficking of progesterone receptors in hypothalamic ventromedial neurons. *Febs j, 282*(6), 1126-1136. doi: 10.1111/febs.13207

Sa, S. I., Fonseca, B. M., Teixeira, N., & Madeira, M. D. (2016). Induction and subcellular redistribution of progesterone receptor A and B by tamoxifen in the hypothalamic ventromedial neurons of young adult female Wistar rats. *Mol Cell Endocrinol, 420*, 1-10. doi: 10.1016/j.mce.2015.11.015

Saito, K., & Cui, H. (2018). Emerging Roles of Estrogen-Related Receptors in the Brain: Potential Interactions with Estrogen Signaling. *Int J Mol Sci, 19*(4). doi: 10.3390/ijms19041091

Sakurai, T., & Mieda, M. (2011). Connectomics of orexin-producing neurons: interface of systems of emotion, energy homeostasis and arousal. *Trends Pharmacol Sci, 32*(8), 451-462. doi: 10.1016/j.tips.2011.03.007

Sanchez, R., Nguyen, D., Rocha, W., White, J. H., & Mader, S. (2002). Diversity in the mechanisms of gene regulation by estrogen receptors - Era affecting genes indirectly. *Bioessays, 24*(3), 244-254. doi: 10.1002/bies.10066

Sandstrom, N. J., & Williams, C. L. (2001). Memory retention is modulated by acute estradiol and progesterone replacement. *Behavioral Neuroscience, 115*(2), 384-393. doi: 10.1037/0735-7044.115.2.384

Sandstrom, N. J., & Williams, C. L. (2004). Spatial memory retention is enhanced by acute and continuous estradiol replacement. *Horm Behav, 45*(2), 128-135. doi: 10.1016/j.yhbeh.2003.09.010

Sarvari, M., Hrabovszky, E., Kallo, I., Galamb, O., Solymosi, N., Liko, I., . . . Liposits, Z. (2010). Gene expression profiling identifies key estradiol targets in the frontal cortex of the rat. *Endocrinology, 151*(3), 1161-1176. doi: 10.1210/en.2009-0911

Schroder, A. L., Pelch, K. E., & Nagel, S. C. (2009). Estrogen modulates expression of putative housekeeping genes in the mouse uterus. *Endocrine, 35*(2), 211-219. doi: 10.1007/s12020-009-9154-6

Seki, S. M., & Gaultier, A. (2017). Exploring Non-Metabolic Functions of Glycolytic Enzymes in Immunity. *Front Immunol, 8*, 1549. doi: 10.3389/fimmu.2017.01549

Sha, D., Jin, H., Kopke, R. D., & Wu, J.-Y. (2004). Choline Acetyltransferase: Regulation and Coupling with Protein Kinase and Vesicular Acetylcholine Transporter on Synaptic Vesicles. *Neurochemical Research, 29*(1), 199-207. doi: 10.1023/B:NERE.0000010449.05927.f9

Shanle, E. K., & Xu, W. (2011). Endocrine disrupting chemicals targeting estrogen receptor signaling: identification and mechanisms of action. *Chem Res Toxicol, 24*(1), 6-19. doi: 10.1021/tx100231n

Sheppard, P. A. S., Choleris, E., & Galea, L. A. M. (2019). Structural plasticity of the hippocampus in response to estrogens in female rodents. *Mol Brain, 12*(1), 22. doi: 10.1186/s13041-019-0442-7

Shi, J., & Simpkins, J. W. (1997). 17 beta-Estradiol modulation of glucose transporter 1 expression in blood-brain barrier. *Am J Physiol, 272*(6 Pt 1), E1016-1022. doi: 10.1152/ajpendo.1997.272.6.E1016

Shirai, N., Houle, C., & Mirsky, M. L. (2015). Using Histopathologic Evidence to Differentiate Reproductive Senescence from Xenobiotic Effects in Middle-aged Female Sprague-Dawley Rats. *Toxicol Pathol, 43*(8), 1158-1161. doi: 10.1177/0192623315595137

Shrestha, P. K., & Briski, K. P. (2015). Hindbrain lactate regulates preoptic gonadotropin-releasing hormone (GnRH) neuron GnRH-I protein but not AMPK responses to hypoglycemia in the steroid-primed ovariectomized female rat. *Neuroscience, 298*, 467-474. doi: 10.1016/j.neuroscience.2015.04.049

Shughrue, P. J., Lane, M. V., & Merchenthaler, I. (1997). Comparative distribution of estrogen receptor-? and -? mRNA in the rat central nervous system. *The Journal of Comparative Neurology, 388*(4), 507-525. doi: 10.1002/(sici)1096-9861(19971201)388:4<507::aid-cne1>3.0.co;2-6

Shughrue, P. J., & Merchenthaler, I. (2000). Estrogen is more than just a "sex hormone": novel sites for estrogen action in the hippocampus and cerebral cortex. *Front Neuroendocrinol, 21*(1), 95-101. doi: 10.1006/frne.1999.0190

Shughrue, P. J., & Merchenthaler, I. (2001). Distribution of estrogen receptor ? immunoreactivity in the rat central nervous system. *The Journal of Comparative Neurology, 436*(1), 64-81. doi: 10.1002/cne.1054

Simerly, R. B., Chang, C., Muramatsu, M., & Swanson, L. W. (1990). Distribution of androgen and estrogen receptor mRNA-containing cells in the rat brain: an in situ hybridization study. *J Comp Neurol, 294*(1), 76-95. doi: 10.1002/cne.902940107

Sirover, M. A. (2012). Subcellular dynamics of multifunctional protein regulation: mechanisms of GAPDH intracellular translocation. *J Cell Biochem, 113*(7), 2193-2200. doi: 10.1002/jcb.24113

Spencer, J. L., Waters, E. M., Romeo, R. D., Wood, G. E., Milner, T. A., & McEwen, B. S. (2008). Uncovering the mechanisms of estrogen effects on hippocampal function. *Front Neuroendocrinol, 29*(2), 219-237. doi: 10.1016/j.yfrne.2007.08.006

Springer, L. N., McAsey, M. E., Flaws, J. A., Tilly, J. L., Sipes, I. G., & Hoyer, P. B. (1996). Involvement of apoptosis in 4-vinylcyclohexene diepoxide-induced ovotoxicity in rats. *Toxicol Appl Pharmacol, 139*(2), 394-401. doi: 10.1006/taap.1996.0180

Srivastava, D. P., Woolfrey, K. M., Jones, K. A., Shum, C. Y., Lash, L. L., Swanson, G. T., & Penzes, P. (2008). Rapid enhancement of two-step wiring plasticity by estrogen and NMDA receptor activity. *Proc Natl Acad Sci U S A, 105*(38), 14650-14655. doi: 10.1073/pnas.0801581105

Stacpoole, P. W. (2012). The pyruvate dehydrogenase complex as a therapeutic target for age-related diseases. *Aging Cell, 11*(3), 371-377. doi: 10.1111/j.1474-9726.2012.00805.x

Sternberg. (1983). Biomedical Image Processing. *Computer, 16*(1), 22-34. doi: 10.1109/mc.1983.1654163

Sterri, S. H., & Fonnum, F. (1980). Acetyl-CoA synthesizing enzymes in cholinergic nerve terminals. *J Neurochem, 35*(1), 249-254.

Sun, J., Aluvila, S., Kotaria, R., Mayor, J. A., Walters, D. E., & Kaplan, R. S. (2010). Mitochondrial and Plasma Membrane Citrate Transporters: Discovery of Selective Inhibitors and Application to Structure/Function Analysis. *Mol Cell Pharmacol, 2*(3), 101-110.

Suzuki, M., Sasabe, J., Miyoshi, Y., Kuwasako, K., Muto, Y., Hamase, K., . . . Aiso, S. (2015). Glycolytic flux controls D-serine synthesis through glyceraldehyde-3-phosphate dehydrogenase in astrocytes. *Proc Natl Acad Sci U S A, 112*(17), E2217-2224. doi: 10.1073/pnas.1416117112

Swerdlow, R. H., & Khan, S. M. (2004). A "mitochondrial cascade hypothesis" for sporadic Alzheimer's disease. *Med Hypotheses, 63*(1), 8-20. doi: 10.1016/j.mehy.2003.12.045

Szego, E. M., Kekesi, K. A., Szabo, Z., Janaky, T., & Juhasz, G. D. (2010). Estrogen regulates cytoskeletal flexibility, cellular metabolism and synaptic proteins: A proteomic study. *Psychoneuroendocrinology, 35*(6), 807-819. doi: 10.1016/j.psyneuen.2009.11.006

Szutowicz, A., Bielarczyk, H., Gul, S., Zielinski, P., Pawelczyk, T., & Tomaszewicz, M. (2005). Nerve growth factor and acetyl-L-carnitine evoked shifts in acetyl-CoA and cholinergic SN56 cell vulnerability to neurotoxic inputs. *J Neurosci Res, 79*(1-2), 185-192. doi: 10.1002/jnr.20276

Szutowicz, A., Bielarczyk, H., Jankowska-Kulawy, A., Pawelczyk, T., & Ronowska, A. (2013). Acetyl-CoA the key factor for survival or death of cholinergic neurons in course of neurodegenerative diseases. *Neurochem Res, 38*(8), 1523-1542. doi: 10.1007/s11064-013-1060-x

Szutowicz, A., Bielarczyk, H., Ronowska, A., Gul-Hinc, S., Klimaszewska-Lata, J., Dys, A., . . . Pawelczyk, T. (2014). Intracellular redistribution of acetyl-CoA, the pivotal point in differential susceptibility of cholinergic neurons and glial cells to neurodegenerative signals. *Biochem Soc Trans, 42*(4), 1101-1106. doi: 10.1042/bst20140078

Szutowicz, A., Jankowska, A., Blusztajn, J. K., & Tomaszewicz, M. (1999). Acetylcholine and acetyl-CoA metabolism in differentiating SN56 septal cell line. *J Neurosci Res, 57*(1), 131-136.

Szutowicz, A., Stepien, M., Bielarczyk, H., Kabata, J., & Lysiak, W. (1982). ATP citrate lyase in cholinergic nerve endings. *Neurochem Res, 7*(7), 799-810.

Szutowicz, A., Tomaszewicz, M., Jankowska, A., & Kisielevski, Y. (1994). Acetylcholine synthesis in nerve terminals of diabetic rats. *Neuroreport, 5*(18), 2421-2424. doi: 10.1097/00001756-199412000-00004

Takahashi, T. A., & Johnson, K. M. (2015). Menopause. *Med Clin North Am, 99*(3), 521-534. doi: 10.1016/j.mcna.2015.01.006

Taki, F. A., Abdel-Rahman, A. A., & Zhang, B. (2014). A comprehensive approach to identify reliable reference gene candidates to investigate the link between alcoholism and endocrinology in Sprague-Dawley rats. *PLoS One, 9*(5), e94311. doi: 10.1371/journal.pone.0094311

Tamrakar, P., Ibrahim, B. A., Gujar, A. D., & Briski, K. P. (2015). Estrogen regulates energy metabolic pathway and upstream adenosine 5'-monophosphate-activated protein kinase and phosphatase enzyme expression in dorsal vagal complex metabolosensory neurons during glucostasis and hypoglycemia. *J Neurosci Res, 93*(2), 321-332. doi: 10.1002/jnr.23481

Taylor, S. C., Berkelman, T., Yadav, G., & Hammond, M. (2013). A defined methodology for reliable quantification of Western blot data. *Mol Biotechnol, 55*(3), 217-226. doi: 10.1007/s12033-013-9672-6

Thacker, J. S., Yeung, D. H., Staines, W. R., & Mielke, J. G. (2016). Total protein or high-abundance protein: Which offers the best loading control for Western blotting? *Anal Biochem, 496*, 76-78. doi: 10.1016/j.ab.2015.11.022

Thomas, P., Pang, Y., Filardo, E. J., & Dong, J. (2005). Identity of an estrogen membrane receptor coupled to a G protein in human breast cancer cells. *Endocrinology, 146*(2), 624-632. doi: 10.1210/en.2004-1064

ThyagaRajan, S., Hima, L., Pratap, U. P., Priyanka, H. P., & Vasantharekha, R. (2019). Estrogen-induced neuroimmunomodulation as facilitator of and barrier to reproductive aging in brain and lymphoid organs. *J Chem Neuroanat, 95*, 6-12. doi: 10.1016/j.jchemneu.2018.02.008

Toran-Allerand, C. D. (2004). Minireview: A plethora of estrogen receptors in the brain: where will it end? *Endocrinology, 145*(3), 1069-1074. doi: 10.1210/en.2003-1462

Toran-Allerand, C. D., Guan, X., MacLusky, N. J., Horvath, T. L., Diano, S., Singh, M., . . . Tinnikov, A. A. (2002). ER-X: A Novel, Plasma Membrane-Associated, Putative Estrogen Receptor That Is Regulated during Development and after Ischemic Brain Injury. *The Journal of Neuroscience, 22*(19), 8391-8401. doi: 10.1523/jneurosci.22-19-08391.2002

Toro-Urrego, N., Garcia-Segura, L. M., Echeverria, V., & Barreto, G. E. (2016). Testosterone Protects Mitochondrial Function and Regulates Neuroglobin Expression in Astrocytic Cells Exposed to Glucose Deprivation. *Front Aging Neurosci, 8*, 152. doi: 10.3389/fnagi.2016.00152

Tovey, E. R., Ford, S. A., & Baldo, B. A. (1987). Protein blotting on nitrocellulose: some important aspects of the resolution and detection of antigens in complex extracts. *Journal of Biochemical and Biophysical Methods, 14*(1), 1-17. doi: 10.1016/0165-022x(87)90002-9

Traish, A. M., Abdallah, B., & Yu, G. (2011). Androgen deficiency and mitochondrial dysfunction: implications for fatigue, muscle dysfunction, insulin resistance, diabetes, and cardiovascular disease. *Horm Mol Biol Clin Investig, 8*(1), 431-444. doi: 10.1515/HMBCI.2011.132

Trenti, A., Tedesco, S., Boscaro, C., Ferri, N., Cignarella, A., Trevisi, L., & Bolego, C. (2017). The Glycolytic Enzyme PFKFB3 Is Involved in Estrogen-Mediated Angiogenesis via GPER1. *J Pharmacol Exp Ther, 361*(3), 398-407. doi: 10.1124/jpet.116.238212

Tristan, C., Shahani, N., Sedlak, T. W., & Sawa, A. (2011). The diverse functions of GAPDH: views from different subcellular compartments. *Cell Signal, 23*(2), 317-323. doi: 10.1016/j.cellsig.2010.08.003

Tsujino, N., & Sakurai, T. (2009). Orexin/hypocretin: a neuropeptide at the interface of sleep, energy homeostasis, and reward system. *Pharmacol Rev, 61*(2), 162-176. doi: 10.1124/pr.109.001321

Tulsulkar, J., Ward, A., & Shah, Z. A. (2017). HO1 and Wnt expression is independently regulated in female mice brains following permanent ischemic brain injury. *Brain Res, 1662*, 1-6. doi: 10.1016/j.brainres.2017.02.006

Tuscher, J. J., Fortress, A. M., & Frick, K. M. (2019). Memory and Epigenetics: Role of Estrogen. 42-51. doi: 10.1016/b978-0-12-801238-3.64551-8

Vahidinia, Z., Alipour, N., Atlasi, M. A., Naderian, H., Beyer, C., & Azami Tameh, A. (2017). Gonadal steroids block the calpain-1-dependent intrinsic pathway of apoptosis in an

experimental rat stroke model. *Neurol Res, 39*(1), 54-64. doi: 10.1080/01616412.2016.1250459

Van Kempen, T. A., Gorecka, J., Gonzalez, A. D., Soeda, F., Milner, T. A., & Waters, E. M. (2014). Characterization of neural estrogen signaling and neurotrophic changes in the accelerated ovarian failure mouse model of menopause. *Endocrinology, 155*(9), 3610-3623. doi: 10.1210/en.2014-1190

Van Kempen, T. A., Milner, T. A., & Waters, E. M. (2011). Accelerated ovarian failure: a novel, chemically induced animal model of menopause. *Brain Res, 1379*, 176-187. doi: 10.1016/j.brainres.2010.12.064

Vargas, K. G., Milic, J., Zaciragic, A., Wen, K. X., Jaspers, L., Nano, J., . . . Franco, O. H. (2016). The functions of estrogen receptor beta in the female brain: A systematic review. *Maturitas, 93*, 41-57. doi: 10.1016/j.maturitas.2016.05.014

Vasconsuelo, A., Milanesi, L., & Boland, R. (2013). Actions of 17beta-estradiol and testosterone in the mitochondria and their implications in aging. *Ageing Res Rev, 12*(4), 907-917. doi: 10.1016/j.arr.2013.09.001

Velarde, M. C. (2014). Mitochondrial and sex steroid hormone crosstalk during aging. *Longev Healthspan, 3*(1), 2. doi: 10.1186/2046-2395-3-2

Vigelso, A., Dybboe, R., Hansen, C. N., Dela, F., Helge, J. W., & Guadalupe Grau, A. (2015). GAPDH and beta-actin protein decreases with aging, making Stain-Free technology a superior loading control in Western blotting of human skeletal muscle. *J Appl Physiol (1985), 118*(3), 386-394. doi: 10.1152/japplphysiol.00840.2014

Vivacqua, A., Bonofiglio, D., Recchia, A. G., Musti, A. M., Picard, D., Ando, S., & Maggiolini, M. (2006). The G protein-coupled receptor GPR30 mediates the proliferative effects induced by 17beta-estradiol and hydroxytamoxifen in endometrial cancer cells. *Mol Endocrinol, 20*(3), 631-646. doi: 10.1210/me.2005-0280

Volker, K. W., & Knull, H. (1997). A glycolytic enzyme binding domain on tubulin. *Arch Biochem Biophys, 338*(2), 237-243. doi: 10.1006/abbi.1996.9819

Volker, K. W., & Knull, H. R. (1993). Glycolytic enzyme-tubulin interactions: role of tubulin carboxy terminals. *J Mol Recognit, 6*(4), 167-177. doi: 10.1002/jmr.300060405

Wada-Kiyama, Y., Suzuki, C., Hamada, T., Rai, D., Kiyama, R., Kaneda, M., & Sakuma, Y. (2013). Estrogen-induced cell signaling in the sexually dimorphic nucleus of the rat preoptic area: potential involvement of cofilin in actin dynamics for cell migration. *Biochem Biophys Res Commun, 434*(2), 287-292. doi: 10.1016/j.bbrc.2013.02.117

Wallace, M., Frankfurt, M., Arellanos, A., Inagaki, T., & Luine, V. (2007). Impaired recognition memory and decreased prefrontal cortex spine density in aged female rats. *Ann N Y Acad Sci, 1097*, 54-57. doi: 10.1196/annals.1379.026

Warner, M., Huang, B., & Gustafsson, J. A. (2016). Estrogen Receptor beta as a Pharmaceutical Target. *Trends Pharmacol Sci*. doi: 10.1016/j.tips.2016.10.006

Weber, M. T., Maki, P. M., & McDermott, M. P. (2014). Cognition and mood in perimenopause: a systematic review and meta-analysis. *J Steroid Biochem Mol Biol, 142*, 90-98. doi: 10.1016/j.jsbmb.2013.06.001

Welinder, C., & Ekblad, L. (2011). Coomassie staining as loading control in Western blot analysis. *J Proteome Res, 10*(3), 1416-1419. doi: 10.1021/pr1011476

Welling, L. L. M., Shackelford, T. K., Ervin, K. S. J., & Choleris, E. (2019). Involvement of the Sex Hormones in Learning and Memory. 66-85. doi: 10.1093/oxfordhb/9780190649739.013.4

Wibowo, E., Calich, H. J., Currie, R. W., & Wassersug, R. J. (2015). Prolonged androgen deprivation may influence the autoregulation of estrogen receptors in the brain and pelvic floor muscles of male rats. *Behav Brain Res, 286*, 128-135. doi: 10.1016/j.bbr.2015.03.003

Wijayaratne, A. L., & McDonnell, D. P. (2001). The human estrogen receptor-alpha is a ubiquitinated protein whose stability is affected differentially by agonists, antagonists, and selective estrogen receptor modulators. *J Biol Chem, 276*(38), 35684-35692. doi: 10.1074/jbc.M101097200

Wilson, M. E., Rosewell, K. L., Kashon, M. L., Shughrue, P. J., Merchenthaler, I., & Wise, P. M. (2002). Age differentially influences estrogen receptor-α (ERα) and estrogen receptor-β (ERβ) gene expression in specific regions of the rat brain. *Mechanisms of Ageing and Development, 123*(6), 593-601. doi: 10.1016/s0047-6374(01)00406-7

Witty, C. F., Gardella, L. P., Perez, M. C., & Daniel, J. M. (2013). Short-term estradiol administration in aging ovariectomized rats provides lasting benefits for memory and the hippocampus: a role for insulin-like growth factor-I. *Endocrinology, 154*(2), 842-852. doi: 10.1210/en.2012-1698

Wong, A. M., Scott, A. K., Johnson, C. S., Mohr, M. A., Mittelman-Smith, M., & Micevych, P. E. (2019). ERalphaDelta4, an ERalpha splice variant missing exon4, interacts with caveolin-3 and mGluR2/3. *J Neuroendocrinol*, e12725. doi: 10.1111/jne.12725

Woolley, C. S. (2007). Acute effects of estrogen on neuronal physiology. *Annu Rev Pharmacol Toxicol, 47*, 657-680. doi: 10.1146/annurev.pharmtox.47.120505.105219

Woolley, C. S., & McEwen, B. S. (1994). Estradiol regulates hippocampal dendritic spine density via an N-methyl- D-aspartate receptor-dependent mechanism. *The Journal of Neuroscience, 14*(12), 7680-7687. doi: 10.1523/jneurosci.14-12-07680.1994

Wright, L. E., Christian, P. J., Rivera, Z., Van Alstine, W. G., Funk, J. L., Bouxsein, M. L., & Hoyer, P. B. (2008). Comparison of skeletal effects of ovariectomy versus chemically induced ovarian failure in mice. *J Bone Miner Res, 23*(8), 1296-1303. doi: 10.1359/jbmr.080309

Wu, T. W., Chen, S., & Brinton, R. D. (2011). Membrane estrogen receptors mediate calcium signaling and MAP kinase activation in individual hippocampal neurons. *Brain Res, 1379*, 34-43. doi: 10.1016/j.brainres.2011.01.034

Wu, W. W., Bryant, D. N., Dorsa, D. M., Adelman, J. P., & Maylie, J. (2013). Ovarian hormone loss impairs excitatory synaptic transmission at hippocampal CA3-CA1 synapses. *J Neurosci, 33*(41), 16158-16169. doi: 10.1523/JNEUROSCI.2001-13.2013

Wu, Y. C., Du, X., van den Buuse, M., & Hill, R. A. (2014). Sex differences in the adolescent developmental trajectory of parvalbumin interneurons in the hippocampus: a role for estradiol. *Psychoneuroendocrinology, 45*, 167-178. doi: 10.1016/j.psyneuen.2014.03.016

Xu, X., Gu, T., & Shen, Q. (2015). Different effects of bisphenol-A on memory behavior and synaptic modification in intact and estrogen-deprived female mice. *J Neurochem, 132*(5), 572-582. doi: 10.1111/jnc.12998

Yan, W., Kang, Y., Ji, X., Li, S., Li, Y., Zhang, G., . . . Shi, G. (2017). Testosterone Upregulates the Expression of Mitochondrial ND1 and ND4 and Alleviates the Oxidative Damage to the Nigrostriatal Dopaminergic System in Orchiectomized Rats. *Oxid Med Cell Longev, 2017*, 1202459. doi: 10.1155/2017/1202459

Yang, S. H., Liu, R., Perez, E. J., Wen, Y., Stevens, S. M., Jr., Valencia, T., . . . Simpkins, J. W. (2004). Mitochondrial localization of estrogen receptor beta. *Proc Natl Acad Sci U S A, 101*(12), 4130-4135. doi: 10.1073/pnas.0306948101

Yao, J., Irwin, R., Chen, S., Hamilton, R., Cadenas, E., & Brinton, R. D. (2012). Ovarian hormone loss induces bioenergetic deficits and mitochondrial beta-amyloid. *Neurobiol Aging, 33*(8), 1507-1521. doi: 10.1016/j.neurobiolaging.2011.03.001

Yao, J., Irwin, R. W., Zhao, L., Nilsen, J., Hamilton, R. T., & Brinton, R. D. (2009). Mitochondrial bioenergetic deficit precedes Alzheimer's pathology in female mouse model of Alzheimer's disease. *Proc Natl Acad Sci U S A, 106*(34), 14670-14675. doi: 10.1073/pnas.0903563106

Yao, J., Rettberg, J. R., Klosinski, L. P., Cadenas, E., & Brinton, R. D. (2011). Shift in brain metabolism in late onset Alzheimer's disease: implications for biomarkers and therapeutic interventions. *Mol Aspects Med, 32*(4-6), 247-257. doi: 10.1016/j.mam.2011.10.005

Yazgan, B., Yazgan, Y., Ovey, I. S., & Naziroglu, M. (2016). Raloxifene and Tamoxifen Reduce PARP Activity, Cytokine and Oxidative Stress Levels in the Brain and Blood of Ovariectomized Rats. *J Mol Neurosci, 60*(2), 214-222. doi: 10.1007/s12031-016-0785-9

Yin, F., Yao, J., Brinton, R. D., & Cadenas, E. (2017). Editorial: The Metabolic-Inflammatory Axis in Brain Aging and Neurodegeneration. *Front Aging Neurosci, 9*, 209. doi: 10.3389/fnagi.2017.00209

Yin, F., Yao, J., Sancheti, H., Feng, T., Melcangi, R. C., Morgan, T. E., . . . Brinton, R. D. (2015). The perimenopausal aging transition in the female rat brain: decline in bioenergetic systems and synaptic plasticity. *Neurobiol Aging, 36*(7), 2282-2295. doi: 10.1016/j.neurobiolaging.2015.03.013

Zeitschel, U., Schliebs, R., Rossner, S., Bigl, V., Eschrich, K., & Bigl, M. (2002). Changes in activity and expression of phosphofructokinase in different rat brain regions after basal forebrain cholinergic lesion. *J Neurochem, 83*(2), 371-380.

Zeng, L., Guo, J., Xu, H. B., Huang, R., Shao, W., Yang, L., . . . Xie, P. (2013). Direct Blue 71 staining as a destaining-free alternative loading control method for Western blotting. *Electrophoresis, 34*(15), 2234-2239. doi: 10.1002/elps.201300140

Zeynalov, E., Rezvani, N., Miyazaki, C., Liu, X., & Littleton-Kearney, M. T. (2014). Reproductive senescence blunts response of estrogen receptor-alpha expression to estrogen treatment in rat post-ischemic cerebral microvessels. *PLoS One, 9*(7), e102194. doi: 10.1371/journal.pone.0102194

Zhang, Q. G., Han, D., Wang, R. M., Dong, Y., Yang, F., Vadlamudi, R. K., & Brann, D. W. (2011). C terminus of Hsc70-interacting protein (CHIP)-mediated degradation of hippocampal estrogen receptor-alpha and the critical period hypothesis of estrogen neuroprotection. *Proc Natl Acad Sci U S A, 108*(35), E617-624. doi: 10.1073/pnas.1104391108

Zhang, Y., Huang, Y., Wang, G., Wang, X., & Wang, Y. (2017). Inhibition of 17-beta-estradiol on neuronal excitability via enhancing GIRK1-mediated inwardly rectifying potassium currents and GIRK1 expression. *J Neurol Sci, 375*, 335-341. doi: 10.1016/j.jns.2017.02.034

Zhang, Z. L., Qin, P., Liu, Y., Zhang, L. X., Guo, H., Deng, Y. L., . . . Hou, W. G. (2017). Alleviation of Ischaemia-reperfusion Injury by Endogenous Estrogen Involves Maintaining Bcl-2 Expression via the ERalpha Signalling Pathway. *Brain Res*. doi: 10.1016/j.brainres.2017.02.004

Zhao, Y., He, L., Zhang, Y., Zhao, J., Liu, Z., Xing, F., . . . Zhang, J. (2017). Estrogen receptor alpha and beta regulate actin polymerization and spatial memory through an SRC-1/mTORC2-dependent pathway in the hippocampus of female mice. *J Steroid Biochem Mol Biol*. doi: 10.1016/j.jsbmb.2017.08.003